1-13-2021

Reassessing Hydrothermal Heat Discharge and the Relationship of Hot Springs in the North Oregon Cascades

Aaron Alexander Orr
Portland State University

Reassessing Hydrothermal Heat Discharge and the Relationship of Hot Springs in the North Oregon Cascades

by

Aaron Alexander Orr

A thesis submitted in partial fulfillment of the
requirements for the degree of

Master of Science
in
Geohydrology

Thesis Committee:
Dr. Robert Perkins, Chair
Dr. Carl Palmer
Dr. John Bershaw

Portland State University
2020

ABSTRACT

Reservoir temperatures of hydrothermal systems in the Pacific Northwest reflect the feasibility of geothermal energy production and the tectonic framework of the region. Multicomponent geothermometry techniques were applied to new and historic water chemistry data in the north-central Oregon Western Cascades and the lower Wind River Valley in southern Washington in order to recalculate reservoir temperatures. Revised reservoir temperatures, water chemistry, and isotope data were used to determine relationships between hot springs in the north-central Oregon Cascades.

Geothermal reservoir temperatures were estimated for the lower Wind River Valley (98.44 ± 0.96°C) and for Austin and Bagby Hot Springs (100.10 ± 1.04°C and 65.29 ± 2.74°C, respectively) using RTEst software and mineral suites reflective of the host rock geology. The estimated reservoir temperature for Austin Hot Springs is lower than previous estimates (180 - 186°C; Ingebritsen et al., 1992; Mariner et al., 1993). The resulting calculated hydrothermal heat output of 48 MW for Austin Hot Springs is lower than the previous estimate of 85 MW (Ingebritsen and Mariner, 2010).

Isotopic evidence indicates that Austin and Breitenbush Hot Springs, located ~27 km apart, are recharged at similar elevations along the crest of the Cascades and may be part of a common hydrothermal system. The data further indicate a component of "andesitic water" (4-8%) in waters discharged from Austin and Breitenbush Hot Springs as well as from hot springs and geothermal wells in Wind River Valley, WA. This, along with extensional structures extending from the central Oregon Western Cascades to the lower Wind River Valley suggest similar mechanisms for the heating and movement of

deep circulating hydrothermal waters near the volcanic arc. Waters from Bagby Hot Springs, which lie ~15 km further west and away from the arc than Austin Hot Springs, do not have the same isotopic signature. Lower estimated reservoir temperatures and recharge elevations, differences in water chemistry, and the lack of an andesitic water signature indicate that the Bagby Hot Springs represent a discreet, localized hydrothermal flow system.

ACKNOWLEDGEMENTS

First and foremost, I would like to thank my adviser Ben Perkins and my committee members—Carl Palmer and John Bershaw—for the help and knowledge they provided to me during this project. I would not have completed this capstone without Ben and his steadfast patience, guidance in geochemical modeling, and nurturing of my understanding of chemistry, hydrology, and geothermal systems.

I would also like to thank Ellen Svadlenak for helping me with the Geochemist's Workbench Software suite and for being an all-around wonderful peer and role model.

Lastly, thank you to the Department of Geology at Portland State University, and all students and faculty therein, for further expanding my understanding and love of all things geological.

TABLE OF CONTENTS

LIST OF FIGURES

LIST OF TABLES

1. INTRODUCTION

The Cascade Range is a volcanic arc extending from northern California to southern British Columbia. Numerous thermal, slightly thermal, and mineral springs discharge along the 1200 km-long volcanic arc, with many of these springs located in the Western Cascades in north-central Oregon. Accurate determinations of geothermal reservoir temperatures are integral in estimating hydrothermal heat discharge within the Cascade Range. Additionally, these temperatures assist in determining the feasibility of geothermal power generation in areas of high heat potential.

Breitenbush and Austin Hot Springs are among the most significant and studied thermal systems in the northern Western Cascades in Oregon due to their high heat potential (Forcella, 1982; Mariner et al., 1990; Ingebritsen et al., 1992; Ingebritsen and Mariner, 2010). These thermal springs represent 300 MW of hydrothermal heat discharge within 50 km of Mount Jefferson (Ingebritsen and Mariner, 2010). Geothermal studies conducted in the 1980s and 1990s estimate a wide range of reservoir temperatures from 84 to 188°C for Austin Hot Springs and 129 to 202°C for Breitenbush Hot Springs (Forcella, 1982; Ingebritsen et al., 1992; Mariner et al., 1993; Bargar, 1994; Pang and Reed, 1998). Along with this wide range of calculated reservoir temperatures, a maximum borehole temperature of 141°C was measured at 3 km depth at Breitenbush Hot Springs (Bargar, 1994). Despite this measured at-depth temperature, a calculated temperature of 174°C was reported based on agreement between anhydrite and sulfate-water isotope geothermometers (Ingebritsen et al., 1992). Furthermore, mineralogy of the measured borehole shows scarce occurrence of anhydrite, which further challenges

reported reservoir temperatures. Utilizing newly developed multicomponent geothermometry techniques, Malkemus (2016) calculated a reservoir temperature for the Breitenbush Hot Springs system 40°C lower than reported in earlier studies, but within 4°C of at-depth temperatures measured in the SUNEDCO-58-28 borehole drilled 3 km to the southeast (Ingebritsen et al., 1992; Malkemus et al., 2017).

A third spring, Bagby Hot Springs, discharges within 20 km of Breitenbush and Austin Hot Springs. Bagby Hot Springs produces more dilute, high pH waters (~9) and a has a lower calculated reservoir temperature (52°C) than Breitenbush and Austin Hot Springs despite also discharging within the Breitenbush formation. Herein, isotope data are used to argue whether Austin and Breitenbush Hot Springs share a common hydrothermal system and if Bagby Hot Springs is in fact separate from Breitenbush and Austin Hot Springs. In addition to evaluating these three springs in the north-central Cascades, two recently installed geothermal wells (>50°C waters) in Wind River, WA are also evaluated. The Wind River fault is located approximately 15 km NW of the Hood River fault zone and follows a similar NW trend as the Clackamas fault zone near Austin, Breitenbush, and Bagby Hot Springs. Isotope and water chemistry data for thermal waters in the Wind River Valley are also referenced in arguing for a common hydrothermal system in the northern Cascades.

2. BACKGROUND

2.1 Heat Flow in the Cascades

The Cascade Mountain Range is located above an active subduction zone in the Pacific Northwest. This volcanic belt is divided into two physiographic subprovinces: the

deeply dissected Western Cascades, and the High Cascades. The bedrock of the Western Cascades is varied in composition, ranging from dacitic ash flows to olivine-bearing basaltic lavas (Blackwell et al., 1982). Bedrock of the High Cascades is mostly basaltic in composition based on total volume.

High rates of Quaternary extrusion, numerous hot and warm springs, and high conductive heat flow in the north-central Cascades make it an area of considerable geothermal energy potential (Blackwell et al., 1982, 1990a, 1993; Priest and Vogt, 1982; Mariner et al., 1990; Ingebritsen et al., 1992, 1994; Ingebritsen and Mariner, 2010). Geothermal investigations conducted in the 1980s produced critical information concerning total heat flow in the Cascades. A substantial shift in heat flow from 40 to ≥100 MW m^{-2} occurs moving east across the Western Cascade Range, with an associated increase in minimum geothermal gradients from 25 to 60+ °C km^{-1} respectively (Blackwell et al., 1982). Heat flow maps for the Pacific Northwest were produced using geothermal gradient wells near and along the Cascades (Figure 1).

2.2 Thermal Springs and Hydrothermal Heat Discharge

Estimates of hydrothermal heat discharge provide insight into the relative importance of thermal waters and the magnitude and distribution of heat loss in the Cascade Range. Seven thermal springs discharge along the north-central Oregon Western Cascades. These springs can be divided into two groups based on relative geographic location: Austin, Bagby, and Breitenbush Hot Springs near 45° latitude and Bigelow, Belknap, Foley, and Terwilliger Hot Springs near 44° latitude. Discharge measurements

from Ingebritsen and Mariner (2010) show that the group of thermal springs between Mt. Hood and Mt. Jefferson—including Austin, Breitenbush, and Bagby Hot Springs—account for approximately ¼ of total hydrothermal heat loss in the central Cascades

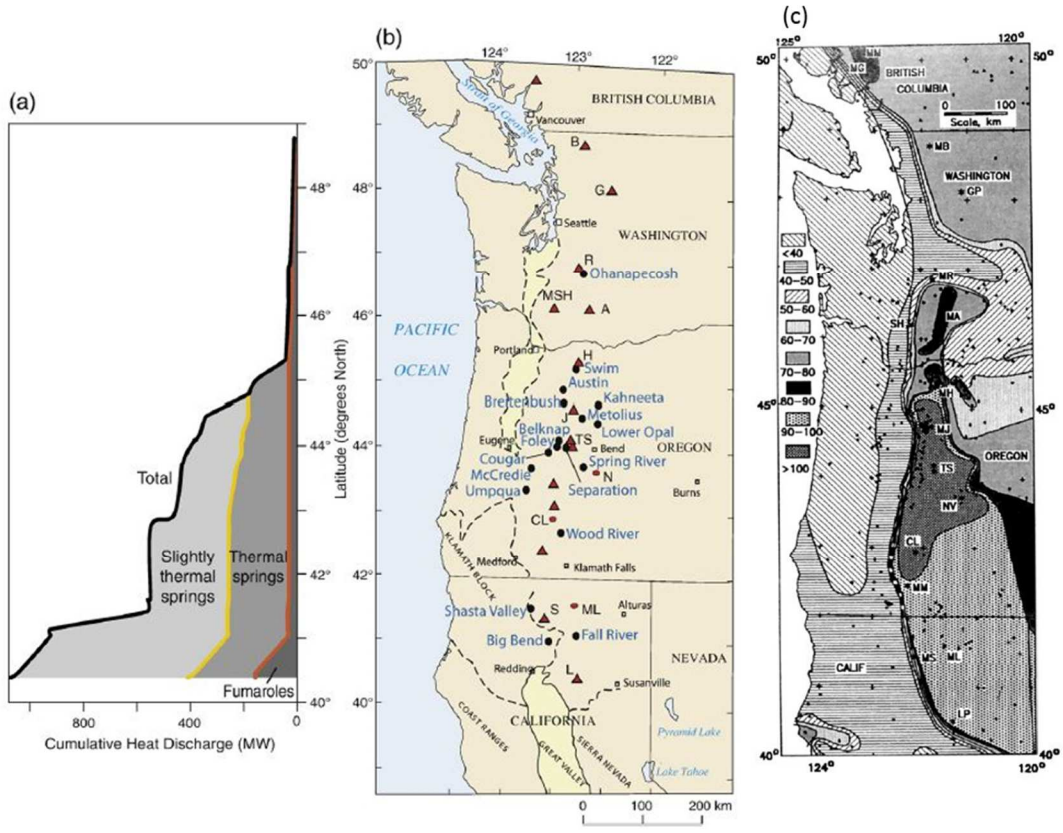

Figure 1: (a) Total cumulative hydrothermal heat discharge in the Pacific Northwest in MW by latitude and medium of discharge. (b) Corresponding thermal and slightly thermal spring locations from northern California to British Columbia (Ingebritsen and Mariner, 2010). (c) Heat flow measurements in the Pacific Northwest in MW m^{-2} in the Pacific Northwest (Blackwell, 1990b).

between 44°45’ and 45°15’ N latitude. The calculated heat output in this portion of the north-central Cascades is 121 MW. Hydrothermal discharge occurs almost exclusively at fumaroles north of 45°15′ latitude (Figure 1). This change from north to south is attributed to higher crustal heat flow and deep permeability caused by Basin and Range

impingement at the point of increased heat discharge (Ingebritsen and Mariner, 2010). However, the total amount of heat hydrothermally discharged at thermal springs may be less than these estimates which are based on older geothermometric studies (Figure 1; Ingebritsen et al., 1992, 1994; Mariner et al., 1993; Ingebritsen and Mariner, 2010). Two simple models have been proposed regarding the geothermal heat source of hot springs in the study area.

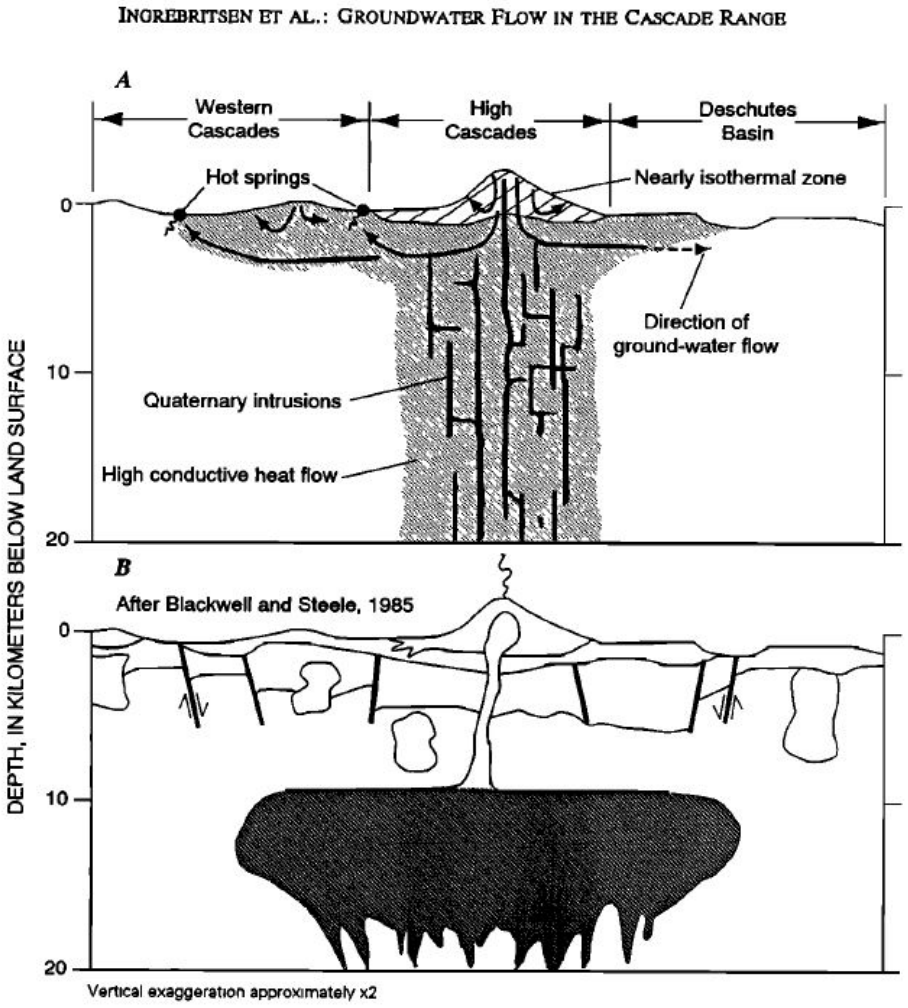

Figure 2. Two simple models of the thermal structure underlying the north-central Cascades, from Ingebritsen et al., 1992. (a) Heat is introduced to regional groundwater flow via young Quaternary intrusions; (b) a laterally extensive midcrustal heat source where heat flow is controlled by faulting near the surface (Blackwell et al., 1982, 1990a)

Ingebritsen et al. (1992) suggest a "lateral flow model" in which there are spatially variable heat sources that are nonetheless narrowly centered on the Quaternary arc, with regional groundwater flow dispersing heat laterally to lower elevations (Figure 2a). Blackwell et al. (1982, 1990a) a laterally extensive mid-crustal heat source underlying both the High Cascades and adjacent older rocks that represents a longer-lived zone of magma interception and crystallization, over which localized, fault-controlled hydrothermal systems are superimposed (Figure 2b). Simulations of heat flow at Breitenbush Hot Springs demonstrate that neither deep thermal structure can be inferred due to due to significant advective heat transport in the system (Ingebritsen et al., 1992).

2.3 Previous Work at Austin, Bagby, and Breitenbush Hot Springs

Bagby, Breitenbush, and Austin Hot Springs are located directly south of the 45°15' latitude line where the contribution to heat discharge by thermal springs along the Cascades increases drastically (Figure 1; Ingebritsen et al., 1992; Ingebritsen and Mariner, 2010). Of the three springs, Austin's calculated hydrothermal output of 85 MW makes up 70% of the calculated 121 MW discharged in this area. The other 30% is made up by Breitenbush Hot Springs in the Western Cascades and Kahneeta Hot Springs on the eastern flanks of the High Cascades (Ingebritsen and Mariner, 2010). Though grouped with these springs, Bagby's contribution is negligible due to its meager groundwater discharge of 1 L s^{-1} (Mariner et al., 1990).

All three hot springs discharge within the Breitenbush Formation, which is composed of Miocene to Oligocene volcanics and volcaniclastics (Figure 5). Bagby is located on the west side of the Breitenbush anticline while Breitenbush Hot Springs lies

east of the N to NE-trending anticlinal axis (Sherrod and Conrey, 1988). Logs from the SUNEDCO-58-28 boring suggest this unit is at least 2 – 3 km thick (Sherrod and Conrey, 1988). Geologic cross sections near Bagby Hot Springs show the Breitenbush formation dominating most of the vicinity, encompassed by the andesite of the Miocene Rhododendron Formation in the north, west, and south (Sherrod and Conrey, 1988). The Breitenbush Formation is unconformably overlain by the basalt of Collawash Mountain approximately 1 km east of the discharge site.

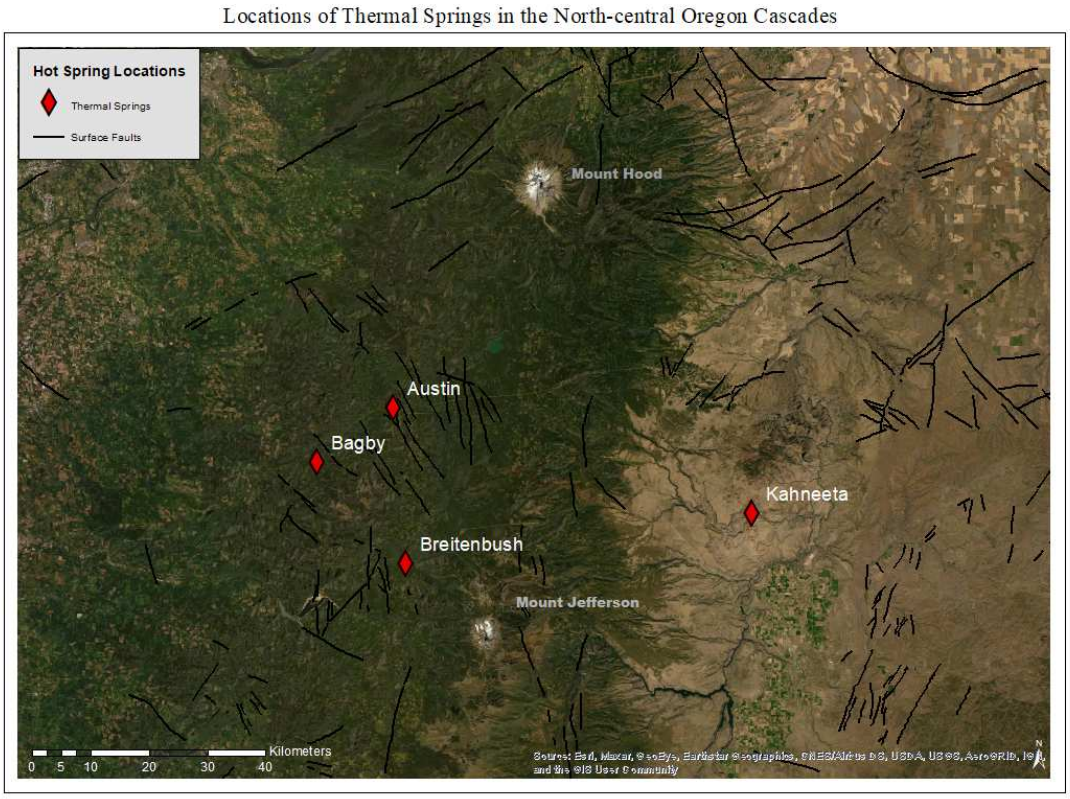

Figure 3. Map of Bagby, Breitenbush, and Austin Hot Springs in the vicinity of Mt. Jefferson. Black lines represent faults in the area. Fault data were downloaded from the US Geological Survey (USGS) Quaternary Faults Database.

Hydrothermal alteration is evident throughout the Breitenbush Formation with the most common secondary minerals being quartz, chalcedony, smectite, zeolites, epidote, calcite, hematite, and mixed clays (Sherrod and Conrey, 1988). These alteration minerals form at different temperatures in hydrothermal systems, suggesting the temperature of these systems has varied since the Oligocene.

Bagby Hot Springs is classified as a Na-mixed anion system with a relatively high pH of 9.4. A reservoir temperature of 52 °C at Bagby Hot Springs was calculated using quartz and cation geothermometers. Generalized stratigraphic cross-sections of the Bagby Hot Springs area show a sequence of basalt, andesite, and volcaniclastic rocks, with petrology in the area ranging from dacite to basaltic andesite (Dyhrman, 1974). Two northwest trending faults have also been documented by Dyhrman (1974) near Bagby Hot Springs, as well as an inferred east-west trending fault intersecting the springs themselves. Na-mixed anion waters of Bagby Hot Springs are similar to thermal waters associated with granitic rocks of the Idaho batholith (Mariner et al., 1980). Tertiary granitic or dioritic rocks are locally exposed in the Bagby Hot Springs area and may be more widespread at depth (Walker et al., 1985).

Breitenbush is classified as a Na-Cl system with a circumneutral pH (Ingebritsen and Mariner, 2010; Malkemus et al., 2017). At Breitenbush Hot Springs, a reservoir temperature estimation of 174 °C was calculated using an anhydrite based geothermometer in conjunction with quartz and cation geothermometers. Reassessment of this temperature using a recently developed multicomponent geothermometry software program (RTEst; Palmer, 2015) yielded a significantly lower temperature of 137 °C

(Malkemus, 2016; Malkemus et al., 2017). The results of this recent study were thermodynamically consistent with a suite of 19 secondary minerals identified in cuttings from the SUNEDCO-58-28 exploratory borehole located 3 km away and agreed with at-depth temperature readings of 141 °C measured in the borehole (Bargar, 1994). The modeled aluminum concentrations calculated assuming equilibrium with K-feldspar essentially matched measured dissolved aluminum concentrations. Earlier higher temperature estimates result in either undersaturation or a greater degree of disequilibrium for most of the identified minerals and aluminum concentrations nearly an order of magnitude higher than measured (Malkemus et al., 2017).

A similar temperature of 186 °C was calculated at Austin Hot Springs using anhydrite and sulfate isotope geothermometers. Similar to Breitenbush, Austin Hot Springs is also classified as a Na-Cl system (Mariner et al., 1993; Ingebritsen et al., 1992). Though it is farther from the crest of the Cascades than Breitenbush Hot Springs, the NW-trending faults may connect Austin Hot Springs to Mt. Jefferson (Sherrod and Conrey, 1988; Ingebritsen and Mariner, 2010).

The upwelling of thermal water at Breitenbush Hot Springs is closely related to the silicic volcanic rocks near Mt. Jefferson based on heat-flow data and 100-degree Celsius isotherms mapped in the study area around Breitenbush, Bagby, and Austin Hot Springs (Blackwell and Baker, 1988; Ingebritsen et al., 1988; Sherrod and Conrey, 1988). Austin Hot Springs' distance from Mt. Jefferson makes its connection to this volcanic center less clear. A NW trending fault zone at Austin Hot Springs could explain the circulation of hydrothermal fluids in this area and provide a hydrologic connection to the

water of Breitenbush Hot Springs (Figure 3). The location of both springs is probably owed to permeability barriers that lead to the zeolitization of the Breitenbush formation, though possible fault controls near Austin Hot Springs probably contribute to its location as well (Sherrod and Conrey, 1988).

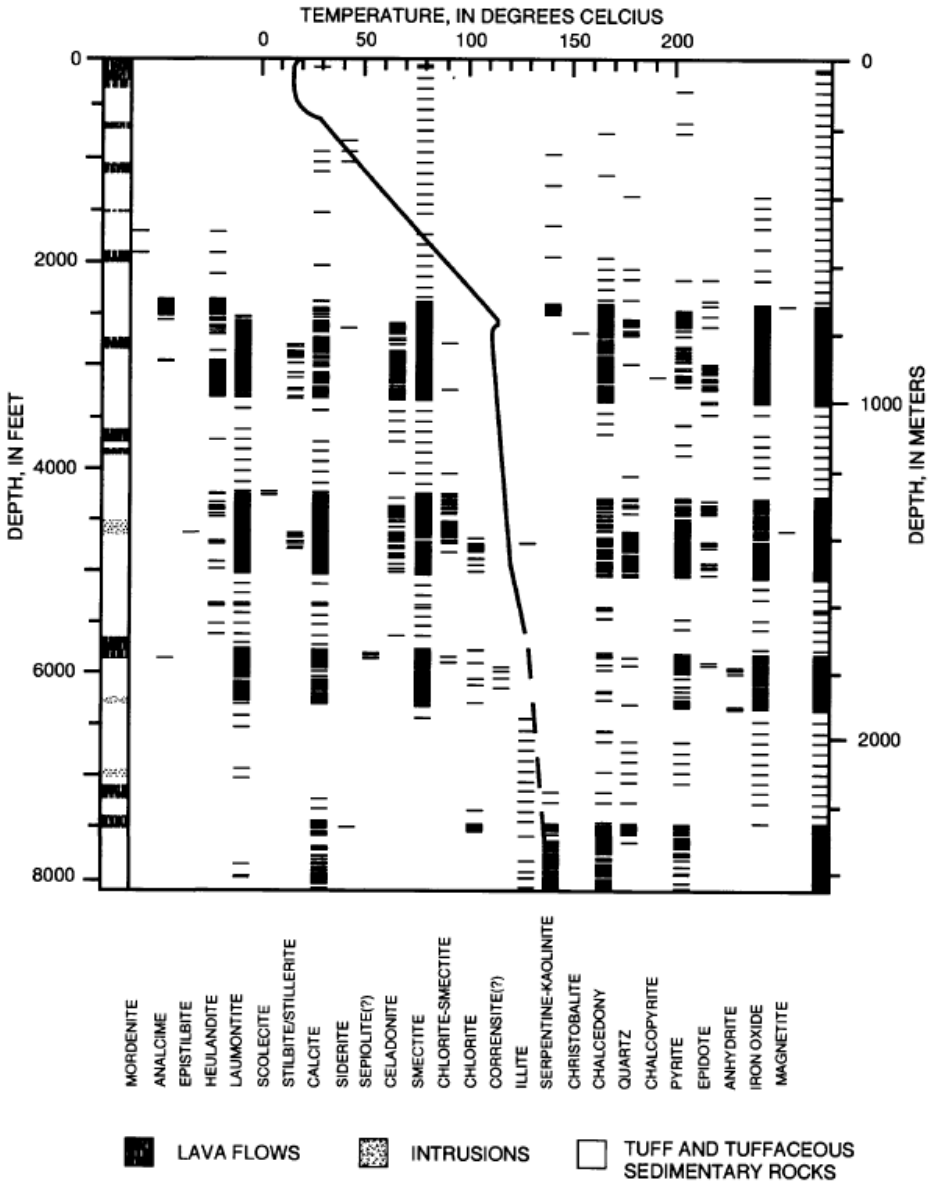

Figure 4. Temperature and minerals observed at increasing depth in SUNEDCO-58 borehole (Sherrod and Conrey, 1988).

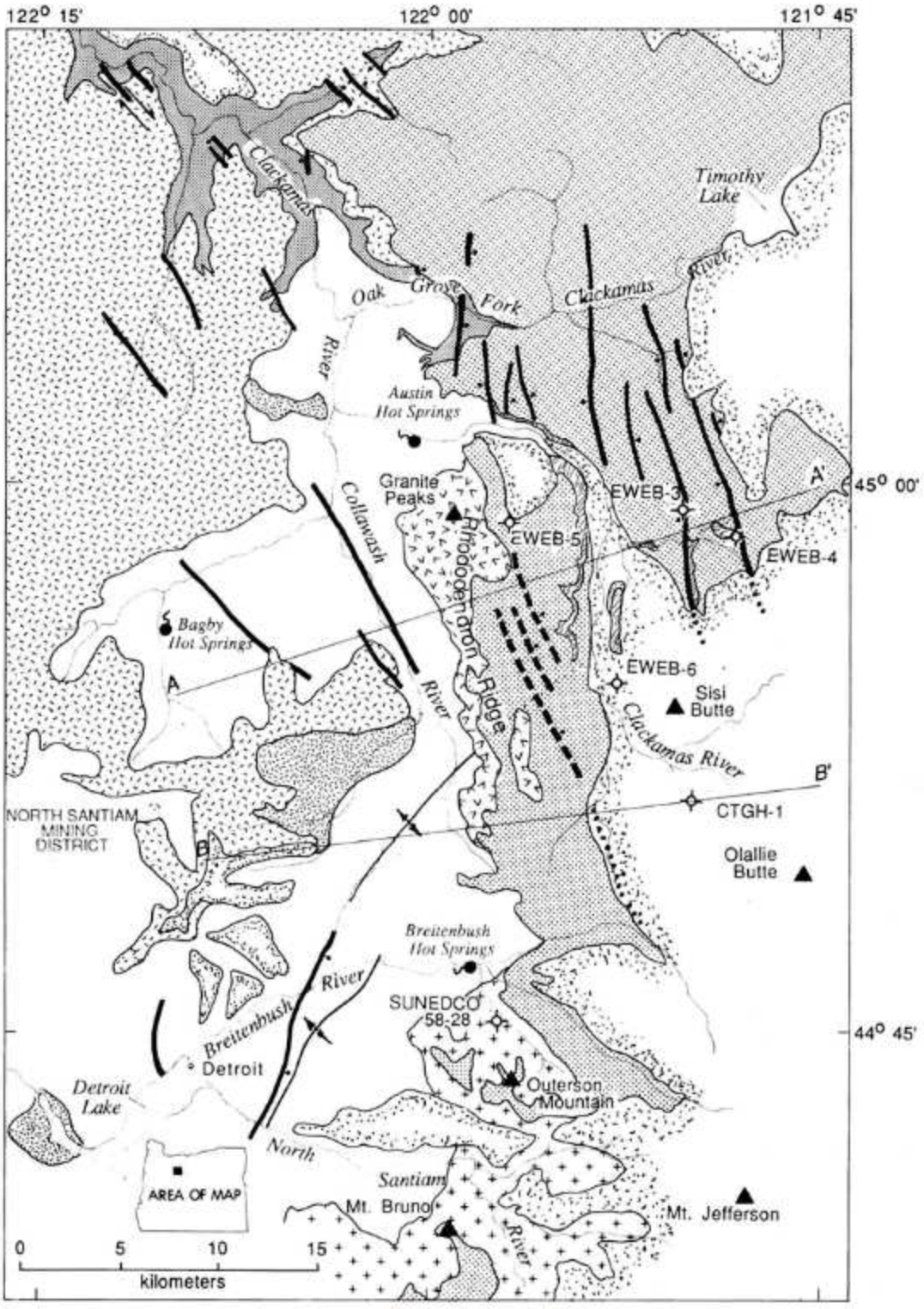

Figure 5. Geologic Map of the Austin-Bagby-Breitenbush area (from Sherrod and Conrey, 1988).

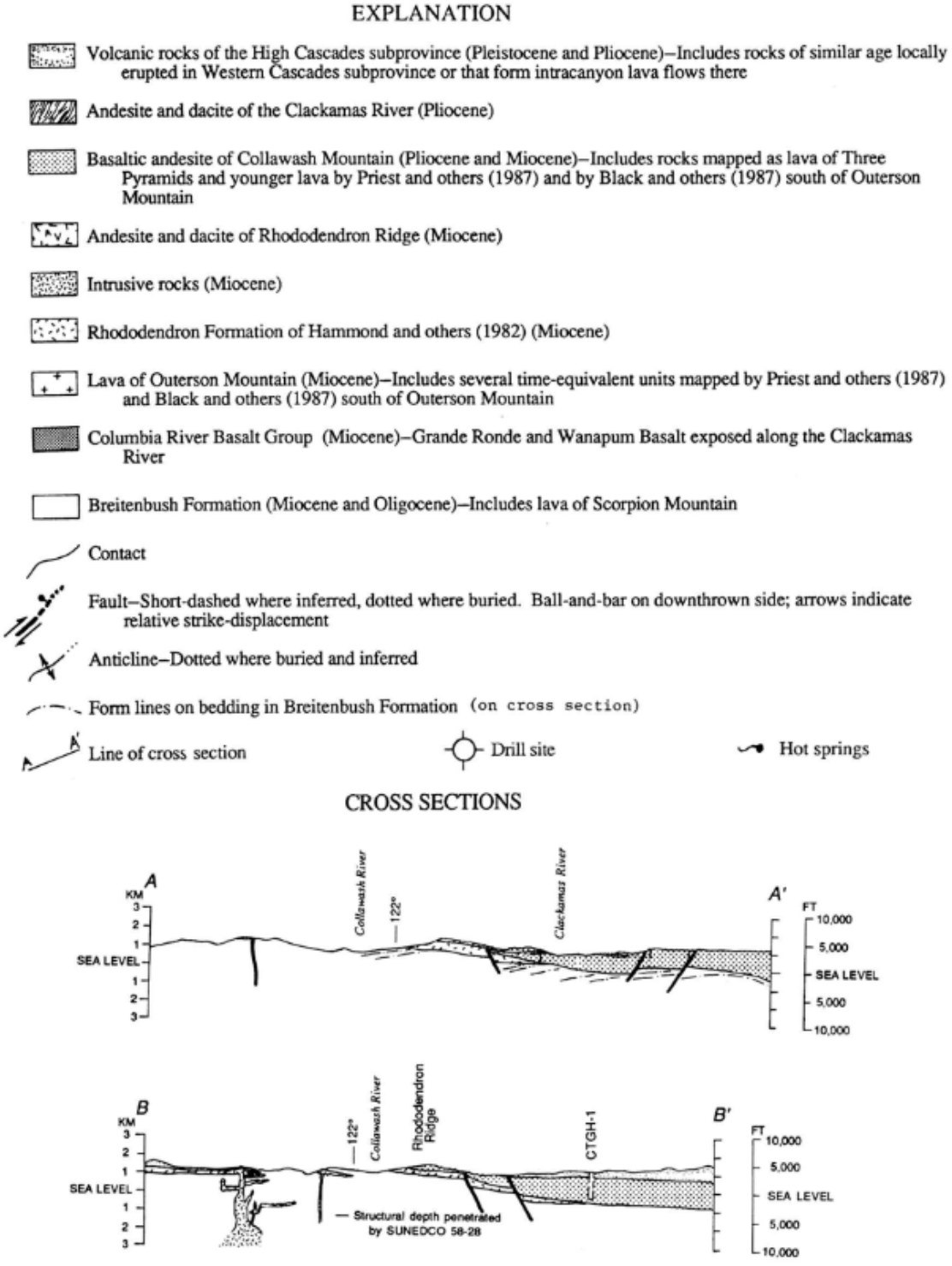

Figure 6. Explanation of geologic units and cross sections from figure 3 (from Sherrod and Conrey, 1988)

δD and $\delta^{18}O$ isotope values were used to calculate a groundwater recharge elevation between 1750 and 2200 m for Breitenbush and Austin Hot Springs (R. Perkins, personal communication, 2018). The inferred recharge elevation range was based on the isotopic values at the intersection of the local meteoritic water line of Brooks et al. (2012) and a trend defined by isotopic signatures of geothermal waters and interpreted as a line of mixing between meteoric water and an "andesitic water" proposed by Giggenbach (1992). The lower limit was calculated using the isotope-elevation model of James et al. (2000) based on values from snow near the crest of the central Oregon Cascades. The higher values were calculated from the isotope-elevation model of Brooks et al. (2012) based on Willamette Valley waters, including from tributaries in the Western Cascades. The fact that geothermal waters from both Breitenbush and Austin Hot Springs plot along the same recharge line indicates that these two geothermal areas are likely recharged at the same elevation along the crest of the High Cascades to the east.

Scarce isotopic data exists in literature for Bagby Hot Springs, though deuterium values suggest Bagby Hot Springs recharges locally compared to other Hot Springs in the area (Mariner et al., 2003). Local circulation of water for Bagby Hot Springs is because drainage divides separate Bagby Hot Springs from the Quaternary arc (Ingebritsen et al., 1992). Although Bagby Hot Springs is classified as a "slightly thermal" spring, its proximity to Austin and Breitenbush Hot Springs remains important in understanding the underlying thermal structure of the north-central Western Cascades.

2.4 Previous Work at Wind River

Wind River Valley is located in Southern Washington, draining into the Columbia River near Carson, WA. A multi-criteria GIS model identified Wind River as one of three locations in Washington that could be used for geothermal energy development (Figure 7; Czajkowski et al., 2013). The valley contains six springs with discharge temperatures ranging from 8 to 53°C (Czajkowski et al., 2013). Numerous faults were identified in the southeast portion of the valley, including the intersecting Wind River Fault and Shipherds Fault Zone (Forson et al., 2017). Wind River Valley also lies 15 km NW of the Hood River fault zone and follows a similar NW trend as other faults along the Columbia River. Geothermal investigations have been heavily focused on springs near the southern boundary of the Shipherds Fault Zone at Wind River Valley. The source of geothermal energy is assumed to be from young intrusives on the east side of the river (Figures 8 and 9).

Various mapping efforts in the past sixty years show that the oldest rocks exposed are the Ohanapecosh Formation—a 300-m thick unit consisting of weathered volcanic and volcaniclastic deposits—which are covered by Oligocene to Pliocene lava flows (Figure 10). Hydrothermal minerals in the strata of the Ohanapecosh Formation were created through low grade zeolite facies metamorphism in the Miocene at temperatures less than 180°C (Berri and Korosec, 1983). The 2017 DNR report suggests the reservoir rocks are Neogene basalts (Forson et al., 2017). The Wind River Fault zone runs through moderately weathered, fine to medium-grained diorite. Young northeast-trending faults in

the lower part of the Wind River Valley likely form barriers to down-valley water flow (Czajkowski et al., 2013).

Figure 7. Map of Wind River Washington. St. Martins and Shipherds Hot Springs discharge along the intersection of the Wind River Fault Zone (WRFZ) and the Shipherds Fault Zone (SFZ) as mapped by Czajkowski et al., 2013.

Springs identified in the lower Wind River Valley are divided into three groups by Czajkowski, 2013. Group A springs are fault-related springs near the southern end of the DNR study area that discharge at the intersection of Shipherds Fault Zone and Wind River Fault Zone. Group B springs are low temperature cold springs in the northern portion of the study area. Group C springs are also cold springs but are distinctly Ca-HCO3 waters. New wells that were sampled as part of this study—installed by Tenzen

Hot Springs Resort—lie very near the mapped trace of the Wind River Fault (Czajkowski et al., 2013).

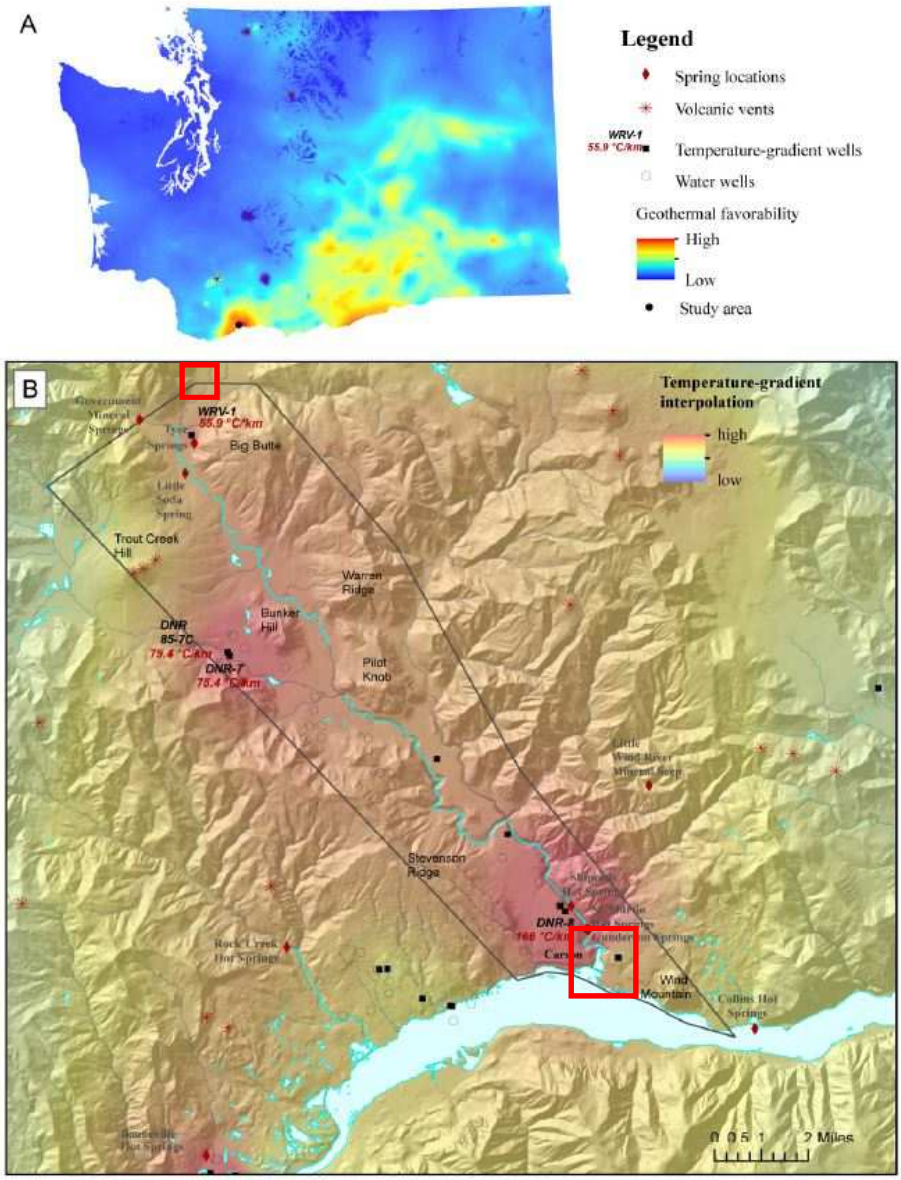

Figure 8. (A) Map of geothermal favorability in the state of Washington. The study area is marked in the southwest portion of the state. (B) Calculated temperature gradient at Wind River. Red diamonds represent springs. Temperature-gradient wells are represented by black squares. The proposed area of interest for the study is within the red square, east of the fault zone (modified from Czajkowski et al., 2013).

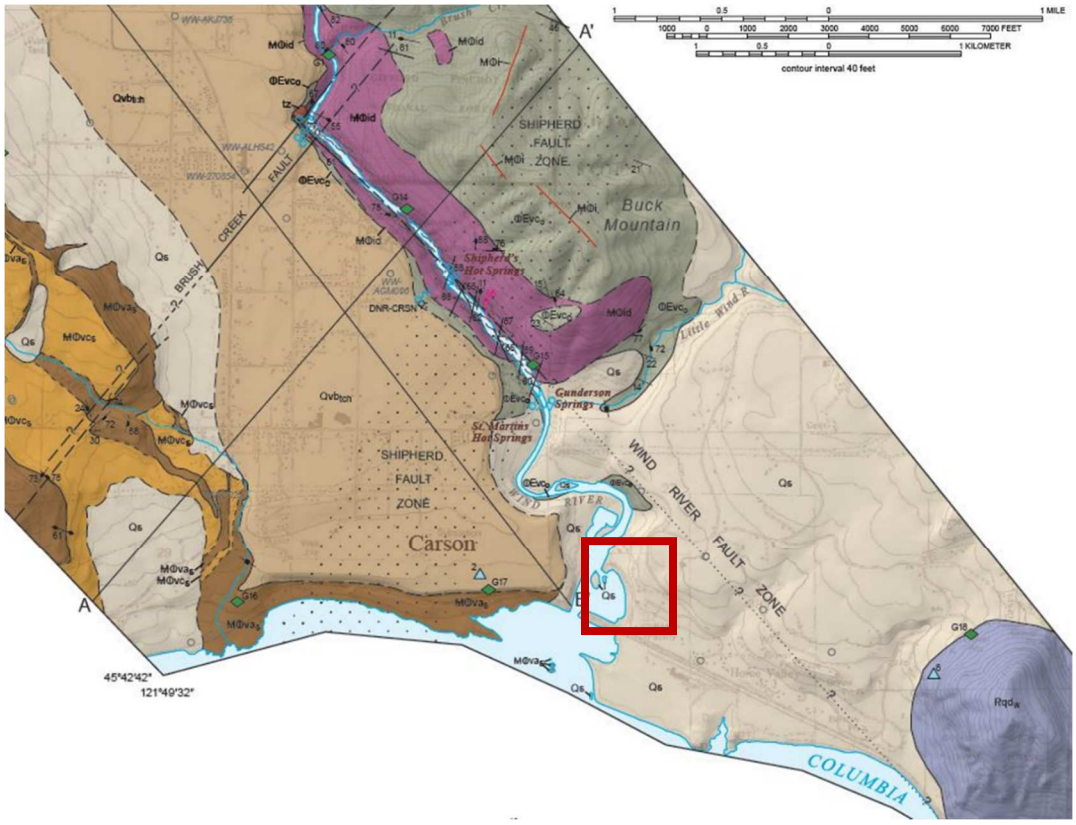

Figure 9. Geology of southern Wind River. Springs discharge at the intersection of the Wind River Fault Zone and Shipherds Fault zone (modified from Czajkowski et al., 2013).

Most of the hot springs in the southern Wind River Valley appear to coincide with the intersection of the Shipherds Fault and Wind River Fault Zones while these wells are installed southeast of the mapped intersection at Shipherds Fault Zone.

Water chemistry and temperature data collected by the Washington DNR have yielded useful at-depth temperature estimations and geothermal temperature gradients. Silica geothermometry results from St. Martins Hot Springs yield a reservoir temperature of 75 °C (Czajkowski et al., 2013). During the early 1980s, borings were drilled in three different locations to establish geothermal gradients. Nearby drill holes show a lithology of Tertiary volcaniclastic and pyroclastic rocks of Oligocene to Miocene age (Berri and

Korosec, 1983). Increased water circulation at depth may be possible due to evidence of increased fracture zones (Berri and Korosec, 1983). Thermal conductivity estimations of underlying lithologies suggest heat flow values ranging from 122 to 157 mW m^{-2}.

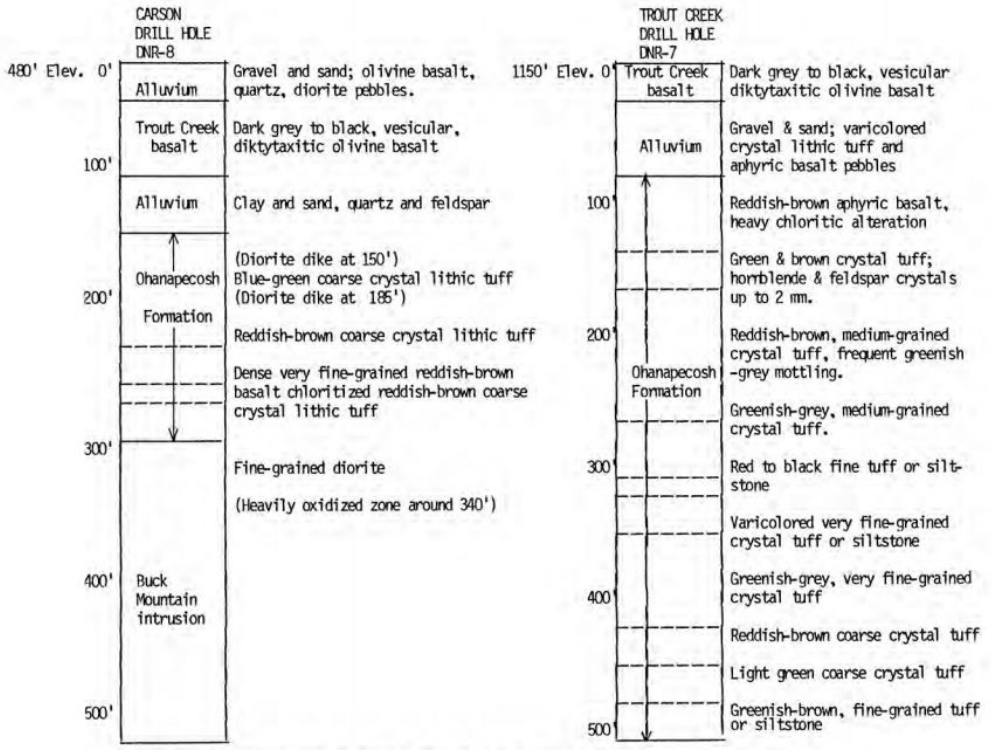

Figure 10. Drill holes from Berri and Korosec, 1983.

2.5 Minerology of Hot Springs

Detailed minerology has been recorded both at the surface and in deep and shallow boreholes near Breitenbush Hot Springs. Hydrothermal minerals found in the Austin-Breitenbush area include chabazite, thomsonite, mesolite, phillipsite, stilbite, heulandite, laumontite, mordenite, and analcime (zeolites); smectite, smectite-illite, celadonite, illite, chlorite, and smectite chlorite (clays), and; sericite, opal, a-cristobalite, b-cristobalite, calcite, chalcedony, quartz, epidote, and adularia (Keith, 1988).

A comprehensive list of alteration minerals observed in the CTGH-1 borehole were recorded by Sherrod and Conrey, 1988. CTGH-1 was drilled near the crest of the cascades, due north of Mt. Jefferson, and intercepts volcanic rocks of the High Cascades subprovince and underlying basaltic andesite of Collawash Mountain. Ubiquitous minerals throughout the 5 km borehole included iron oxides, smectite, and heulandite. From approximately 2000 to 3000 m depths, thomsonite, analcime, chabazite were present, and from 3000 m down heulandite, mordenite, a-cristobalite, chalcedony, celadonite, and quartz were observed. The measured high temperature endmember of the CTGH-1 borehole is slightly under 100 degrees Celsius (Bargar, 1994). Because these minerals reflect the younger basaltic andesite of the High Cascades, these minerals were not referenced when selecting the suite for Austin.

Mineralogy in the SUNEDCO-58-28 borehole is reported by Bargar, 1994. The SUNEDCO-58-28 borehole was drilled 3 km southeast of Breitenbush Hot Springs and intercepts the lava of Outerson Mountain and the Breitenbush Formation (Sherrod and Conrey, 1988). Most mineral observations were beneath depths of 2000 m, assumed to be present at levels where past or current aquifers exist. Ubiquitous hydrothermal minerals within these sections include heulandite, laumontite, calcite, celadonite, smectite, chalcedony, quartz, pyrite, and iron oxides. The maximum measured temperature in the SUNEDCO-58 borehole is 141 degrees Celsius, which is consistent with new geothermometry estimations (Bargar, 1994; Malkemus, 2016; Malkemus et al., 2017).

List of Minerals at Austin Hot Springs

Table 1. Reported by Boden 1985 and summarized by Bargar 1997 using samples from two shallow boreholes near Austin Hot Springs (andesitic and microdioritic outcrops). Zeolites and clays were also listed in *Keith, 1988.

Zeolites	Silica Minerals	Clays	Carbonates	Iron Oxides	Others
Epistilbite	Cristobalite	Smectite	Calcite	Hematite	Pyrite
Stilbite	Quartz	Celadonite	Dolomite	Magnetite	Epidote
Laumontite	Chalcedony	Chlorite	Siderite		Antigorite
Mesolite		Illite			
Analcime					
Mordenite					
Heulandite					

List of Minerals at Bagby Hot Springs

Table 2. Surface mineralogy reported by Walker et al., 1985. Celadonite with Magnetite veins reported by Dyhrman, 1974

Zeolites	Silica Minerals	Clays	Carbonates	Iron Oxides	Others
Nontronite	Chalcedony	Chlorite	Calcite		
Saponite					
Stilbite					
Laumontite					
Leonhardite					
Heulandite					

List of Minerals at Lower Wind River

Table 3. Mineralogy reported by Wise, 1961 for the Ohanapecosh formation. Hydrothermal alteration minerals proximal to breccias and quartz veins were reported by McGowan 1985 (M).

Zeolites	Silica Minerals	Clays	Carbonates	Iron Oxides	Others
Heulandite	Quartz		Calcite		
Laumontite					
Analcime					
Stilbite					
Scolecite					
Mordenite					
Grifithite					
Smectite (M)					
Chlorite (M)					
Illite (M)					

2.6 Advances in Geothermometry

The discharge temperature of hydrothermal fluids at or near the surface is lower than at its reservoir depth due to the cooling of geothermal fluids during ascent. Geothermometry techniques utilize the chemistry of thermal waters collected at or near the surface to back calculate the temperatures at depth in the geothermal reservoir. Geothermometry relies on the principles that 1) chemical equilibrium is achieved between groundwater and specific minerals within the reservoir host rocks, 2) the processes that control this equilibrium are temperature-dependent, and 3) no mixing of waters or re-equilibration of the indicator occurs between the reservoir and the surface (Fournier, 1977). Based on the third principle, it is assumed that geothermometry techniques calculate reservoir temperatures at whatever the most recent point of equilibration was before reaching the surface.

Geothermometry techniques of the 1970s relied on known reference concentrations of silica and specific cations at certain temperatures. These known concentrations are compared to ion concentrations in a sample to estimate the reservoir temperature of the system. The most commonly used cation geothermometers are sodium, potassium, and calcium (Spycher et al., 2014). The 1980s saw a development in geothermometry where instead of using one or several single component geothermometers to calculate reservoir temperature, multicomponent geothermometry could be used to estimate temperature based on comparisons between bulk water chemistry and a chosen mineral assemblage (Reed and Spycher, 1984). However, early versions of this multicomponent geothermometry required tedious minute adjustments

during use and relied on visually subjective grouping of data (Spycher et al., 2014). Furthermore, most reported chemistries for wells and springs lack aluminum concentrations, which is critical for using aluminosilicate minerals for geothermometry. A method of estimating aluminum concentrations for use in multicomponent geothermometry, the FixAl method, was proposed by Pang and Reed (1998), though this requires assumed equilibrium with a phase like K-feldspar. Other issues have been addressed by new software programs, namely GeoT (Spycher et al., 2014) and RTEst (Palmer, 2015). Ultimately, the accuracy of any geothermometry calculation is dependent upon the selection of a mineral suite that adequately reflects the reservoir conditions.

3. METHODS

3.1 Field Methods

Three distinct points of discharge were identified at the Bagby Hot Springs site, which is administered by the Mt. Hood National Forest. Bagby Springs 1 is used to provide water to the historic bathhouse. Flow from this spring was estimated at 2 L/s. A seep that lies immediately adjacent to Bagby Springs 1 is identified herein as Bagby Side Springs. Flow from this seep is relatively insignificant, likely < 0.1 L/s. Bagby Springs 2 lies approximately 70 m south of Bagby Springs 1 and provides water to a bathing tub. Discharge from this spring is estimated at 1 L/s. Samples from Bagby were collected in late October 2018 and early July 2019. All five spring samples were collected in low-density polyethylene bottles placed directly in the discharge of the springs.

Two wells are located near the east bank of Wind River near 45.71881, -121.78836 (WR AAT715) and 45.71924, -121.78830 (WR AAT724), ~0.5 km from the

mouth of the river. Samples were collected at the Tenzen Hot Springs site in the lower Wind River Valley. Both samples from Tenzen Hot Springs were collected in early December 2018 from flowing artesian wells within 0.05 km of one another. Wells were purged at least one full well-volume of water before samples were collected in low-density polyethylene bottles.

Prior to filtering, grab samples from WR AAT715, WR AAT724, and Bagby Hot Springs were collected in LDPE bottles. Well samples from WR AAT724 were collected from outflow tubing while samples from WR AAT715 were collected directly from the flowing artesian well. Samples for ion analysis at both locations were then filtered through a 0.45-micron polyethersulfone membrane syringe filter and collected into acid washed, LDPE bottles. Samples intended for cation analysis for acidified to < pH 2 using trace-metal grade HNO_3. All samples were filled to prevent air bubbles in the headspace of the LDPE bottles. After collection all samples were stored in an ice-filled cooler before being transferred to a refrigerator at the Portland State University laboratory. At each location field measurements of discharge temperature, specific conductance, electrical conductivity, oxidation-reduction potential, pH and dissolved oxygen content were obtained using a calibrated YSI Professional Plus multimeter, either directly in the spring discharge or, for the wells, in sample bottles. Discharge temperatures at both locations were low enough that cooling of the water was not necessary before measuring. Oxidation-reduction potential was measured using a combination platinum electrode with an Ag/AgCl (4M KCl) reference electrode calibrated using a Zobell solution. pH was calibrated using pH 4.0, 7.0, and 10.0 buffer standards. Field alkalinity measurements

were obtained at Tenzen Hot Springs using a HACH digital titrator equipped with either 0.16 or 1.6 N H_2SO_4 and green-methyl red indicator for total alkalinity; a phenolphthalein indicator was also used to determine carbonate alkalinity.

3.2 Laboratory Methods

Total alkalinity was re-measured at Portland State University within 24-hours of sample collection. 50 mL samples were titrated with 0.1 N HCl at room temperature. pH values were recorded using an Oakton Ion 510 series pH meter every 0.1 mL until pH was well below the bicarbonate equivalence point (generally to < 3 pH). Alkalinity values were then calculated from recorded measurements using the Gran function (Gran, 1952).

Major anions (Cl^-, Br^-, F^-, NO_2^-, NO_3^-, and SO_4^{2-}) were analyzed using liquid chromatography via an LC25 Dionex chromatography instrument attached with a Dionex CD25 conductivity detector, GP50 gradient pump, and an As40 automated sampler. A mixture of 4.5 millimolar Na_2CO_3 and 0.8 millimolar $NaHCO_3$ was used as the carrier fluid. Major, minor, and trace cations in samples were analyzed using an Agilent 7900 series quadrupole ICP-MS. Cation and anion concentrations were determined by comparing measurements to known standards prepared from commercial NIST-traceable stock solutions.

Samples were sent to four different laboratories for isotope analysis. Deuterium and ^{18}O were analyzed at Northern Arizona University Stable Isotope Laboratory using an LGR Liquid Water Isotope Analyzer DLT-100. Boron-11 isotopes were analyzed at the University of Calgary Isotope lab. Samples for boron analysis were not acidified prior

to shipment. Sulfur and oxygen isotopes in sulfate were analyzed at the University of Waterloo Isotope Lab. Sulfide was precipitated out of solution using zinc acetate. The remaining solution was then re-filtered using a 0.45-micron filter. Lithium-6/lithium-7 isotopes were analyzed at ALS Scandinavia using ICP-SMFS. Samples for lithium analysis were collected in acid-washed LDPE bottles and then filtered through a pre-washed 0.2-micron cellulose filters. Samples were then acidified to pH < 2 before shipment.

3.3 Modeling Software

RTEst (Palmer, 2015) is a computer program that estimates reservoir temperatures using measured water chemistries and a user-selected suite of minerals believed to be at or near equilibrium with the aqueous system. This program interfaces in conjunction between The Geochemist's Workbench (GWB; Bethke et al., 2019) to calculate shifts in chemistry and mineral saturation indices with changing temperature and a Model-Independent Parameter Estimation and Uncertainty Analysis (PEST) program to perform optimization calculations of key parameters (temperature, CO_2 fugacity, and loss or gain in water). RTEst determines the temperature at which the weighted sum of the squares of mineral saturation indices (theoretically "0" at saturation) are minimized (Palmer, 2015). RTEst minimizes the objective function via PEST, providing the most likely parameters for a selected suite of minerals close to saturation with the system.

3.4 Multicomponent Geothermometry Mineral Selection

Mineral suites were selected based on ubiquity in surface mineralogy, borehole mineralogy, chemical modeling, and likely saturation minerals based on lithology, temperature, and pH (Palmer et al., 2014). Hot Springs were assumed either low temperature systems in tholeiitic host rock (Bagby, Tenzen, Austin; LT-T) or medium temperature systems in tholeiitic host rock (Austin; MT-T).

Alteration mineral assemblages from the CTGH-1 and SUNEDCO-58-28 exploratory boreholes completed near Breitenbush Hot Springs (Bargar 1988; Bargar 1994) were referenced when identifying key alteration minerals (i.e., saturation index close to 0) for Austin and—to a lesser extent—Bagby Hot Springs. The three locations share similar geologies, namely the volcanic and volcaniclastic rocks of the Breitenbush Formation. Minerals identified in these boreholes were considered when selecting minerals assumed at equilibrium with Austin and Bagby Hot Springs. Similarly, boreholes analyzed by Czajkowski et al. (2013) and mineralogy of the Ohanapecosh Formation by Wise (1961) provide a starting point for mineral selection at Tenzen Hot Springs. Zeolites and clay minerals for Bagby and Wind River Hot Springs were selected based on surface mineralogy and minerals that form in similar hydrothermal zones (Utada, 2001)

Historic water chemistry data for Austin Hot Springs compiled by Mariner et al. (1993) were used as the input for GWB basis species. To accommodate for unknown aluminum concentrations in the springs, aluminum values were set in equilibrium with potassium feldspar, illite, albite, and a low aluminum well at Breitenbush. Other

unknown trace element concentrations were set to negligible concentrations of one part per trillion in order to account for the undersaturation of other minerals in the system.

4. RESULTS

4.1 Ion Chemistry

Chemical data for all samples collected and analyzed in this study as well as select data from prior studies are presented in Tables 4 and 5. For major cations and silica, analytical percent recoveries measured in quality control samples range between 97.1 and 102.2% and average 100.3%, while the percent recoveries for Cl, SO4 and F ranged between 96.3 and 100.1%. Analytical percent recoveries for trace elements range between 87.5 and 102.3% with an overall average of 99.7%. Relative standard deviations (RSD) measured in duplicate samples are 0.1 – 4.8% for major cations, 1.8 – 7.7% for anions, and 0.2 – 20% for trace elements, excluding iron. The RSD for Fe measured in duplicates of Bagby Spring 2 collected in July 2019 is 40.5%. However, the measured Fe concentration is ≤1 µg/l and less than 3x the calculated detection limit of 0.33 µg/L. Comparable levels of Fe were measured in the Bagby field blank, though this was the only analyte detected in a field blank. A F concentration of 0.016 mg/l was detected in a single laboratory blank: however, the measured concentration is only 3.2% of the lowest measured sample concentration. The maximum RSD between laboratory-measured alkalinities was 4.0%. RSD values for field-based alkalinity measurements made in July 2019 using a HACH digital titrator were 5.4 – 11.1% and the field-based alkalinities were lower than (91-98% of) laboratory values.

Table 4. Measured field parameters for the Wind River and Austin-Breitenbush-Bagby Hot Springs. Shipherds and St. Martins data from Malkemus (2016). Historic Breitenbush, Bagby, and Austin Hot Springs data from Mariner et al. (1993) and Ingebritsen et al. (1992).

Sample ID	Collection Date	Latitude	Longitude	Temperature	pH	Eh
				(°C)	(23°C)	(mV)
WR AAT715 (Tenzen 1)	12/4/2018	45.71881	-121.78836	64.5	8.33	-40
WR AAT724 (Tenzen 2)	12/4/2018	45.71924	-121.78830	56.3	8.42	-21
Shipherds 1	11/16/2015	45.73475	-121.8024	34.7	9.4	288
Shipherds 2	11/16/2015	45.73420	-121.8021	39.3	9.1	282
St. Martin Well	11/16/2015	45.72917	-121.7980	51.5	8.2	26
St. Martin Tap	11/16/2015	45.72881	-121.7962	51.6	8.18	-32
Bagby Spring 1A	10/17/2018	44.93582	-122.17267	57.6	9.57	85
Bagby Side Spring	10/17/2018	44.93574	-122.17253	52.6	9.49	75
Bagby Spring 2A	7/1/2019	44.93556	-122.17258	56.9	9.57	63
Bagby Spring 1B	10/17/2018	44.93582	-122.17367	57.6	9.67	85
Bagby Spring 2B	7/1/2019	44.93556	-122.17358	56.9	9.7	63
Austin*	1972	45.02124	-122.00982	86	7.4	[1]nr
Breitenbush*	1980	45.78167	-121.9750	84	7	[1]nr
Bagby*	1977	44.93583	-122.1725	58	9.4	[1]nr

*From Ingebritsen et al. (1992)

[a]CBE: Charge balance errors after speciation in Geochemist's Workbench (Bethke et al., 2019)

[b]TDS: Total dissolved solids of analytes in the system

Table 5. Major ion chemistry for the Wind River and Austin-Breitenbush-Bagby Hot Springs. Shipherds and St. Martins data from Malkemus (2016). Historic Breitenbush, Bagby, and Austin Hot Springs data from Mariner et al. (1993) and Ingebritsen et al. (1992).

Sample ID	SiO_2	Na	K	Ca	Mg	HCO_3	Cl^-	SO_4	F	[a]CBE	[b]TDS
	(mg/L)	(mg/L)	(mg/L)	(mg/L)	(mg/L)	(mg/L)	(mg/L)	(mg/L)	(mg/L)	(%)	(mg/kg)
WR AAT715 (Tenzen 1)	69	490	8.5	125	0.03	23	800	23	0.91	8.10	1570
WR AAT724 (Tenzen 2)	71	420	6.7	73	0.02	33	760	15	0.91	-0.96	1410
Shipherds Spring 1	46.3	48.4	0.49	3.7	0.05	33	35.1	11	0.5	-0.42	198
Shipherds Spring 2	45.3	47.5	0.45	3.8	0.45	38.5	32.7	12	0.32	-0.52	201
St. Martins Well	45	395	10	78.5	1.48	16.4	658	14	0.6	5.30	1215
St. Martins Tap	44.9	393	10	78.1	1.48	14.8	660	13	0.61	5.10	1212
Bagby Spring 1A	78.1	53.5	0.67	3.21	0.0023	78	14.7	40.7	0.67	-14.06	287
Bagby Side Spring	78.4	52.3	0.69	3.28	0.0041	74	16.3	40.5	0.66	-12.54	283
Bagby Spring 2A	77.1	51.0	0.69	3.15	0.0016	75	15.7	41.7	0.68	-11.25	280
Bagby Spring 1B	74.7	59.0	0.78	3.78	0.002	72	14.1	40.5	0.52	-8.28	282
Bagby Spring 2B	77.1	57.5	0.784	3.69	0.002	68	13.52	40.27	0.52	-8.85	285
Austin*	81	305	6.4	35	0.1	36	390	130	1.4	2.78	903
Breitenbush*	163	745	31	95	1.1	137	1200	140	3.7	-0.88	2454
Bagby*	74	53	0.7	3.3	<0.05	69	14	42	[1]nr	-8.49	266

*From Ingebritsen et al. (1992)

[1]nr: Not reported in study

[2]nd: Below ICP-MS detection limit

[3]bdl: Either below detection limit or interfering peaks in chromatography data

Table 6. Minor and trace ion chemistry for the Wind River and Austin-Breitenbush-Bagby Hot Springs. Shipherds and St. Martins data from Malkemus (2016). Historic Breitenbush, Bagby, and Austin Hot Springs data not reported for these analytes.

Sample ID	Fe	Mn	Li	Sr	As	Ba	Al	Br	B	Rb	V
	µg/L	µg/L	µg/L	µg/L	µg/L	µg/L	µg/L	µg/L	µg/L	µg/L	µg/L
WR AAT715 (Tenzen 1)	36	11	340	210	27	92	8	[2]nd	4200	[2]nd	[2]nd
WR AAT724 (Tenzen 2)	5	6.5	304	93	20	46	12	[2]nd	4000	[2]nd	[2]nd
Shipherd's Spring 1	7.9	0.57	20.7	6.9	12.0	[2]nd	33	136	963	[1]nr	[1]nr
Shipherd's Spring 2	10.7	nd	21.5	6.8	11.2	[2]nd	29	125	957	[1]nr	[1]nr
St. Martin Well	7.4	3.2	222	76.3	1.6	3.7	10	2037	3589	[1]nr	[1]nr
St. Martin Tap	8.8	3.3	221	76.1	1.6	3.8	8	2092	3616	[1]nr	[1]nr
Bagby Spring 1A	0.75	0.04	18	22	15.6	0.29	47.6	[3]bdl	64	2.6	0.21
Bagby Side Spring	0.90	0.03	19	22	15.5	0.27	45.5	[3]bdl	67	2.6	0.21
Bagby Spring 2A	0.81	0.12	19	23	15.9	0.32	47.7	[3]bdl	65	2.5	0.20
Bagby Spring 1B	0.67	[1]nd	23	24	15.9	0.29	50.1	[3]bdl	[1]nr	2.6	0.25
Bagby Spring 2B	0.96	[1]nd	23	23	16.9	0.28	48.8	[3]bdl	[1]nr	2.5	0.22

[1]nr: Not reported in study
[2]nd: Below ICP-MS detection limit
[3]bdl: Either below detection limit or interfering peaks in ion chromatography data

Ion chemistry data for well samples WR AAT715 and WR AAT724 (Tenzen wells) plot as Na-Cl waters. Analytical percent recoveries were similar to results from Bagby Hot Springs. WR AAT724 is slightly more dilute than WRAAT715 with lower Na, Ca, and SO_4 concentrations. Concentrations are similar regardless, and this may be attributable to different rates of cooling and sorption between WRAAT715 and WR AAT724. This contrasts with previously collected data by Malkemus, (2016) for Shipherds Hot Springs which plots as Na-mixed anion waters (Figure 11). The Tenzen well waters are similar St. Martins tap samples reported by Malkemus (2016) with respect to temperature, total dissolved solids, pHs, and ion concentrations with the exception of Mg, As, and Br (Tables 4, 5, and 6). Shipherds Hot Springs samples are much more dilute, with ion concentrations approximately an order of magnitude less than the Tenzen and St Martins samples (Tables 4, 5, and 6). The pH of Shipherds Hot Springs (9.10 – 9.40) is also significantly higher than measured at Tenzen and St. Martins (8.18-8.42). Cooler discharge temperatures and lower ion concentrations could be attributed to water mixing along Shipherds fault zone before reaching the surface or cooling and mineral precipitation during lateral of vertical movement of groundwater.

Bagby Hot Springs waters are Na-mixed-anion-type waters while Austin and Breitenbush Hot Springs are distinctly Na-Cl waters (Figure 12). Percent recovery of all analytes for Bagby Hot Springs is 90-110%. Final charge balance errors for July samples (Bagby 1b and 2b) are approximately -8%. This could be due to the speciation of Si to $H_3SiO_4^-$ (increasing the total concentration of negative ions within the system), a measurement error yielding higher pH than actual values, or loss of CO_2 during ascent and discharge.

Water chemistries are consistent between the three springs at Bagby, with an average TDS of 283 mg/kg and a standard deviation of 2.55 mg/kg (<1%) between all samples. The values of total dissolved solids for Bagby Hot Springs are significantly lower than that of Austin or Breitenbush Hot Springs (900 vs ~2500 mg/kg). Measured pH values for Bagby Hot Springs (9.49 to 9.70 at STP) are considerably higher than the circumneutral pH of other hot springs in the region including Austin and Breitenbush Hot Springs (7.0 to 7.4). As is the case in most of these systems, there are no discernable seasonal differences in the ion chemistry of Bagby Hot Springs waters based on the margin of cumulative measurement errors. However, the volumetric discharge of Bagby Side Spring was too low in the summer to collect samples or conduct field measurements, suggesting evaporation or mixing with near-surface water.

4.2 Isotope Chemistry

Isotopic values for all thermal waters plot below the local meteoric water lines of Brooks et al. (2012) with the exception of Bagby Hot Springs (Figure 14). Results for δD and $\delta^{18}O$ are relative to Vienna Mean Standard Ocean Water (VSMOW). δD results have an error of between ±0.02 and 0.04‰, and $\delta^{18}O$ results have an error of between ±0.03 and 0.11‰ for both collection dates. δD values from Bagby Hot Springs vary slightly between collection dates with a mean of -88.60‰ and a standard deviation of 0.22‰, with higher values in July samples (-88.44 vs. -88.77‰). $\delta^{18}O$ values vary by 0.79‰ between October and June collection dates, with a mean of -13.06‰ and higher values in July samples (-12.66 vs. -13.44‰). The margin of δD error for at least one Bagby sample (Bagby 1b) overlaps the local meteoric water line. The closest point to Bagby Hot

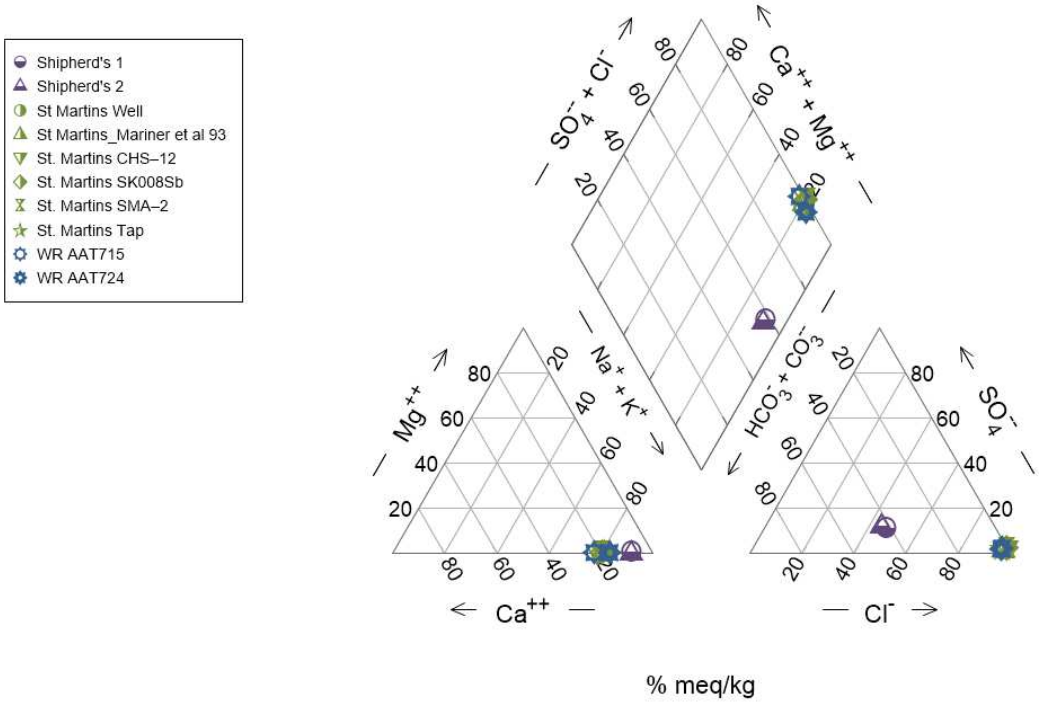

Figure 11. Piper diagram of thermal waters from Wind River.

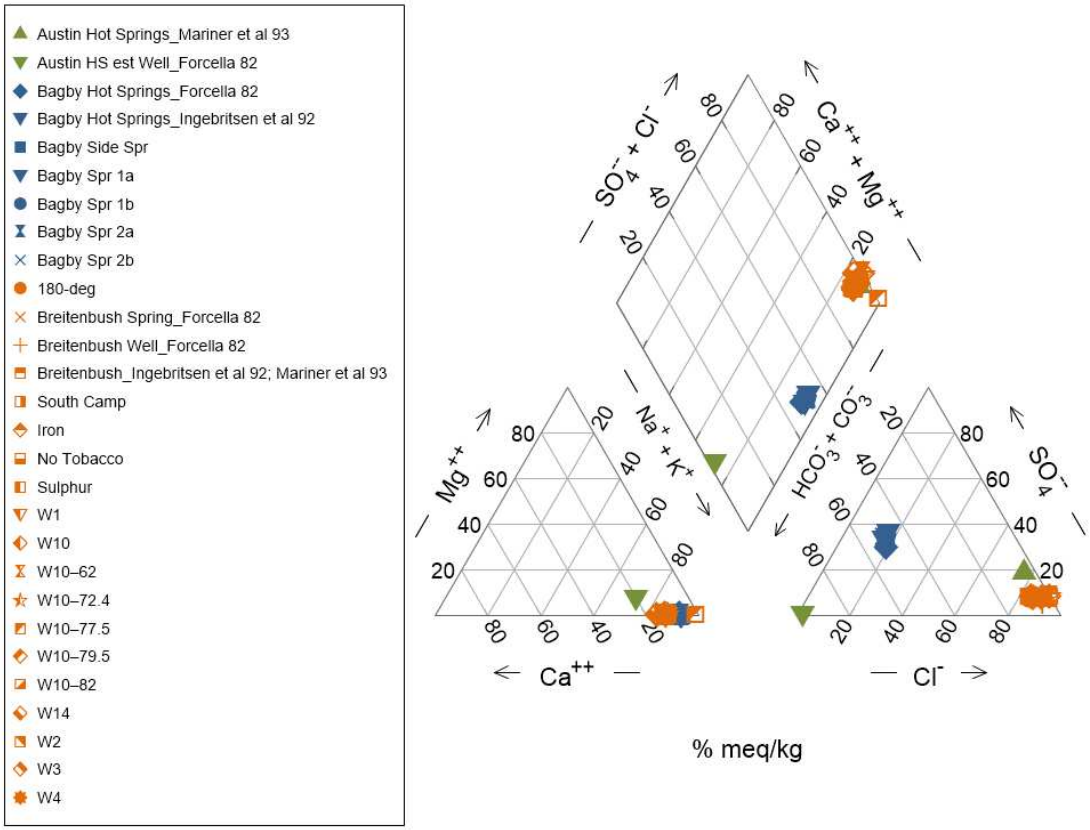

Figure 12. Piper diagram of thermal waters from the north-central Oregon Western Cascades.

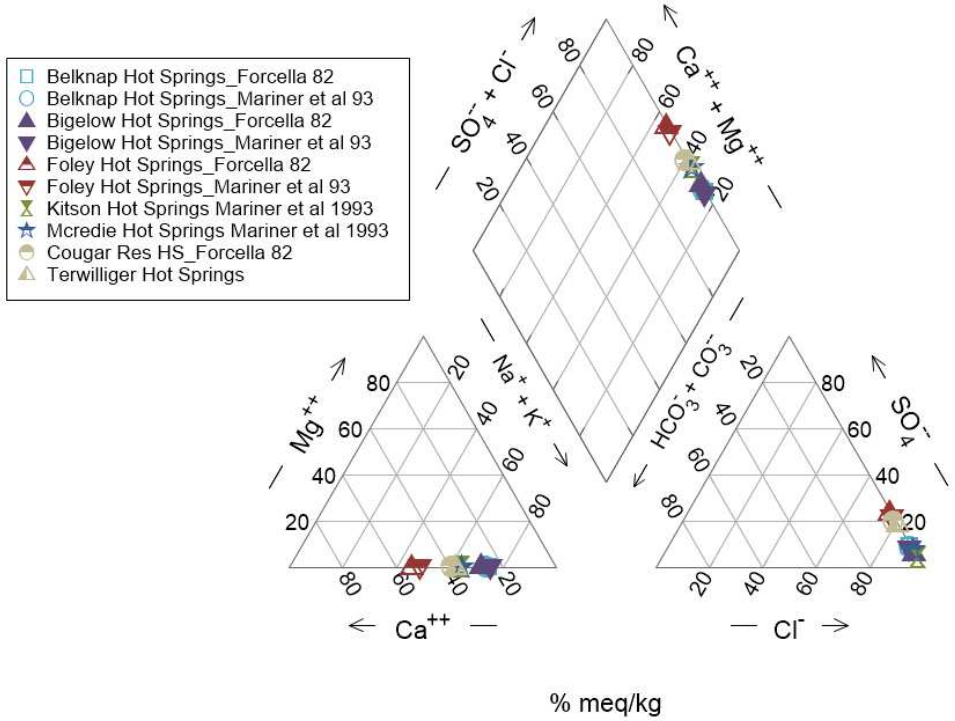

Figure 13. Piper diagram of the southern group of springs in the central Oregon Western Cascades

Springs on the LMWL when intersected with the trendline of Bagby Hot Spring samples is (-12.41‰, -88.24‰), which is 0.20‰ less than the $\delta^{18}O$ and 0.04‰ greater than the δD values of Bagby 1b (Figure 14). The isotopic values for WR AAT715 and AAT724 (Tenzen Wells) are consistent, with means of -91.42 ±0.13‰ and -12.32 ±0.012‰ for δD and $\delta^{18}O$ values, respectively. Tenzen well sample data do not cluster with Shipherds or St. Martins Hot Springs, though values appear to fall on a trendline with St. Martins data (Figure 14).

Estimated recharge elevations of Bagby Hot Springs and the Wind River wells were calculated using the isotopic lapse-rate models of James, 2000 and Brooks et al., 2012 (Figure 15). Bagby Hot Springs recharges between 832 and 880 meters using δD values and methods by James (2000) and between 1612 and 1643 meters based on the model by Brooks et al. (2012). Using the same models and $\delta^{18}O$ values for each system, Bagby Hot Springs recharges between 953 and 1425 (James, 2000) and between 1630 and 1934 meters. The model of Brooks et al. (2012) is more suitable for Bagby Hot Springs based on its proximity to the Willamette Valley study area, as the James (2000) study area lies in the high eastern side of the Cascades. However, this still leaves a ~300-meter difference in the spread between the δD calculated elevation and the $\delta^{18}O$ calculated elevation. The discrepancies between a) larger standard deviations in $\delta^{18}O$ values between autumn and summer and b) differences in recharge elevations using the same elevation model warrant collecting duplicate samples for Bagby Hot Springs in autumn and summer to rule out physical processes that would cause this variation.

Table 7. Isotope chemistry of select thermal waters along the Western Cascades

Sample	δD (‰)	$\delta^{18}O$(‰)	Source	Date
Bagby				
Bagby 1	-88.69	-13.47	This Study	10/17/2020
Bagby 1 (Repeat)	-88.21	-12.61	This Study	7/1/2019
Bagby 2	-88.86	-13.42	This Study	10/17/2020
Bagby 2 (Repeat)	-88.49	-12.70	This Study	7/1/2019
Bagby Side Springs	-88.74	-13.08	This Study	10/17/2020
Breitenbush				
W1	-96.65	-12.59	Malkemus et al., 2017	11/19/2014
W2	-98.08	-12.83	Malkemus et al., 2017	2/21/2015
W3	-96.08	-12.61	Malkemus et al., 2017	11/19/2014
W4	-97.05	-12.60	Malkemus et al., 2017	11/19/2014
W10	-96.96	-12.77	Malkemus et al., 2017	10/7/2014
W14	-98.27	-12.76	Malkemus et al., 2017	10/7/2014
W10-62	-97.42	-12.26	Malkemus et al., 2017	6/30/2015
W10-82	-96.74	-12.58	Malkemus et al., 2017	6/30/2015
180 degree	-93.59	-11.81	Malkemus et al., 2017	11/19/2014
Iron	-95.63	-12.52	Malkemus et al., 2017	11/19/2014
No Tobacco	-94.96	-12.39	Malkemus et al., 2017	11/19/2014
Sulphur	-96.39	-12.91	Malkemus et al., 2017	11/19/2014
South Camp	-94.82	-12.07	Malkemus et al., 2017	6/30/2105
Austin				
Austin Hot Springs	-93	-11.9	Mariner et al., 1993	1972
Wind River				
WR AAT715	-91.29	-12.31	This Study	12/4/2018
WR AAT724	-91.55	-12.33	This Study	12/4/2018
St. Martins Tap	-88.61	-11.55	Malkemus, 2016	11/16/2015
St Martins Well	-88.751	-11.8	Malkemus, 2016	11/16/2015
St Martins CHS-12	-95.10	-11.47	Czajkowski et al., 2013	8/8/2012
Shipherds 1	-84.818	-11.88	Malkemus, 2016	11/16/2015
Shipherds 2	-84.80	-11.73	Malkemus, 2016	11/16/2015
Shipherds-12	-86.30	-11.82	Czajkowski et al., 2013	8/27/2012

Other Isotopes of Bagby Hot Springs (This Study)	$\delta^{18}O$-SO_4 (‰)	$\delta^{34}S$-SO_4 (‰)	$\delta^{11}B$ (‰)	$\delta^{7}Li$ (‰)
Bagby 1	5.39	9.17	-4.8	2.47
Bagby 1 Repeat	5.14	9.15	na	2.71

Though Wind River Valley is not located in the study area for Brooks et al. (2000), these elevation models were used for Tenzen wells as no isotopic lapse models were found for the Columbia River Gorge area. The calculated recharge for thermal waters at Tenzen wells is 1155 meters using the δD elevation model and 1520-1530 meters using the $\delta^{18}O$ elevation model.

A trendline for Wind River Valley thermal waters was created using the values determined for the Tenzen wells and previously determined values for Martins Hot Spring. The R^2 value for this trendline is 0.9459. The intersection of this line produces a δD value of -94.82 and a $\delta^{18}O$ value of -13.28. When applying the elevation models from Brooks et al. (2012) to this point, the calculated recharge for thermal waters at Wind River Valley is between 1870 ($\delta^{18}O$) and 1930 (δD) meters (Figure 15).

Trendlines of isotope data from the Wind River Valley and from Breitenbush and Austin wells and springs are highlighted in Figure 16. These trendlines were used to calculate isotope ratios that match the LMWL in order to determine elevation. Though the $\delta^{18}O$ and δD trendline for Breitenbush-Austin and Wind River systems mimic evaporative effects on geothermal waters, their respective δD /$\delta^{18}O$ slopes of 3.20 and3.65 are shallower than that of typical evaporative trends of between 4 and 7 (Clark, 2015). An evaporative trend should also produce increasing chloride concentrations; however, a plot of chloride concentrations vs. δD values for the St Martins and Tenzen wells yields a negative correlation (Figure 17). When extrapolated, the δD /$\delta^{18}O$ trendline of St. Martins and Tenzen wells intersects with the andesitic water ratio of $\delta^{18}O = 10$ ±2‰ and δD = -20 ±10‰ proposed by Giggenbach (1992). This ratio is exclusive to

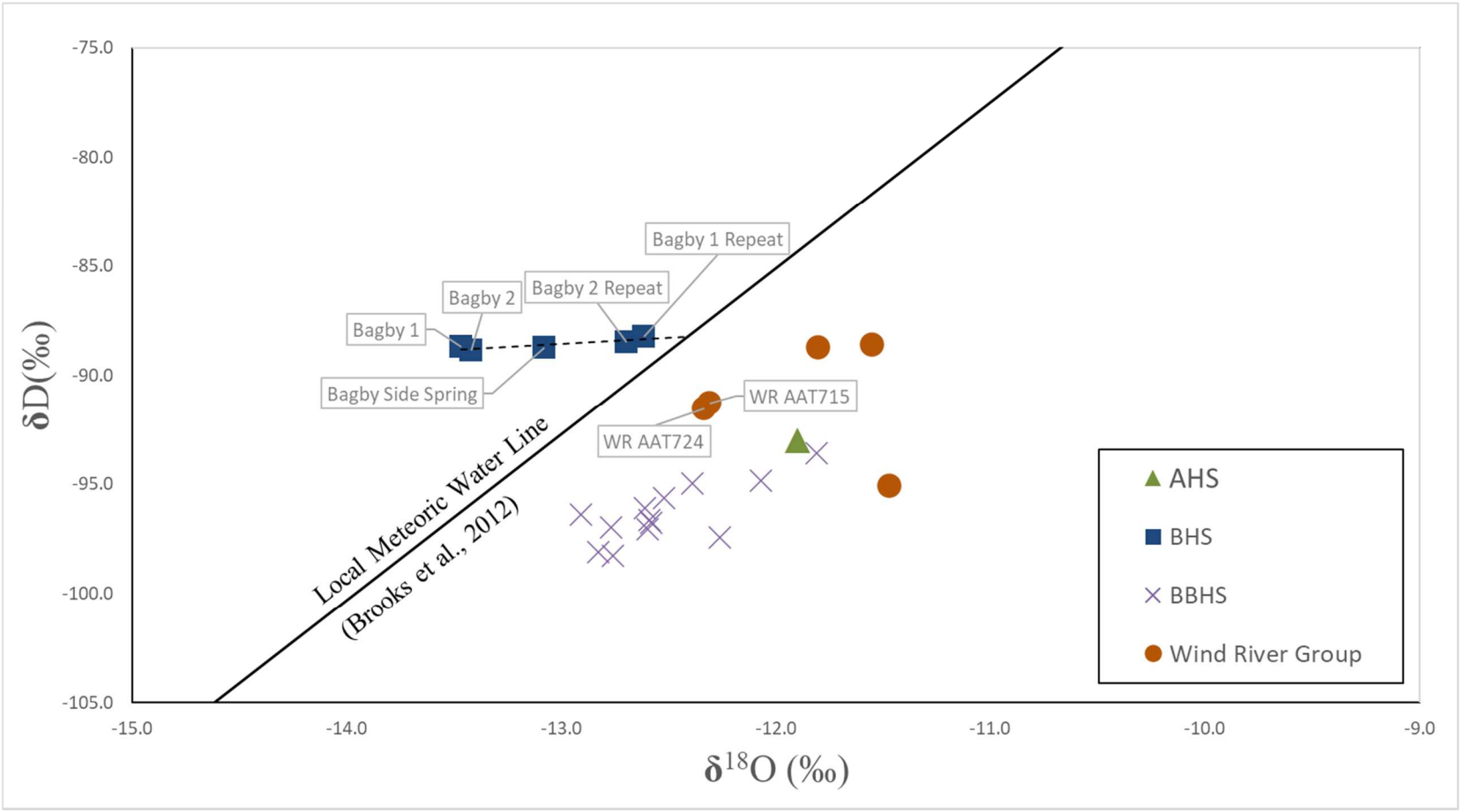

Figure 14. δD and $\delta^{18}O$ values relative to the Local Meteoric Water Line by Brooks et al. (2012)

waters from geothermal and volcanic systems along convergent plate boundaries in the Pacific Northwest. While typical $\delta^{18}O$ values for magma and solid rocks lie between 5 and 10‰, ratios for most other "magmatic waters" fall in the range of $\delta^{18}O = 7 \pm 2‰$ and $\delta D = -65 \pm 2‰$ (Taylor, 1974; Dilles et al., 1992; Bindeman, 2008). These "magmatic waters" are waters that have originated from primary magmas not modified by fractional crystallization or assimilation. High-$\delta^{18}O$ magmas are hypothesized to have exchanged with—or derived from—high-$\delta^{18}O$ metasedimentary silicate rock (Bindeman, 2008). These rocks crystallize from or exchange with seawater at surface temperatures. Alternatively, low- $\delta^{18}O$ represent remelting or exchange with hydrothermally altered rocks that have been heated by meteoric waters. This would be reflected by lower $\delta^{18}O$ waters in the hot spring systems. However, trendlines produced from these data extrapolate out to ratios of high-$\delta^{18}O$ andesitic magma values (Giggenbach, 1992). Therefore, it is more likely that there is an "andesitic water" component in these hot springs that is produced from recycled seawater in magmas related to subduction processes (Giggenbach, 1992). δD and $\delta^{18}O$ data suggest that meteoric waters in both areas have mixed with andesitic seawater from the subducted slab at depth. Breitenbush and Austin Hot Spring waters have $\delta D/\delta^{18}O$ ratios indicating 4 to 8% mixing with andesitic water (R. Perkins, personal communication, 2018*)*. St. Martins and Tenzen wells have a similar mixing ratio of between 4.2% and 8.5%.

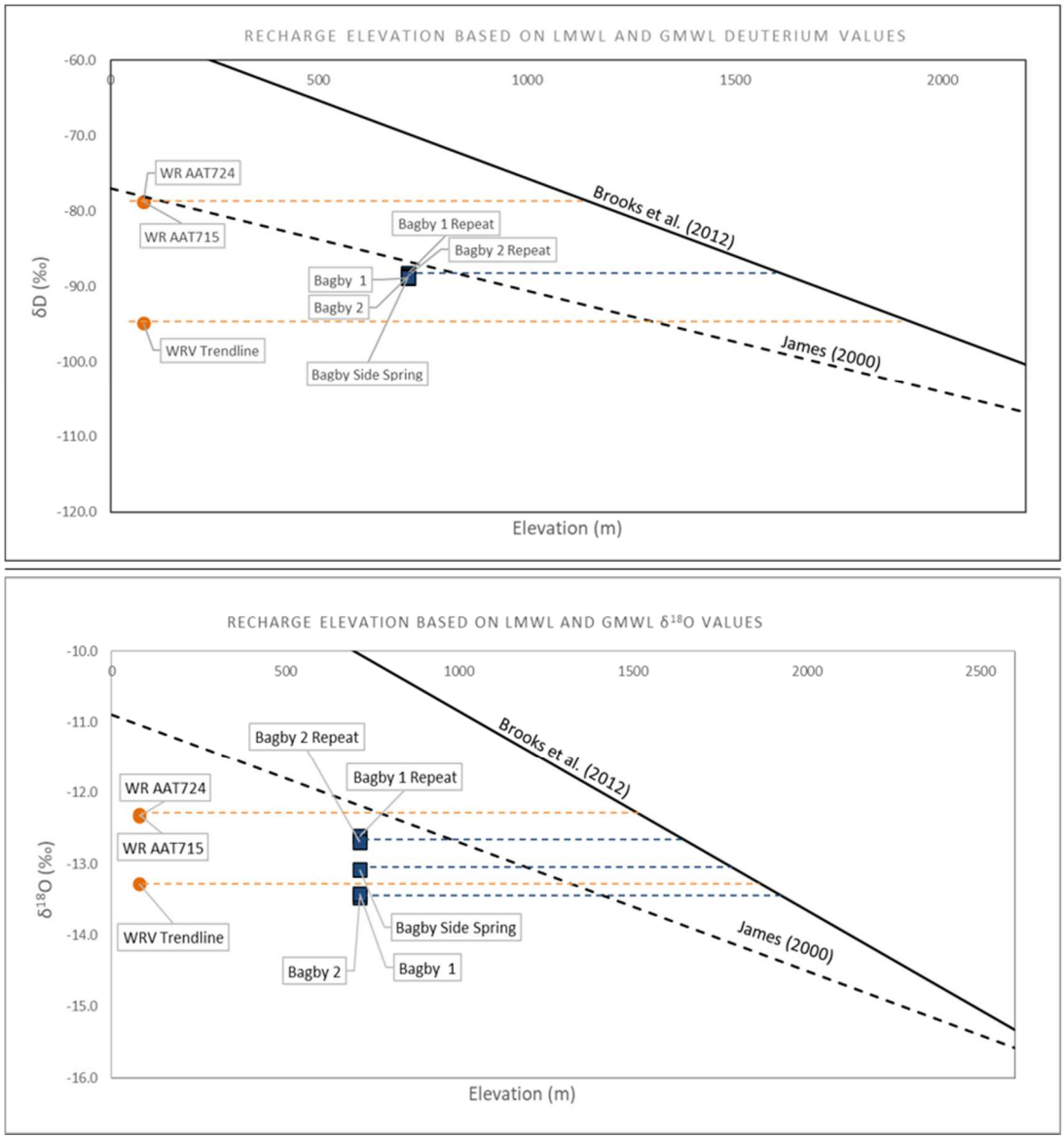

Figure 15. Recharge elevations of Tenzen Wells and Bagby Hot Springs based on GMWL recharge elevations (James, 2000) and LMWL recharge elevations (Brooks et al., 2012). The model from James (2000) applies to near-crest recharge for groundwater on the east side of the Cascades. The model from Brooks et al. (2012) applies to surface waters in the Willamette Valley. "WRV trendline" was calculated from the intersection of the trendline in Figure 16 (bottom left).

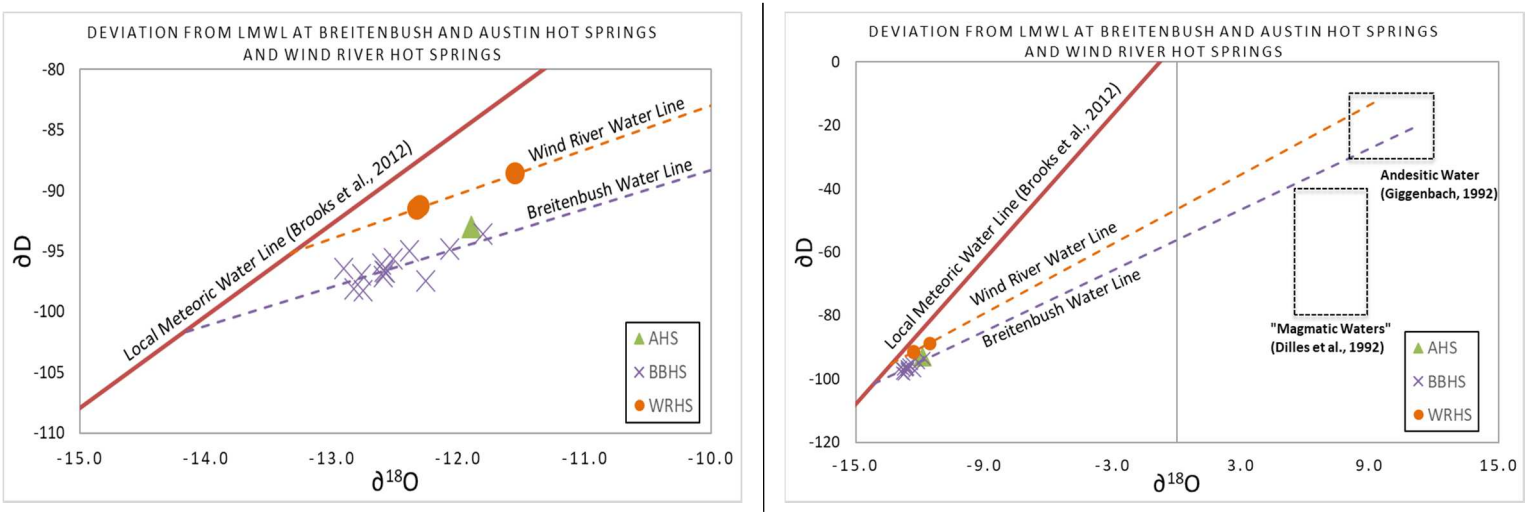

Figure 16. Water lines of Wind River and Breitenbush/Austin. The graph on the right project trendlines from the graph on the left. Boxes indicate andesitic water values from Giggenbach, 1992. R^2 for the Wind River series is 0.9459.

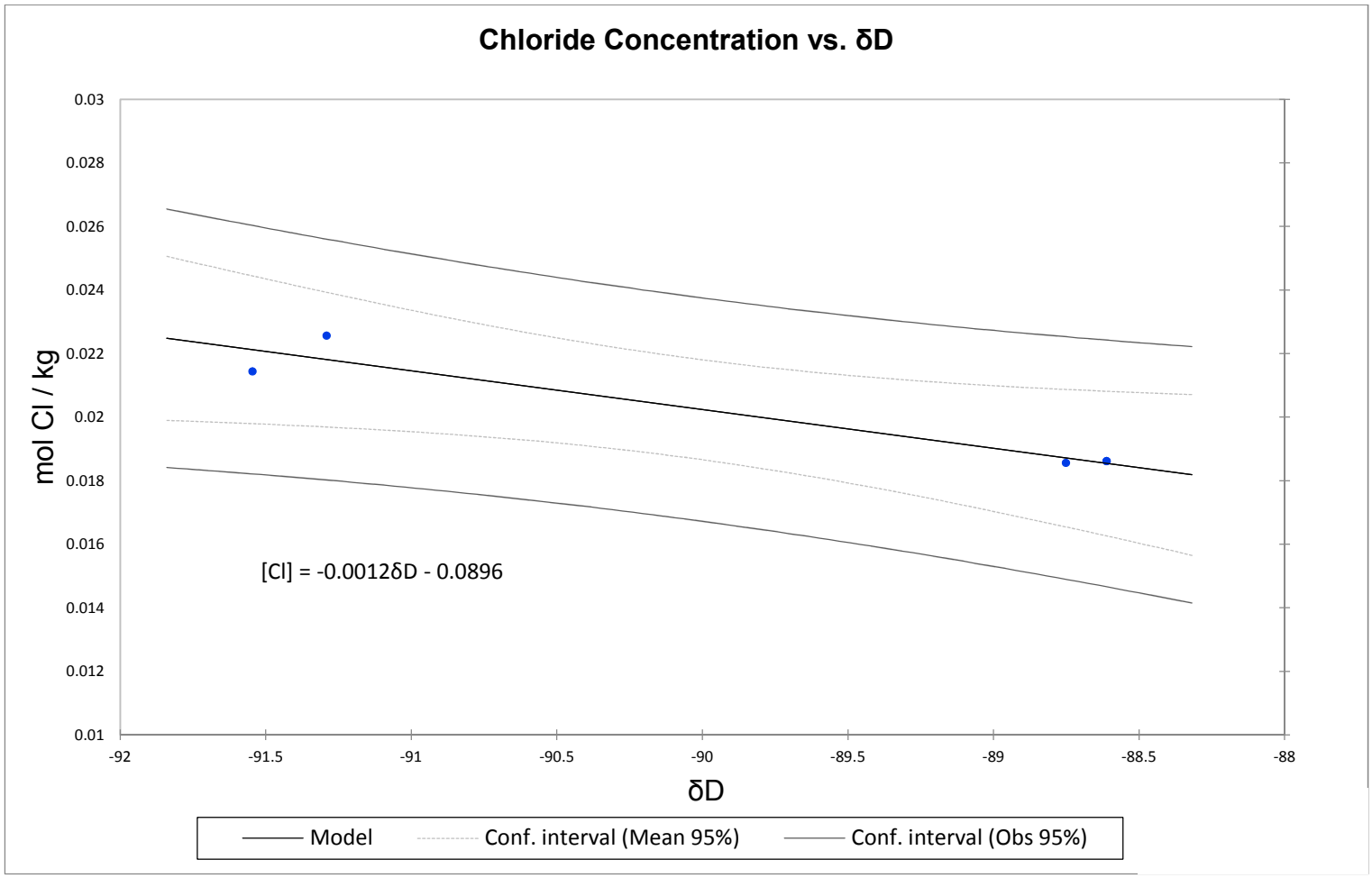

Figure 17. Chloride concentrations between St. Martins (left) and Tenzen wells (right). Decreasing chloride concentrations with decreasing δD values suggest the cause of a shallow meteoric water line at Wind River is not evaporative.

Therefore, it is more likely that there is an "andesitic water" component in these hot springs that is produced from recycled seawater in magmas related to subduction processes (Giggenbach, 1992). δD and $\delta^{18}O$ data suggest that meteoric waters in both areas have mixed with andesitic seawater from the subducted slab at depth. Breitenbush and Austin Hot Spring waters have $\delta D/\delta^{18}O$ ratios indicating 4 to 8% mixing with andesitic water (Malkemus et al., 2017*)*. St. Martins and Tenzen wells have a similar mixing ratio of between 4.2% and 8.5%.

$\delta^{11}B$

Bagby 1 spring has a $\delta^{11}B$ value of -4.8‰ relative to the National Institute of Standards and Technology (NIST) SRM 951(a). This ratio is consistent with subaerial geothermal fluids of Yellowstone (-6.7 to +3.1‰) and closely matches the $\delta^{11}B$ values (-5.9 to -3.6‰) of calcite springs and higher pH (7.9 – 8.2) springs in the Yellowstone hydrothermal system (Palmer and Sturchio, 1990; Palmer, 1991). Similar $\delta^{11}B$ values are sourced from rhyolites and volcanic tuffs. The $\delta^{11}B$ values of altered and fresh rhyolites (-9.7 to -5.2‰) and volcanic tuffs (-9.5 to -4.9‰) are closest to the value of -4.8‰ obtained from Bagby Hot Springs. Island- and back-arc settings are enriched in ^{11}B (-2.3 to +14.2‰; Spivack, 1986; Palmer, 1991; Ishikawa and Nakamura, 1994).

A rhyolitic and tuffaceous ^{11}B signature for Bagby Hot Springs waters is consistent with their circulation through the silica-rich tuff of the Breitenbush Fm. Fresh Mid Ocean Ridge Basalt (MORB) is considerably more depleted in ^{11}B than the continental host rock of Bagby Hot Springs, though the ratios at Bagby more closely coincide with median $\delta^{11}B$ of MORB (Figure 18; Barth, 1993). A shift towards

isotopically light boron was observed in Icelandic rhyolites that have formed from—or have assimilated—fluid-altered crust; this phenomenon was observed in subaerial alteration by meteoric water and not in seawater-altered crust (Marschall, 2018). Comparable ^{11}B data must be obtained at Breitenbush and Austin Hot Springs before a definitive case can be made for the influence of andesitic water on boron concentrations of these system.

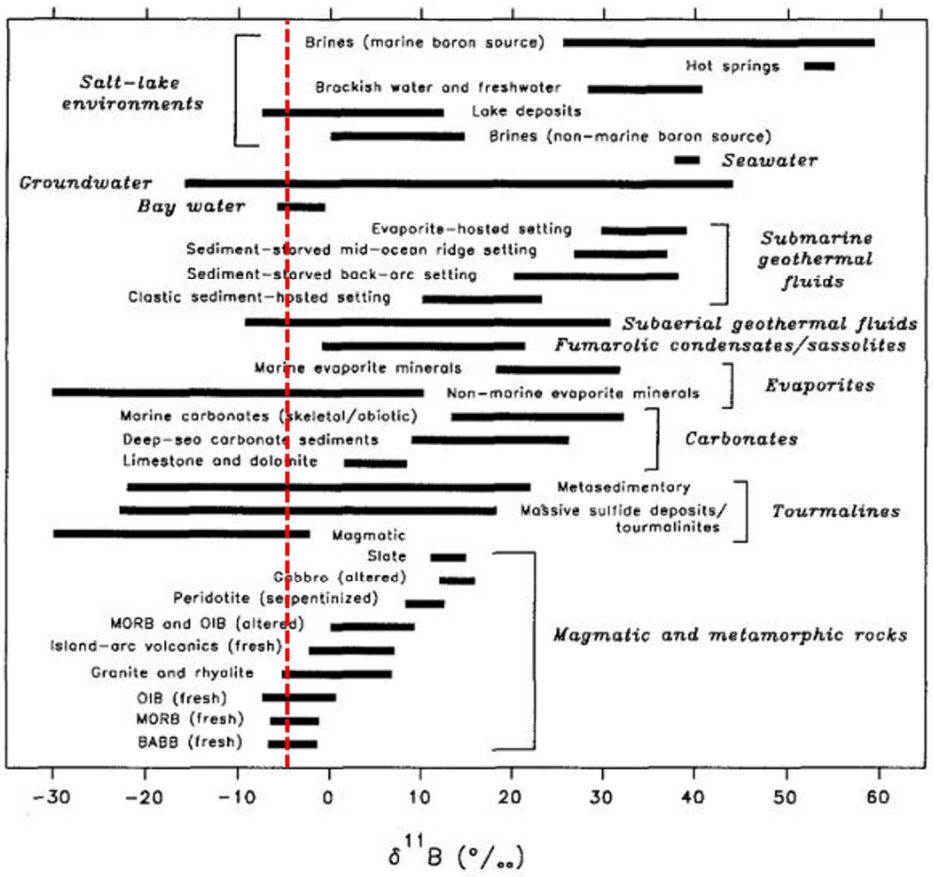

Figure 18. $\delta^{11}B$ of Bagby superimposed on ranged of $\delta^{11}B$ from geologic and hydrologic sources from Barth (1993). Boron may be undergoing increased rate of fractionation due to the low temperature of its Reservoir water (Barth, 1993).

$\delta^{18}O\text{-}SO_4$ and $\delta^{34}S\text{-}SO_4$

$\delta^{34}S$ values are relative to the Vienna-Canyon Diablo Troilite (VCDT) and $\delta^{18}O$ are relative to VSMOW. Bagby Hot Springs has an average $\delta^{18}O\text{-}SO_4$ value of 5.27‰ with a standard deviation of 0.13‰, and an average $\delta^{34}S$-SO4 value of 9.16‰ with a standard deviation of 0.01‰. When plotting $\delta^{18}O\text{-}SO_4$ vs. $\delta^{34}S\text{-}SO_4$, Bagby Hot Springs falls outside of the seawater and atmospheric sulfate ratios of Möller et al. (2006). This is not indicative of mixing between the two sources, as the thermal waters in this study were highly saline and/or largely carbonate controlled. A more telling analog is the Spring BC-1 collected from the Rocky Mountain Trench in south-eastern British Columbia. Not only are $\delta^{34}S\text{-}SO_4$ ratios similar (8.9 and 9.16‰), but the water chemistry of the site is comparable to Bagby Hot Springs as well (Allen et al., 2006). BC-1 is considered a "Na-Ca-HCO_3-SO_4" type water based on its ion concentrations with respect to Stiff diagrams and has a calculated reservoir temperature of 32.5°C using chalcedony and Na-K-Ca geothermometers. BC 1 host rock is presumed to be cretaceous granite, and discharges from Hall Lake Fault, similar to the structural setting and proposed silicic host rock for Bagby Hot Springs.

Mariner et al. (1993) provide a list of $\delta^{18}O\text{-}SO_4$ data for various hot springs along the Cascades including Breitenbush and Austin Hot Springs. When plotting $\delta^{18}O\text{-}SO_4$ values against δD values, distinct groupings are observed for Austin and Breitenbush, the more southerly "central springs" (Terwilliger, Belknap, Foley, Bigelow, McCredie), and Bagby Hot Springs (Figure 19). A more prominent trendline is discernable for sulfate

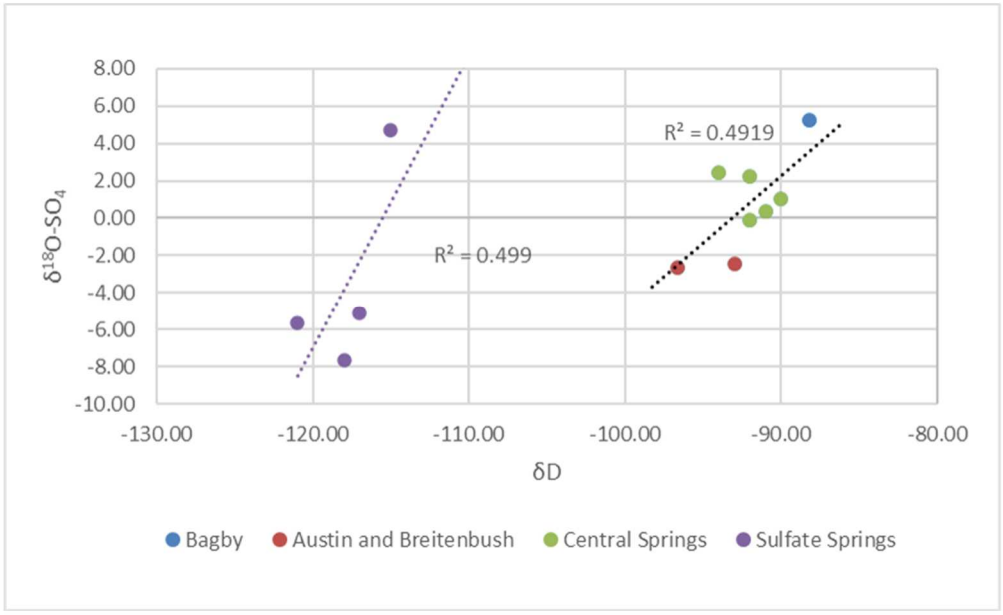

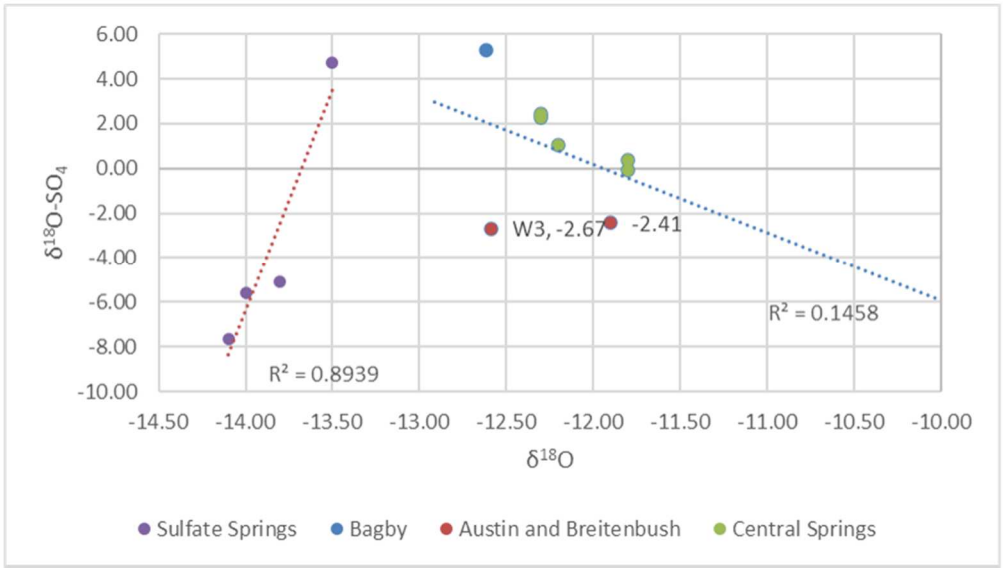

Figure 19. $\delta^{18}O$-SO_4 vs. δD (top) and $\delta^{18}O$ (bottom). Data for all points but Bagby are from Ingebritsen et al. (2013). "Sulfate Springs" are Na-SO_4 springs of the Modoc Plateau, northern CA. "Central Springs" encompass the group of hot springs in the central Oregon Cascades (Figure 14).

springs of California when considering $\delta^{18}O\text{-}SO_4$ vs. $\delta^{18}O$ (Mariner et al., 1993), while the trendline for the north-central Cascade springs is less significant (Figure 19).

$\delta^{34}S\text{-}SO_4$ can be used to trace inter-aquifer mixing, but $\delta^{34}S\text{-}SO_4$ values are only reported for Bagby Hot Springs (9.16‰) in this study (Dogramaci et al., 2001). With more data for other north-central Cascade springs (Breitenbush, Austin, central Oregon Cascade hot springs), inter-aquifer mixing and sulfate sources/reductions can be determined using $\delta^{34}S\text{-}SO_4$ vs. SO_4/Cl plots. Inclusion of $\delta^{34}S\text{-}SO_4$ data from Austin and Breitenbush Hot Springs could also constrain mineralogic controls on $\delta^{34}S\text{-}SO_4$. Pyrite and chalcopyrite in the Cascades are more enriched in $\delta^{34}S$ (pyrite: 2.3‰, chalcopyrite: 2.4‰) than other sulfide minerals (galena: -0.3‰, sphalerite: 1.4‰).

$\delta^{7}Li$

$\delta^{7}Li$ values are relative to the LSVEC lithium carbonate standard. Bagby 1 Springs has an average $\delta^{7}Li$ value of 2.59‰ and a standard deviation of 0.12‰. Isotope geothermometry methods from Millot and Negrel (2007) yield temperatures above 200°C which is higher than expected for this system (Figure 20). $\delta^{7}Li$ results for Bagby Hot Springs are within the expected range of values for hydrothermal systems (-3 to 26‰) and below reported values for submarine hydrothermal and low-temperature groundwater systems (5 to 11‰ and 6 to 29‰; Penniston-Dorland et al., 2017; Millot and Negrel, 2007).

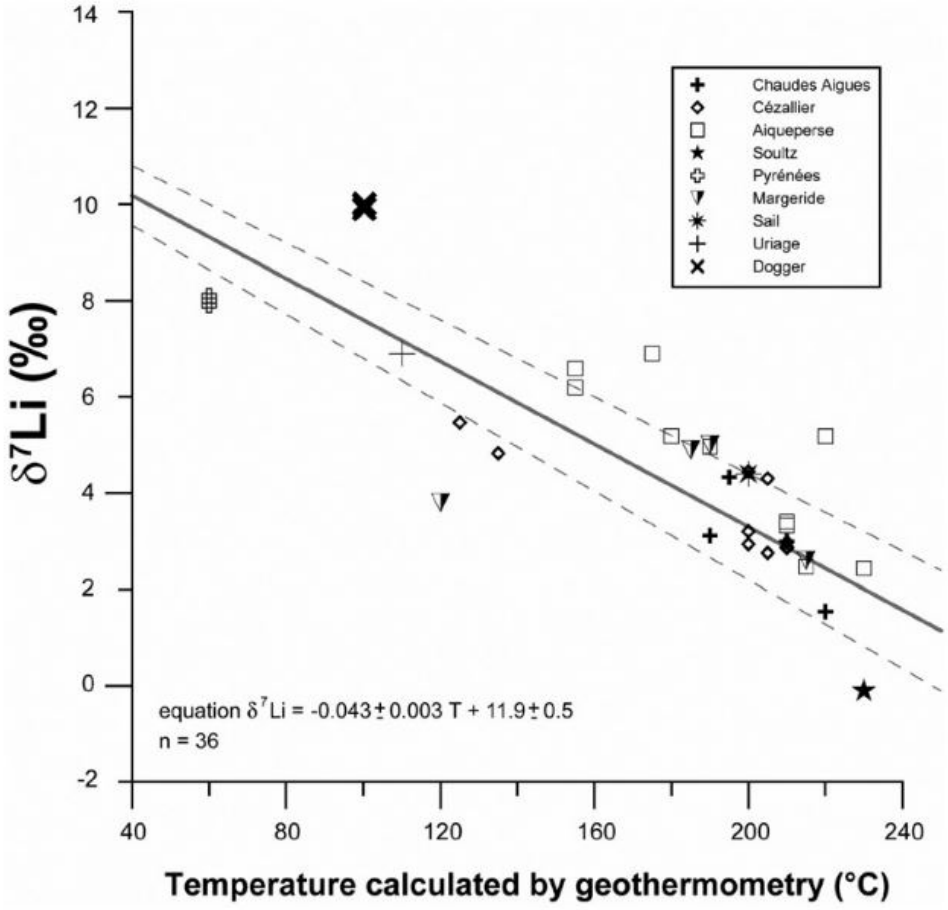

Figure 20. Lithium geothermometer from Millot and Negrel (2007).

4.3 Geothermometry Results

Several classical geothermometers were used to establish a range of possible reservoir temperatures and to better constrain mineral suites for both Bagby and Wind River (Table 8). These temperatures were calculated using only equilibrium temperatures and do not consider the CO_2 fugacity of each system. Sulfate and anhydrite geothermometers suggest a higher temperature of approximately 180°C for Austin Hot Springs, whereas chalcedony and cation geothermometers provide a low endmember of approximately 90°C.

Previous Geothermometers and Reservoir Temperature Calculations

Table 8. Reservoir temperatures in °C previously calculated using different "classical" geothermometers for Bagby and Austin Hot Springs and Wind River wells.

Hot Spring	Alpha Cristobalite[1]	Chalcedony[2]	Na/K[3]	Na/K[4]	K/Mg[5]	Sulfate
Bagby Spring 1A	73	96	86	76	105	81
Bagby Side Spring	73	96	89	78	98	N/A
Bagby Spring 2A	72	95	90	80	111	N/A
WR AAT724 (Tenzen Well 2)	68	90	98	87	143	N/A
WR AAT715 (Tenzen Well 1)	67	89	102	91	144	N/A
Austin Hot Springs*	75	98	112	101	116	186

**Historic data from Mariner et al. 1990; [1]Fournier, 1977; [2]Fournier, 1989; [3]Fournier, 1979; [4]Giggenbach, 1988; [5]Giggenbach, 1986*

Austin Hot Springs

Three chalcedony-based mineral assemblages were used to calculate the reservoir temperature of Austin Hot Springs: 1) chalcedony, heulandite, laumontite, illite; 2) chalcedony, heulandite, laumontite, celadonite; 3) chalcedony, calcite, mordenite-K, illite, albite, clinoptilolite-K, beidellite-Na. All three suites contain minerals identified in both the SUNEDCO-58-28 borehole and in shallow boreholes and microdioritic outcrops near Austin Hot Springs. All suites 1 and 2 contain minerals observed at these sites. The range of temperatures for Austin Hot Springs using these three models lie between 100.1 and 106.5°C (Table 9).

A "no-silica" model for suite 3 was created to compare mineral saturations in the absence of a purely SiO_2 mineral control. In the model that omits chalcedony it is assumed that silica is controlled by clay and zeolite minerals that have formed due to low temperature hydrothermal alteration including mordenite-K, clinoptilolite-K, and beidellite-Na. Both the chalcedony and "no-silica" models have a similar log f(CO_2) of -2.19 and -2.10 respectively, suggesting loss of CO_2 at the surface. The mineral suite includes minerals identified in nearby shallow boreholes and in the SUNEDCO-58 borehole (Keith, 1988; Bargar and Oscarson, 1997; Boden, 1985) illite, calcite, and smectite.

A quartz-based mineral selection (quartz, chlinochlore-14A, phengite, prehnite) for Austin Hot Springs yields a higher reservoir temperature of 128.7°C and log f(CO_2) of -2.15 (Table 9). Though this is a higher temperature than with the chalcedony suite, it still lies far below the previously estimated 186°C using anhydrite and sulfate geothermometers (Ingebritsen et al., 1992). Because Austin Hot Springs discharges at

86°C, α-cristobalite was not considered as a silica controlling mineral for Austin Hot Springs because calculated temperatures were consistently below discharge.

Based on the absolute value of the total number of standard deviations away from equilibrium (n_SD) each mineral suite was, chalcedony-based suites are a better fit for determining reservoir temperatures at Austin Hot Springs (Table 9, Figure 21). Furthermore, using minerals observed at the site yielded greater n_SD values for quartz suites. The lowest n_SD value was obtained using minerals commonly found in medium temperature geothermal systems (Palmer et al., 2014).

Aluminum concentrations for Austin Hot Springs were calculated via equilibrium with K-feldspar, albite, or illite, or assumed to be approximately 1.0 μmol/kg. The average calculated aluminum concentration using the three minerals was 68.4 μg/L with a standard deviation of 10.8 μg/L. K-feldspar, albite, and illite saturation indices were -0.1478, -0.2890, and -1.0103 respectively when equilibrium is assumed with chalcedony, heulandite, celadonite, and laumontite. Despite the deviation in modeled aluminum concentrations, calculated reservoir temperatures are between 100.1 and 106.5°C.

CO_2 fugacity was calculated using three methods: optimizing CO_2 fugacity in RTEst (-2.19), allowing calcite to precipitate (-2.17), and adding or removing CO_2 until calcite is at equilibrium at discharge temperature (-2.62). Changing CO_2 fugacity had an impact on the overall mineral suite selected, but reservoir temperatures remained between 100.1 and 106.5 °C (Table 9).

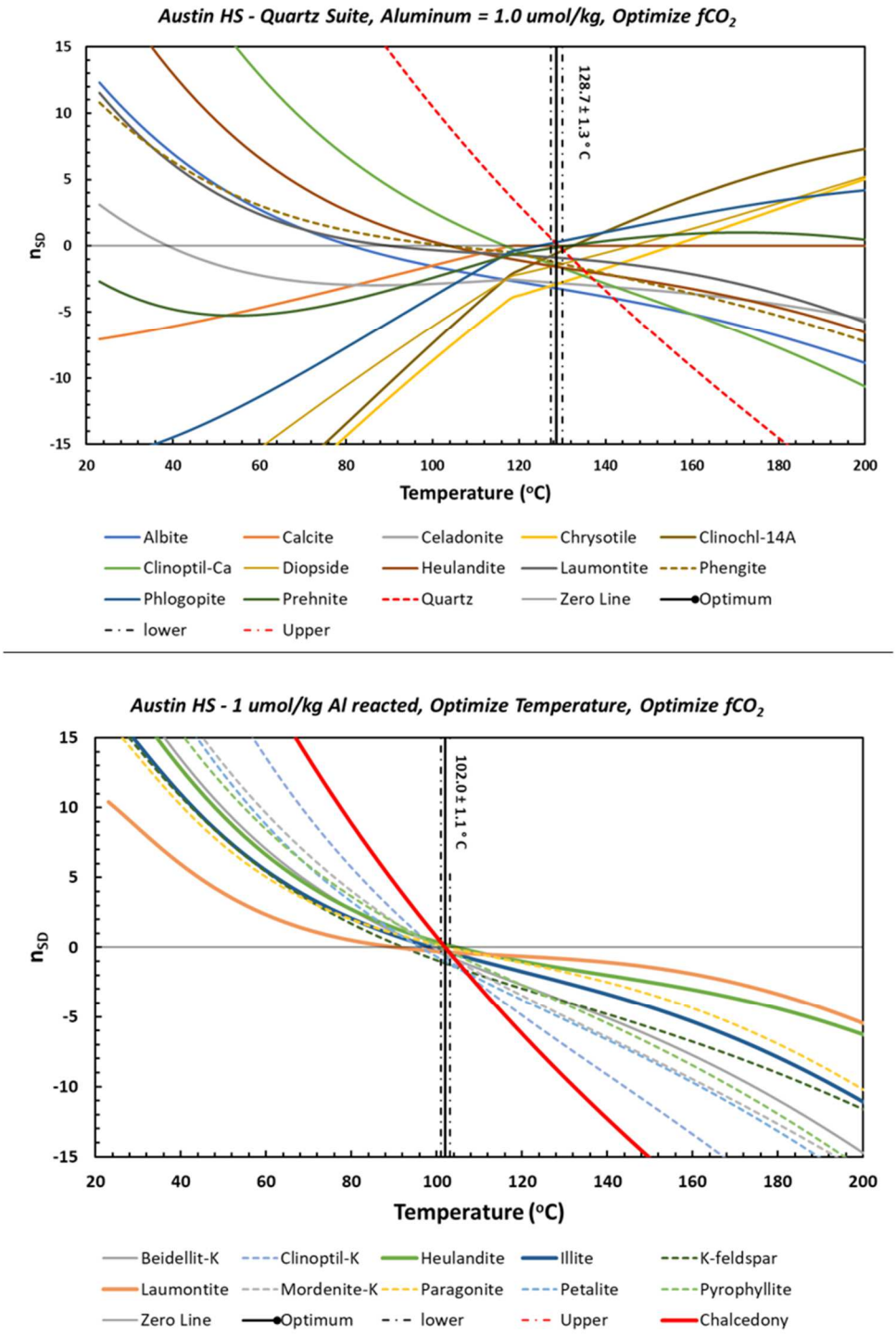

Figure 21. Comparison between "Suite 1" (chalcedony, illite, laumontite, heulandite) and the best-fit quartz suite (quartz, clinochlore-14A, phengite, prehnite).

Table 9. Chalcedony models for Austin Hot Springs. Mineral suites were selected based on borehole mineralogy of SUNEDCO-58 and nearby shallow boreholes (Keith, 1988; Bargar and Oscarson, 1997; Boden, 1985).

Mineral Suite	[Al]	CO2 Control	Temperature	log f(CO2)	mean|nsd|	Calculated pH	Final Al
Chalcedony Heulandite Illite Laumontite	1.0 µmol/kg	Sliding CO2 Fugacity	102.0	-1.682	0.152	6.781	27.01
Chalcedony Heulandite Celadonite Laumontite	1.0 µmol/kg	Sliding CO2 Fugacity	100.1	-2.918	0.135	7.71	31.52
Chalcedony Calcite Mordenite-K Illite Albite Clinoptilolite-K Beidellite-Na	K-Feldspar	Sliding CO2 Fugacity	106.5	-2.19	0.674	7.262	68.6
Quartz Clinochlore-14A Phengite Prehnite	1.0 µmol/kg	Sliding CO2 Fugacity	128.7	-2.15	0.201	7.291	27.0

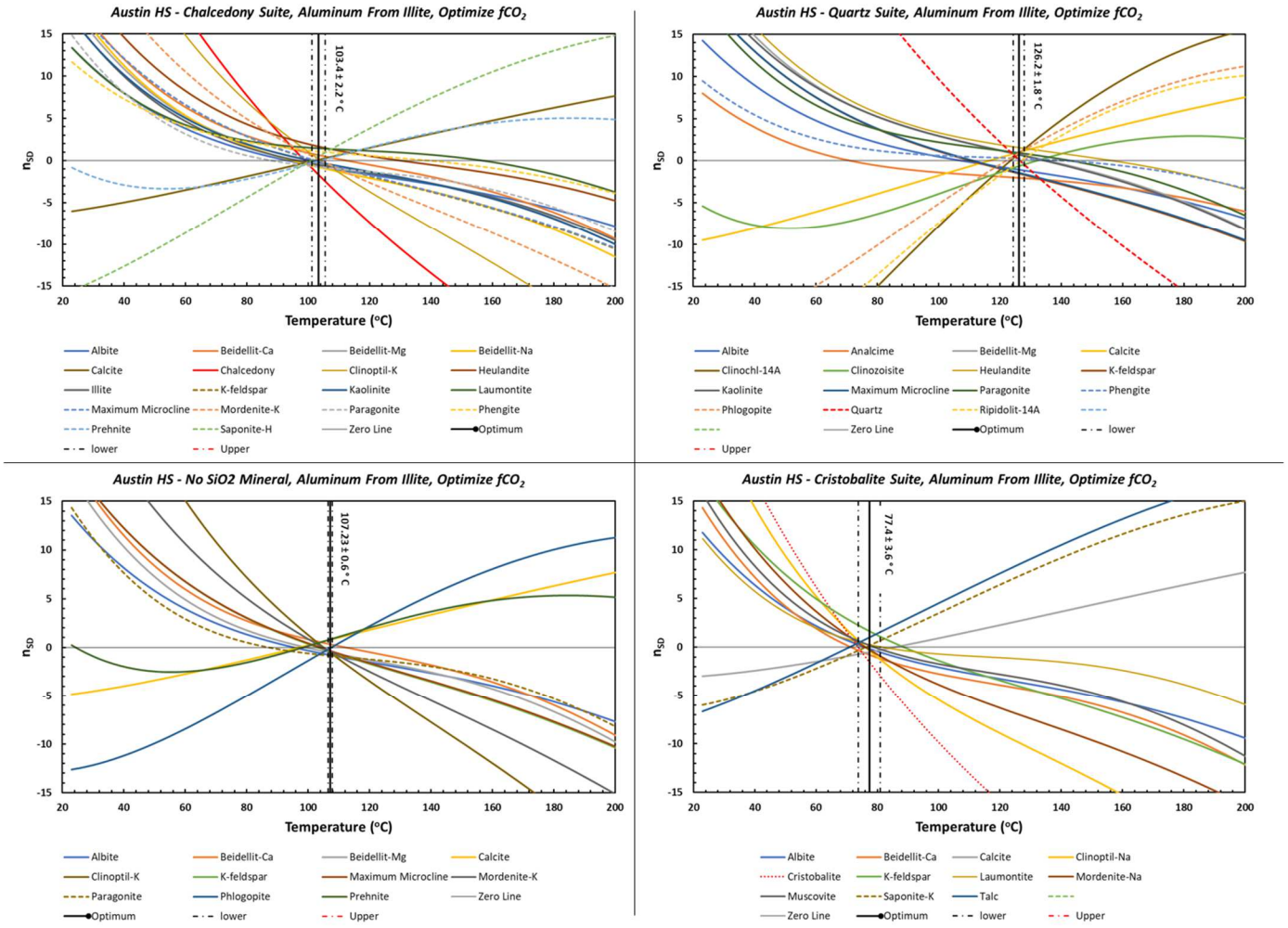

Figure 22. Comparison of silica controlling minerals for Austin Hot Springs. Silica controlling minerals outlined in red.

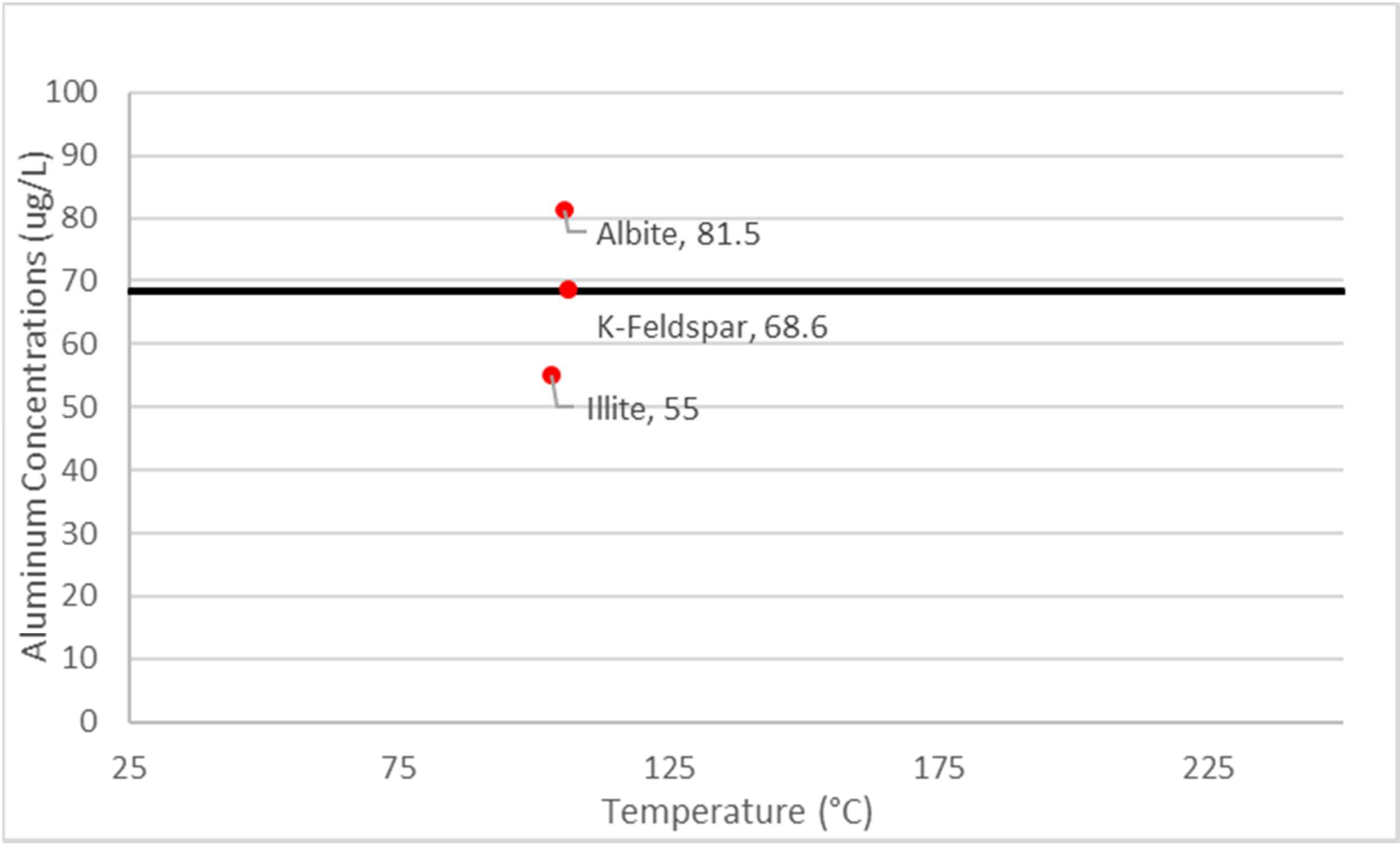

Figure 23. Calculated aluminum concentrations for Austin Hot Springs using different aluminum-bearing minerals. Black line represents average aluminum concentrations of albite, K-feldspar, and illite.

Bagby Hot Springs

Chalcedony- and cristobalite-based mineral assemblages were used to calculate the reservoir temperature of Austin Hot Springs. Low alteration temperature clay and zeolite minerals were considered in both models, particularly heulandite and laumontite. Models using both cristobalite and chalcedony were made due to the presumed low reservoir temperature (<100 °C) of Bagby Hot Springs. Cristobalite and chalcedony geothermometers are optimal for reservoir temperatures below 150°C (Fournier, 1977).

A mineral suite consisting of cristobalite, calcite, albite, and laumontite yields a reservoir temperature of 65.3°C and a log f(CO_2) of -2.77 at this temperature. These minerals were selected based on surface mineralogy reported by Walker el al. (1985) and alteration minerals found in Ca- and Na- silicate alkaline systems (albite and laumontite; Utada, 2001). The average of the absolute value of the number of standard deviations away from equilibrium each mineral (n_SD) for this suite is equal to 0.344.

A chalcedony mineral suite (chalcedony, calcite, clinoptilolite-Ca) indicates a higher reservoir temperature of 93.7°C and log f(CO_2) of -2.19. However, in this model all other minerals are more undersaturated than in the cristobalite model (Figure 24). When a fourth mineral is considered in this model (heulandite), the n_SD value is 0.500. This is higher than the value for the Cristobalite suite (0.344). Clays and zeolites (laumontite, heulandite, kaolinite) are also not as well represented using the chalcedony suite over the cristobalite suite. Though a greater CO_2 fugacity is consistent with outgassing observed at the site, this mineral suite of chalcedony, calcite, and clinoptilolite-Ca overemphasizes equilibrium with calcium and carbonate and neglects other likely clays and zeolites at equilibrium with the system. Using expected equilibrium

minerals such as heulandite, laumontite, and muscovite in conjunction with chalcedony in the model yields a higher objective function and therefore a poorer fit.

Aluminum concentrations for Bagby Hot Springs were both measured and calculated via equilibrium with K-feldspar, albite, heulandite, or illite. The measured aluminum concentration at Bagby 1 is 50.13 μg L^{-1}. Modeled aluminum concentrations ranged from lows of 27.24 (K-feldspar) and 101.8 (heulandite) μg L^{-1} to much higher values of 409.6 (albite) and 591.1 (illite) μg L^{-1}. Temperature ranges using the cristobalite suite remained narrow (67.2 to 73.5 °C) despite large deviations in modeled aluminum concentrations. Saturation indices of aluminum minerals at the calculated reservoir temperature using the cristobalite suite were: K-feldspar = 0.2227, Albite = -0.1046, Illite = -0.8373, Heulandite = 0.8204. The K-feldspar aluminum model correlated best with measured values (27.24 vs. 50.13 μg/L) and yielded a temperature of 69.8°C. Log f(CO_2) ranged from -1.68 ([Al] from illite) to -2.77 ([Al] from albite).

CO_2 fugacity was calculated using the same methods for Austin Hot Springs. Optimizing the CO_2 fugacity in RTEst yielded a log f(CO_2) of -2.77. Adding CO_2 yielded a similar result of -2.96. Allowing calcite to precipitate yielded a CO_2 fugacity far above atmospheric at all temperatures as calcite was oversaturated at all temperatures.

Table 10. Calculated aluminum concentrations using aluminum-bearing minerals and resulting temperature and f(CO_2) for Bagby Hot Springs

[Al]	Mineral Suite	Al (µg/L)	Temperature (°C)	log f(CO2)
Measured	Cristobalite Beidellite-Mg K-Feldspar Heulandite	50.13	68.2	-2.35
Heulandite	Cristobalite Beidellite-Mg K-Feldspar Heulandite	101.8	67.2	-1.94
K-Feldspar	Cristobalite Beidellite-Mg Albite Heulandite	27.24	69.8	-2.69
Illite	Cristobalite Beidellite-Mg K-Feldspar Heulandite	591.1	71.7	-1.68
Albite	Cristobalite Beidellite-Mg K-Feldspar Heulandite	409.6	73.5	-2.77

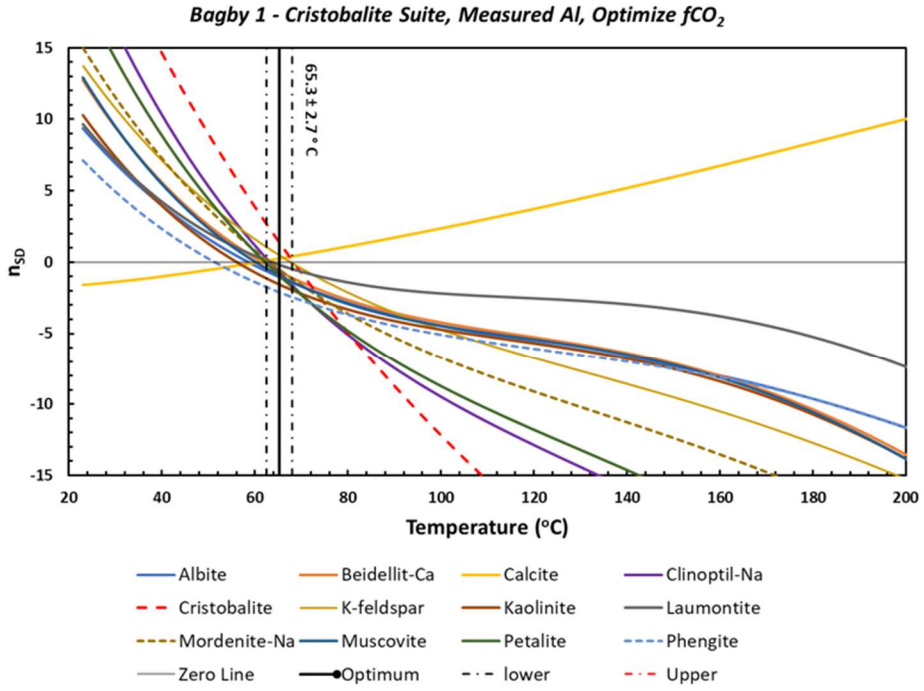

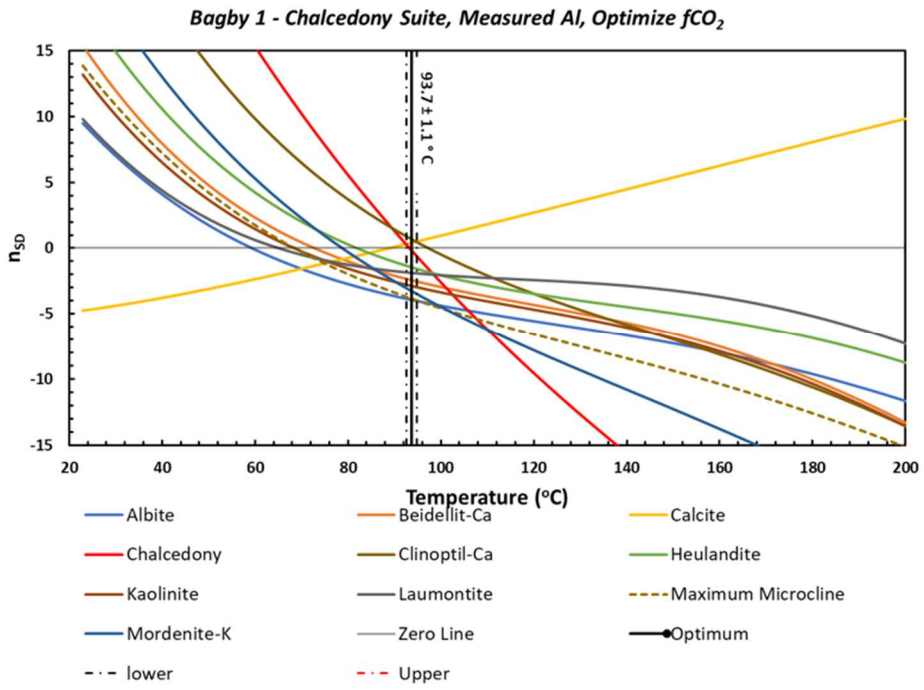

Figure 24. Suite: Cristobalite, Calcite, Laumontite, Albite. Suite 2: Chalcedony, Calcite, Clinoptilolite-Ca.

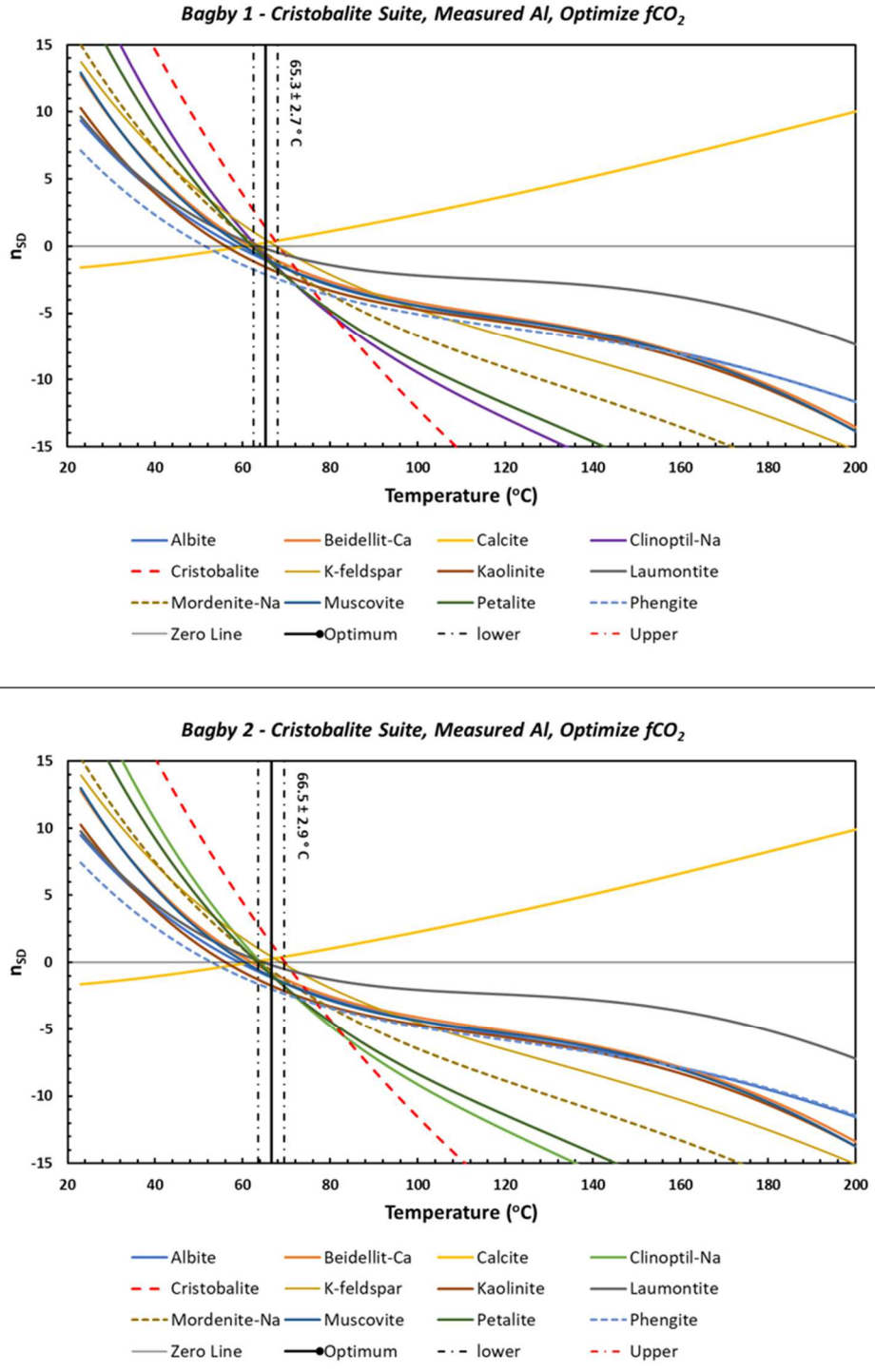

Figure 25. Cristobalite suite models for Bagby 1 and Bagby 2.

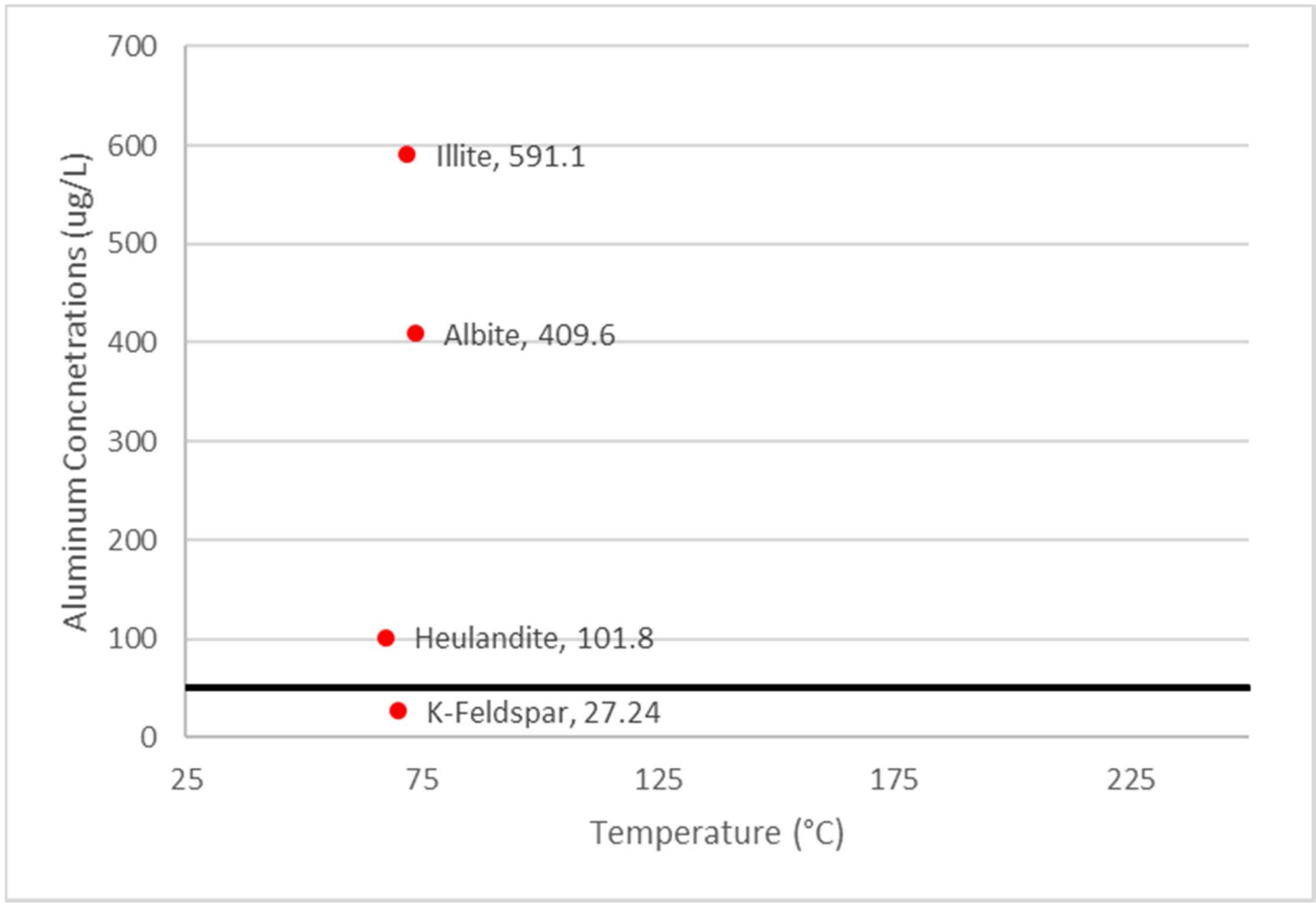

Figure 26. Calculated aluminum concentrations for Bagby Hot Springs using different aluminum-bearing minerals. Black line represents the measured aluminum concentration Bagby 1.

Wind River: Tenzen Wells

Similar to Bagby Hot Springs, both chalcedony- and cristobalite-based mineral suite were considered for calculating the reservoir temperature at Tenzen Wells in Wind River Washington. Assemblages were selected based on mineralogy of the Ohanapecosh Fm. and hydrothermal alteration minerals reported by Wise (1961) and McGowan (1985) including heulandite, mordenite, laumontite, and smectite.

WR ATT724 (i.e. "Tenzen well 2") has a temperature of 66.2°C based on a cristobalite mineral suite (cristobalite, calcite, mordenite-Na, clinoptilolite-Ca). Log $f(CO_2)$ at this temperature was calculated as -2.65. WR AAT715 yields a similar temperature and log $f(CO_2)$ of 63.9°C and -2.80 respectively using a similar suite of minerals (cristobalite, calcite, mordenite-Na, daphnite-14A), though this would be lower than the discharge temperature of WR AAT715 (64.5°C).

A chalcedony mineral suite (chalcedony, clinoptilolite-Ca, calcite) yields a reservoir temperature of 87.6°C for AAT724. Other minerals are significantly under- or oversaturated when this chalcedony mineral suite is used (Figures 27 and 28). However, reservoir temperatures using the chalcedony model agree with previously reported calculated reservoir temperatures of both St. Martins and Shipherds Hot Springs (~90°C; Berri and Korosec, 1983; Czajkowski et al., 2013; Malkemus, 2016). The lower n_SD values supports the chalcedony suite for WR AAT715: the average n_SD for the chalcedony suite (chalcedony, clinoptilolite-Ca, Calcite, Daphnite-14A) is 0.103, compared to 0.178 from the cristobalite suite used for the same well.

Aluminum concentrations for Tenzen wells were both measured and calculated via equilibrium with K-feldspar, albite, heulandite, or illite. The measured aluminum

concentration at WR AAT724 is 12.0 μg L^{-1}. Modeled aluminum concentrations ranged from lower endmembers of 5.924 (heulandite) and 101.8 (K-feldspar) μg L^{-1} to higher endmembers of 76.9 (albite) and 125.0 (illite) μg L^{-1}. Wide deviations in modeled aluminum concentrations provide a constrained temperature range of 64.4 to 66.3°C using cristobalite mineral suites at lower calculated aluminum concentrations and 95.9 to 98.0°C using chalcedony mineral suited at higher calculated aluminum concentrations. Saturation indices of aluminum minerals at the calculated reservoir temperature using the chalcedony suite were: K-feldspar = -0.3539, Albite = -0.4255, Illite = -0.5871, Heulandite = -0.0203. Log f(CO_2) ranged from -2.69 ([Al] from heulandite) to -1.98 ([Al] from illite and albite).

CO_2 fugacity was calculated using the same methods for Austin and Bagby Hot Springs. Optimizing the CO_2 fugacity in RTEst yielded a log f(CO_2) of -2.60 when modeling reservoir temperature with a cristobalite mineral suite. Adding CO_2 yielded a similar result of -2.62. Allowing calcite to precipitate yielded a CO_2 fugacity far above atmospheric as calcite was oversaturated at all temperatures.

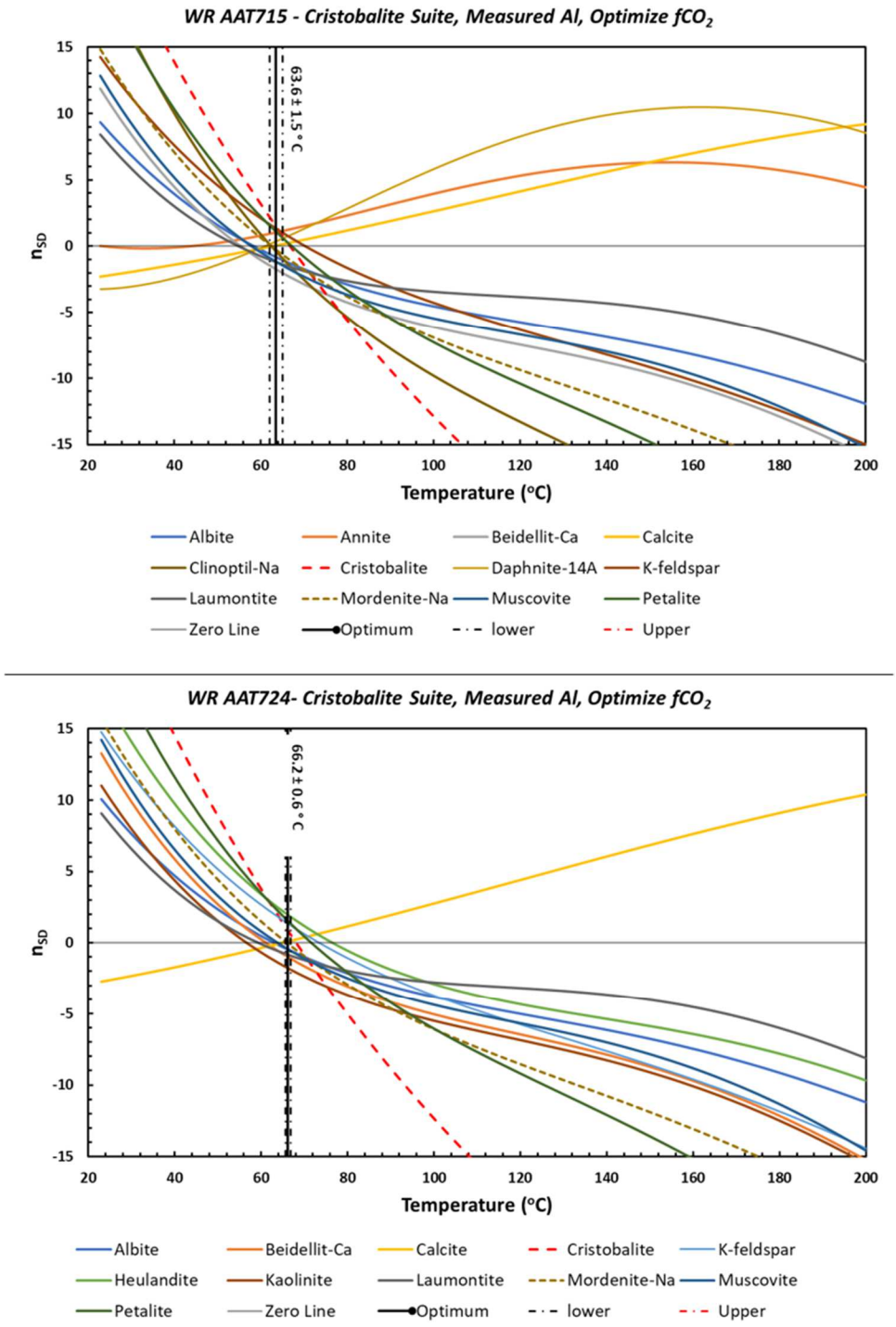

Figure 27. Comparison of cristobalite mineral suite geothermometry for WR AAT715 and WR AAT724.

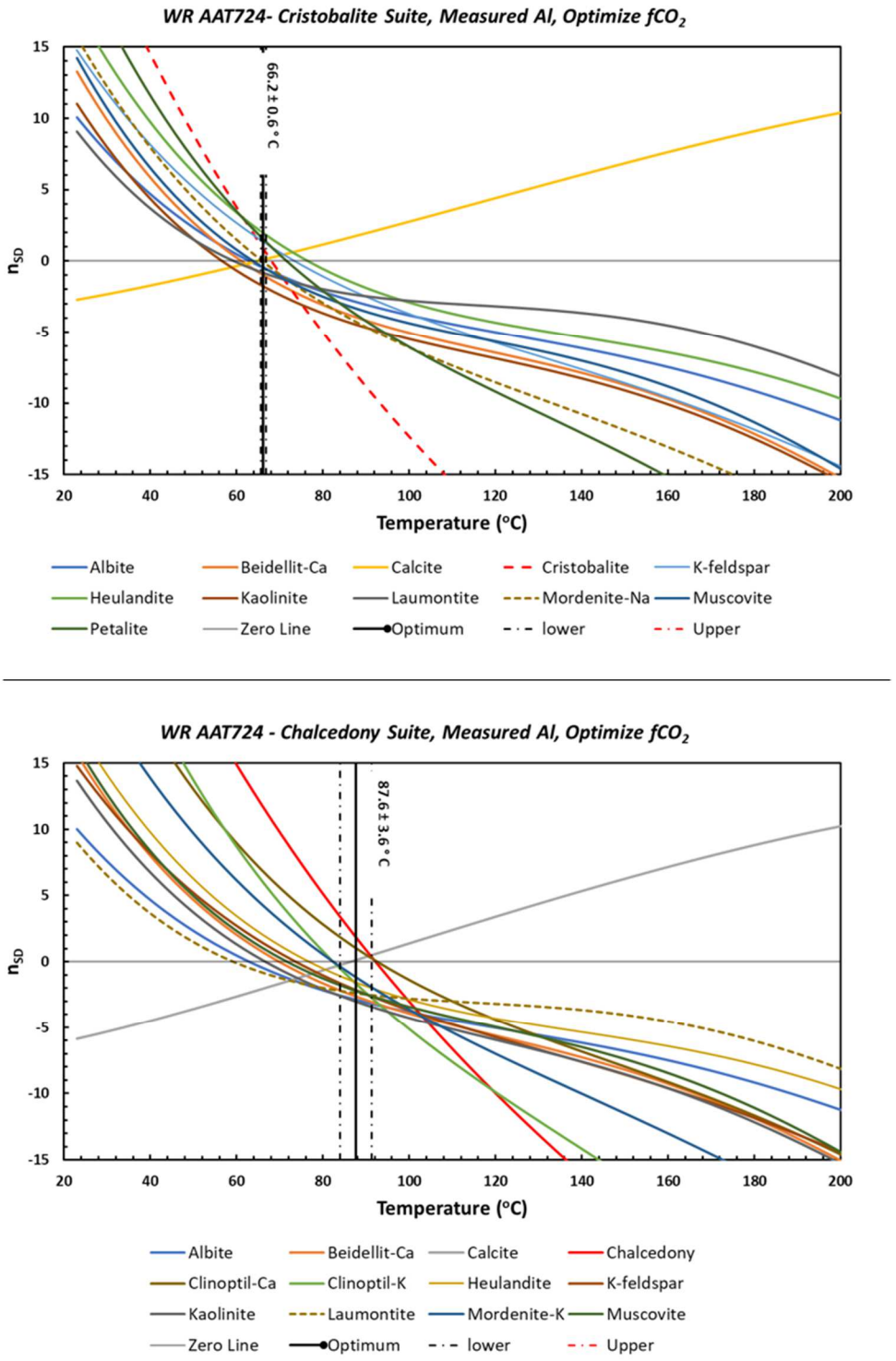

Figure 28. Cristobalite vs. Chalcedony mineral suite for WR AAT724. Silica controlling minerals outlined in red.

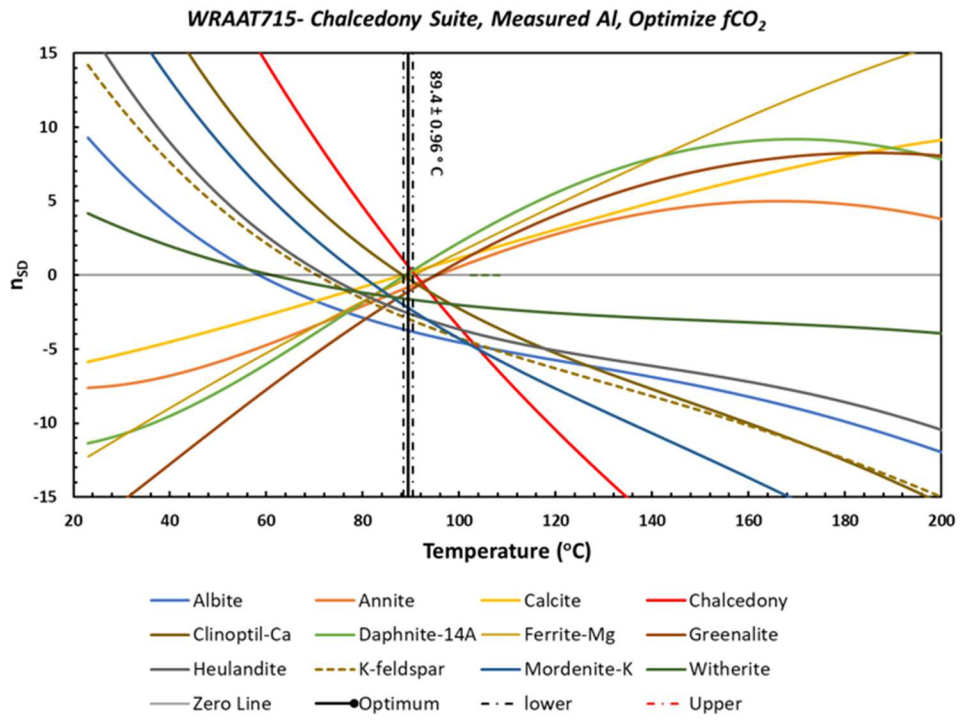

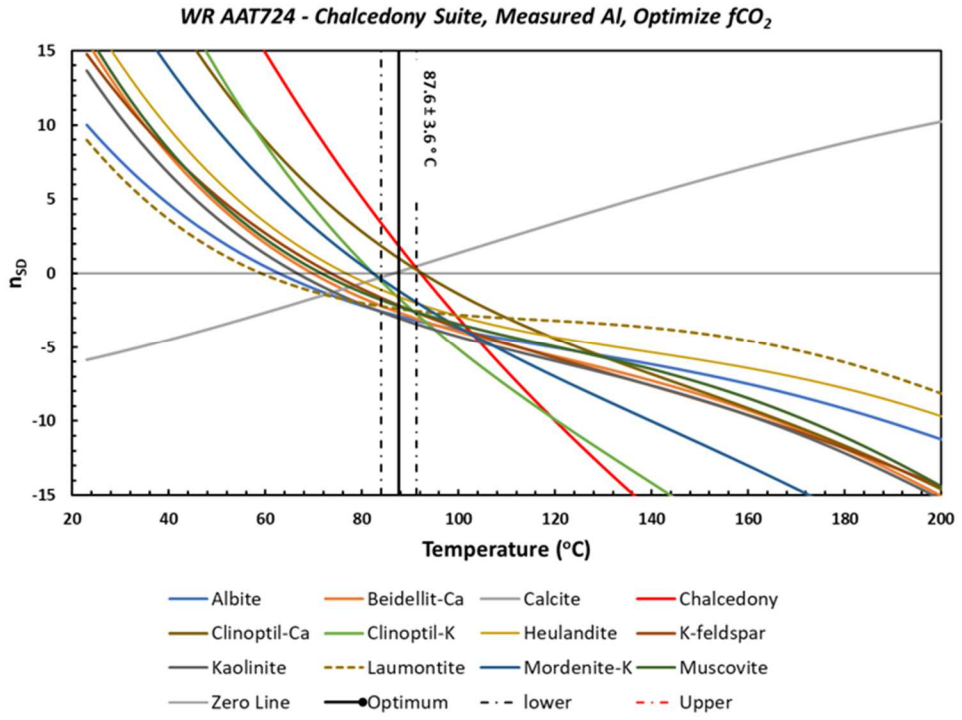

Figure 29. Comparison of chalcedony mineral suites for WR AAT715 and WR AAT724.

Table 11. Calculated aluminum concentrations using aluminum-bearing minerals and resulting temperature and f(CO_2) for Tenzen Wells (AAT724)

[Al]	Mineral Suite	Al (µg/L)	Temperature (°C)	log f(CO2)
Measured	Cristobalite Calcite Mordenite-Na Heulandite	12	68.5	-2.60
K-Feldspar	Cristobalite Calcite Mordenite-Na Heulandite	6.744	66.3	-2.64
Heulandite	Cristobalite Calcite Mordenite-Na Laumontite	5.924	64.4	-2.69
Illite	Chalcedony Calcite Mordenite-K Clinoptilolite-K	125	95.9	-1.98
Albite	Chalcedony Calcite Mordenite-K Clinoptilolite-K	76.9	98	-1.98

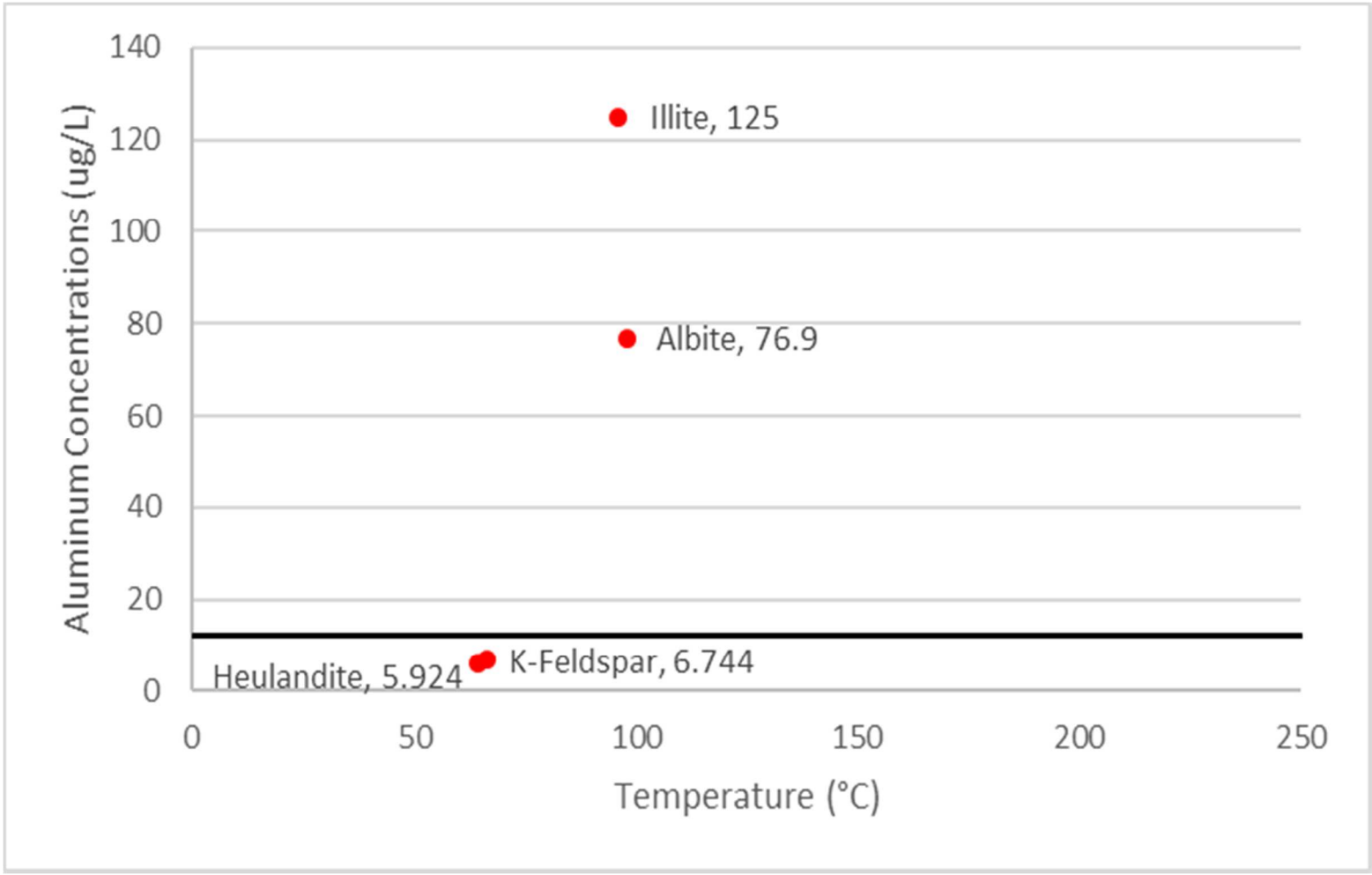

Figure 30. Calculated aluminum concentrations for WR AAT724 using different aluminum-bearing minerals. Black line represents the measured aluminum concentration WR AAT724.

5. DISCUSSION

5.1 Hot Springs of the North-central Cascades

5.1a Austin and Breitenbush Hot Springs

Austin and Breitenbush Hot Springs were reported with similar reservoir temperatures by Ingebritsen et al., 1992 (174 and 186°C), but new lower reservoir temperature estimates for Breitenbush Hot Springs (137 to 141°C; Malkemus, 2016; Malkemus et al., 2017) suggest that the reservoir temperature for Austin Hot Springs should be reevaluated. I calculated a reservoir temperature of between 100.1 (chalcedony suite) and 128.7°C (quartz suite) for Austin Hot Springs, much lower than the previous estimates. This is strictly due to the lower equilibrium temperatures of the minerals selected than the original anhydrite-sulfate geothermometer. However, the minerals used in the chalcedony-based suite are more consistent with mineralogic observations at Austin and Breitenbush Hot Springs than quartz- and anhydrite-based geothermometers (Keith, 1988; Bargar and Oscarson, 1997; Boden, 1985).

The more constrained temperature range of 104.5 to 106.5°C using the chalcedony suite is also more suitable than the quartz suite for Austin Hot Springs' reservoir because chalcedony is more likely than quartz to control silica concentrations at temperatures below 180°C, and likely to be the only silica control at temperatures lower than 110°C (Arnórsson, 1975). However, temperatures calculated using the quartz model are still 60°C lower than previously reported values, indicating that the heat output of Austin hot springs is lower than previously calculated regardless of the choice of silica geothermometer.

Piper diagrams for Austin and Breitenbush thermal waters suggest their waters are similar. Both are considered Na-Cl waters, and ion ratios at both sites are similar for the elements that were measured at Austin Hot Springs. The most pronounced differences between the ion chemistry of both waters are the lower overall TDS and higher ratios of Ca^{2+} and SO_4^{2-} at Austin Hot Springs (Figure 33). Similarities in cation ratios between Austin and wells W14 and W2 at Breitenbush support the possibility of mineral precipitation before discharge. Regardless of ion ratios, lower chloride values at Austin Hot Springs (390 mg/L) preclude it from emanating from the same groundwater flowpath as Breitenbush Hot Springs (1200 mg/L), though this does not suggest they are heated by different sources.

While Breitenbush Hot Springs is near enough Mt. Jefferson for its waters to be heated solely by a narrow intrusive heat source beneath Mt. Jefferson, Austin Hot Springs may be too far away for its previously reported reservoir temperature to be explained by this heat source (Sherrod et al., 1996). The lower calculated reservoir temperature of between 100.1 and 106.5°C supports a scenario where hydrothermal water is cooled as it travels north-northwest along the NW trending Clackamas River fault zone that runs through the discharge point of Austin Hot Springs. Austin Hot Springs is also simply farther away from Mt. Jefferson than Breitenbush Hot Springs which could account for its lower temperature; another possibility is that Austin Hot Springs is heated by Quaternary intrusions in the High Cascades beneath both Mt. Jefferson and Mt. Hood (Figure 32).

A localized Quaternary intrusion beneath Mt. Jefferson has been speculated as the heat source for Breitenbush Hot Springs (Sherrod et al., 1996).

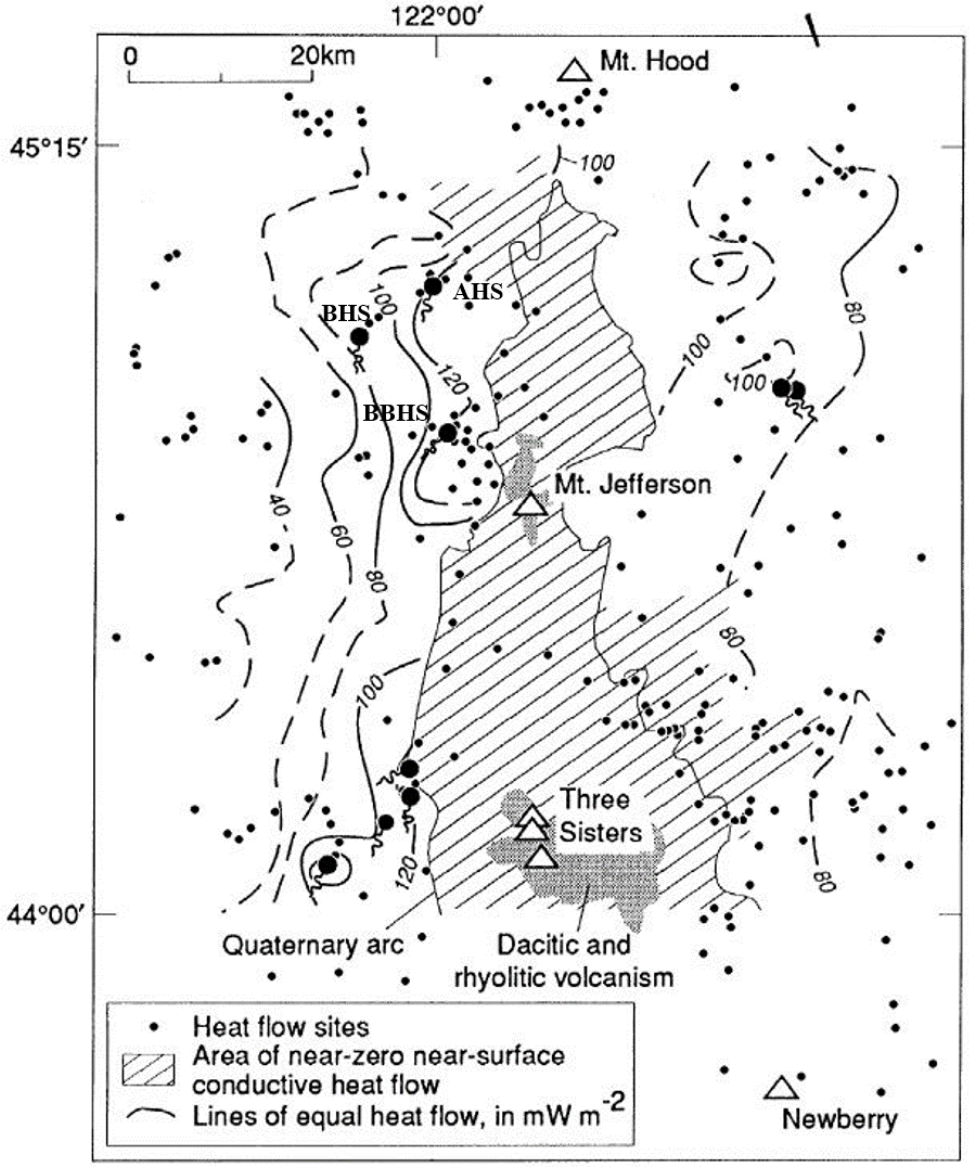

Figure 31. Conductive heat isotherm heat map from Ingebritsen et al. (1989). AHS: Austin Hot Springs; BHS: Bagby Hot Springs; BBHS: Breitenbush Hot Springs.

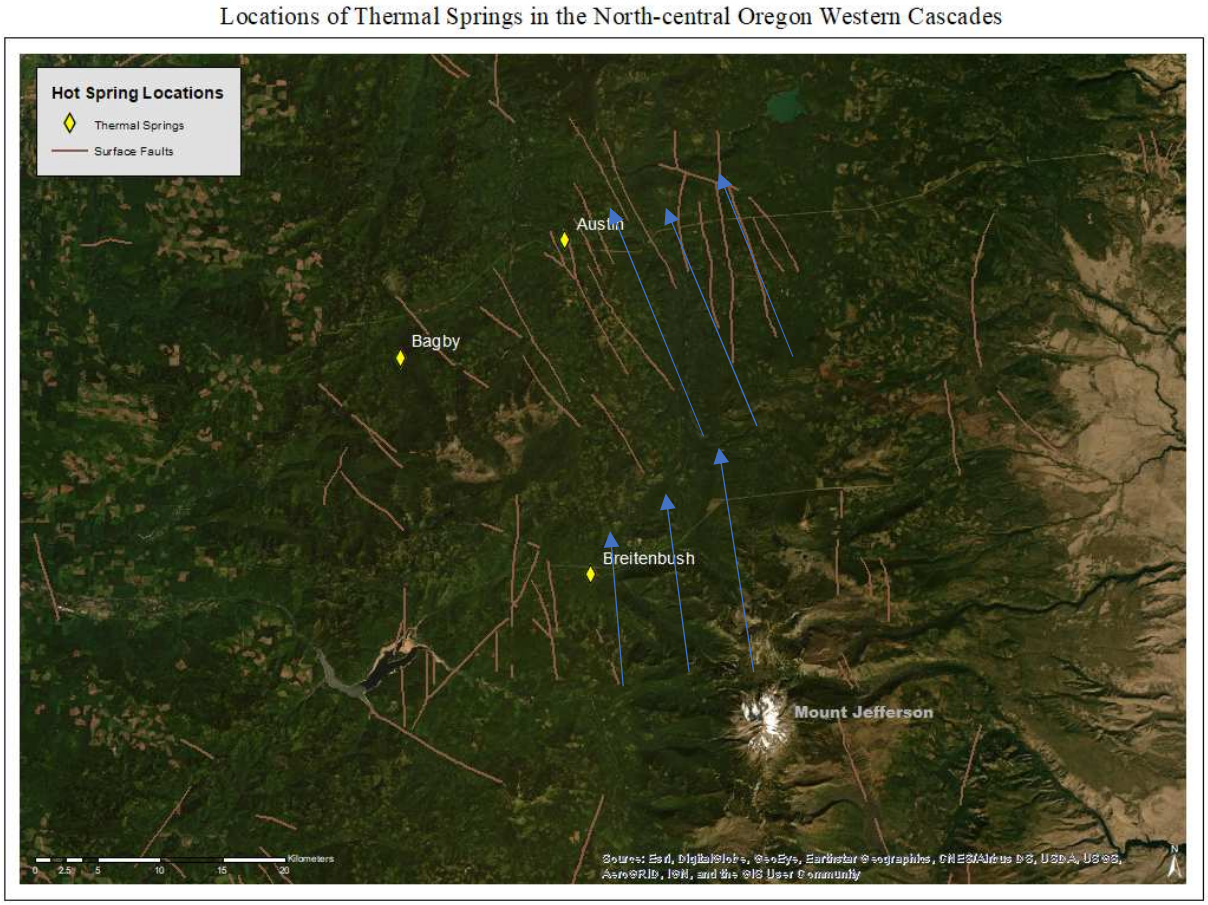

Figure 32. Representation of possible generalized groundwater flow direction from Mt. Jefferson to Austin Hot Springs where groundwater is heated by a narrow Quaternary intrusion beneath Mt. Jefferson.

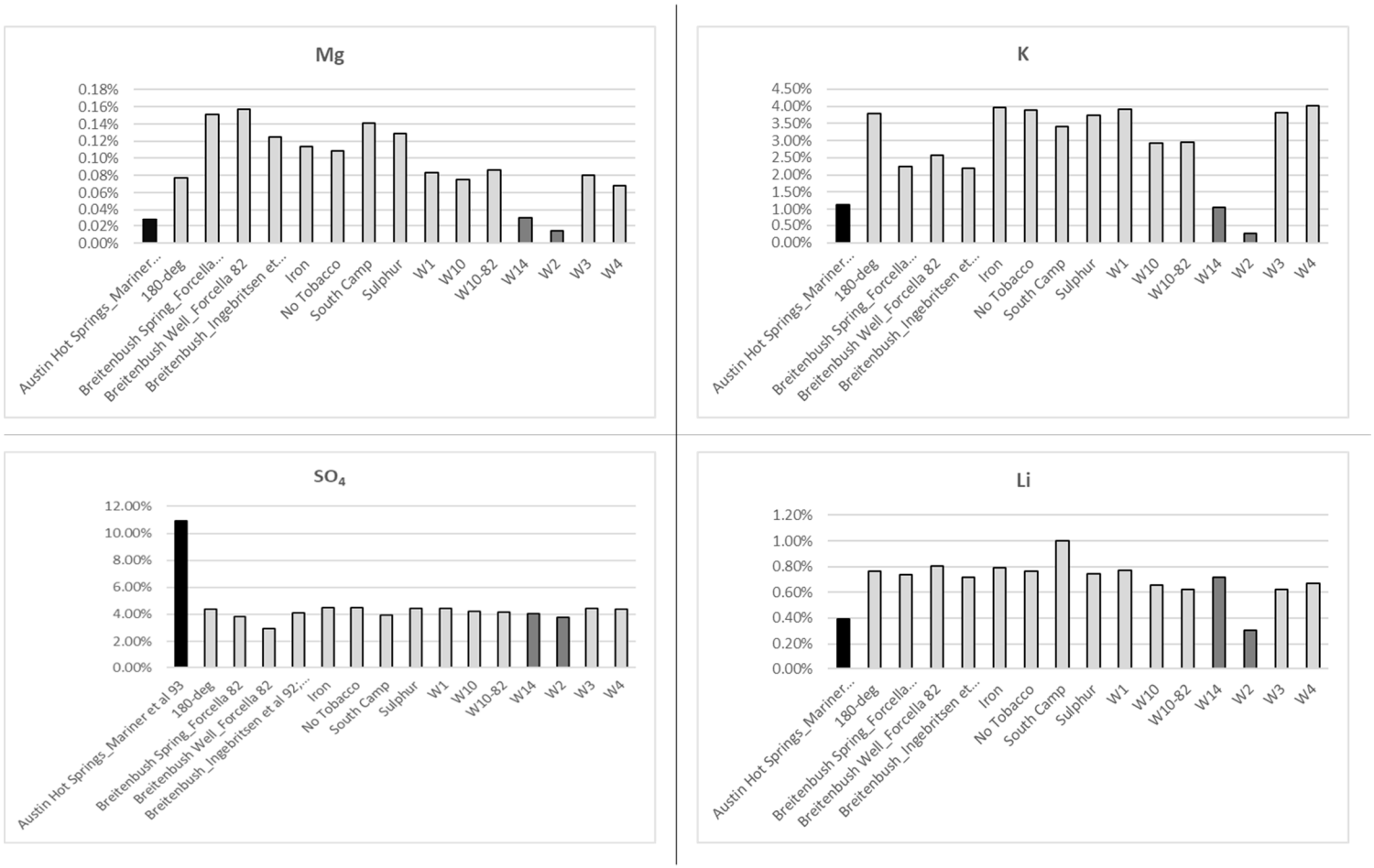

Figure 33. Ion chemistry of Austin Hot Springs vs. thermal wells at Breitenbush. Austin Hot Springs is highlighted in black. Two Breitenbush wells that have likely experienced mineral precipitation are highlighted in gray. Mg, Li, and K values are relative to total cation concentrations. SO4 concentrations are relative to total anion concentrations.

If this is also assumed to be the heat source for Austin Hot Springs, then the combination of the following factors most strongly support that the two systems share a common hydrothermal system: 1) faults between Breitenbush and Austin Hot Springs act as a conduit for groundwater movement northwestward, 2) water compositions are similar at both sites, though Austin has a lower TDS. Other factors that support the connection between the two systems are the proposed shared "andesitic water mixing line" (Malkemus et al., 2017; Giggenbach, 1992) of both sites and lower reservoir temperatures at Austin Hot Springs. The latter suggests cooling and re-equilibration of groundwater as it travels northward.

High $^{3}He/^{4}He$ ratios of Austin (5.7) and Breitenbush (6.5) Hot Springs suggest deep thermal circulation (Ingebritsen et al., 1992). High $^{3}He/^{4}He$ ratios at Breitenbush and Austin Hot Springs also indicate some dissolved constituents originate from magmatic sources (Ingebritsen et al., 1992).

5.1b Bagby Hot Springs

Temperature estimations for Bagby Hot Springs using a cristobalite-based suite yield a temperature of 65.3°C. This temperature is above the measured discharge temperatures of 58 °C and is more reasonable than the previously estimated reservoir temperature estimation of 52°C (Ingebritsen et al., 1992). This temperature difference is inconsequential to the total hydrothermal heat discharge of the region due to its low discharge rate of approximately 1 $L\text{-}s^{-1}$.

$\delta^{18}O$ and δD values measured at Bagby Hot Springs suggest the upper limit for recharge elevation of Bagby Hot Springs is between 1600-1650 meters using the local

meteoric water data from Brooks et al. (2012). The lower recharge elevation limit for Bagby Hot Springs is between 850 and 900 meters using $\delta^{18}O$ values in snow vs. Elevation (James, 2000). These modeled recharge elevations are considerably lower than Austin and Breitenbush Hot Springs and suggest localized recharge at elevations lower than the crest of the Cascades. Values of $\delta^{18}O$ and δD for Bagby also do not suggest mixing with magmatic andesitic water (Malkemus et al., 2017*).* This opposes the proposed regional deep groundwater flow model of Austin and Breitenbush Hot Springs and instead suggests a shallower localized system independent from other hydrothermal waters in the north-central Cascades. However, this does prompt the question of a heat source for Bagby Hot Springs. Based on lower recharge elevations, reservoir temperatures, and discharge volumes, the source of heat likely stems from the geothermal gradient of the study area. Geothermal gradients for the Western Cascade Range (28.8 °C/km) and the Western Cascade-High Cascade Boundary (61.3 °C/km) suggest source water for Bagby Hot Springs must reach a depth of 1-2 km to be heated to its calculated reservoir temperature (Blackwell, 1978).

The $\delta^{18}O/\delta D$ ratio of Bagby Hot Springs falls to the left of the LMWL for samples collected in October 2018. These measurements were consistent in δD concentrations, but not $\delta^{18}O$ concentrations. Provided these values are not the result of laboratory error, the most likely explanation for this depletion of ^{18}O is oxygen exchange between water and CO_2 in the organic soil layers near the surface (Clark and Fritz, 1997). However, samples collected during the summer of 2019 lie close enough to the local

meteoric water line that the lab reported standard deviation of 0.21‰ may be sufficient in explaining this depletion of ^{18}O (Figure 14).

Bagby Hot Springs' deviation from Breitenbush and Austin Hot Springs in terms of pH, water chemistry, and temperature also suggests it is independent of the common system for Breitenbush and Austin (Figure 32). Bagby discharges further west from Austin and Breitenbush Hot Springs along an 80-mW m^{-2} isotherm (Figure 31). This, along with Bagby's lower $^{3}He/^{4}He$ ratio (1.2), dilute waters, and $\delta D/\delta^{18}O$ ratios close to the LMWL (Brooks et al., 2012) suggest a 1-2 km deep local flow system independent from Austin and Breitenbush Hot Springs.

5.1c Total Cumulative Heat Discharge

The lower estimated reservoir temperature of 104.5 to 106.5°C for Austin Hot Springs implies a significant decrease in the estimate of overall hydrothermal heat discharge in the north-central Oregon Cascades. The advective heat discharge can be estimated using the following equation (Ingebritsen et al., 2001; Ingebritsen and Mariner, 2010):

$$\mathbf{Q_{hydrothermal} = Cl_{flux} c_w (T_{geo} - T_{Rch})/Cl_t}$$

where Cl_{flux} represents the hydrothermal chloride flux (obtained from measurements reported by the USGS Cascades Volcano Observatory) c_w is the heat capacity of the fluid, T_{geo} is the maximum fluid temperature at depth calculated from multicomponent chemical geothermometry, T_{Rch} is the recharge temperature (between 0 and 5 degrees

Celsius in the Cascade Range), and Cl_t is the chloride concentration measured in the spring water. The value calculated for $Q_{hydrothermal}$ reflects heat advected away from a deep heat source as opposed to heat discharged from thermal springs at the surface. Here, the reservoir temperature for Austin Hot Springs, $T_{geo,}$ is 100.1 to 106.5°C rather than the previous estimate of 186 °C and all other variables—including the recharge temperature, T_{Rch} = 2.5°C—remain as the values used in Ingebritsen and Mariner (2010). The resulting value for total hydrothermal heat advection from Austin is then 47 to 49 MW, or ~44% less than the earlier estimate of 85 MW produced using a temperature of 186°C. This changes the total overall thermal spring heat discharge of the north-central Cascades from 121 MW to 84 MW (27% decrease) and the total heat discharge by thermal and "slightly thermal" springs from 311 to 278 MW (11% decrease; Figures 34 and 35). While this is significantly less than previously calculated, it is still a substantial contribution to total hydrothermal heat discharge. Due to the high volume of water discharged at Austin (120 L s^{-1}) compared to Breitenbush and Bagby (12 and 1 L s^{-1}), Austin remains the major contributor to the hydrothermal heat discharge of north-central Oregon despite its lower calculated reservoir temperature. The recalculated reservoir temperature of Bagby Hot Springs does not significantly change the value (< 1 MW) of heat discharge in the region due to its paltry discharge. While the differences in cumulative heat output do not change the fact that there is a large influx of heat discharged by thermal springs between 44°45'N and 45°15'N, the lower temperatures reduce the favorability of geothermal energy exploration in the region.

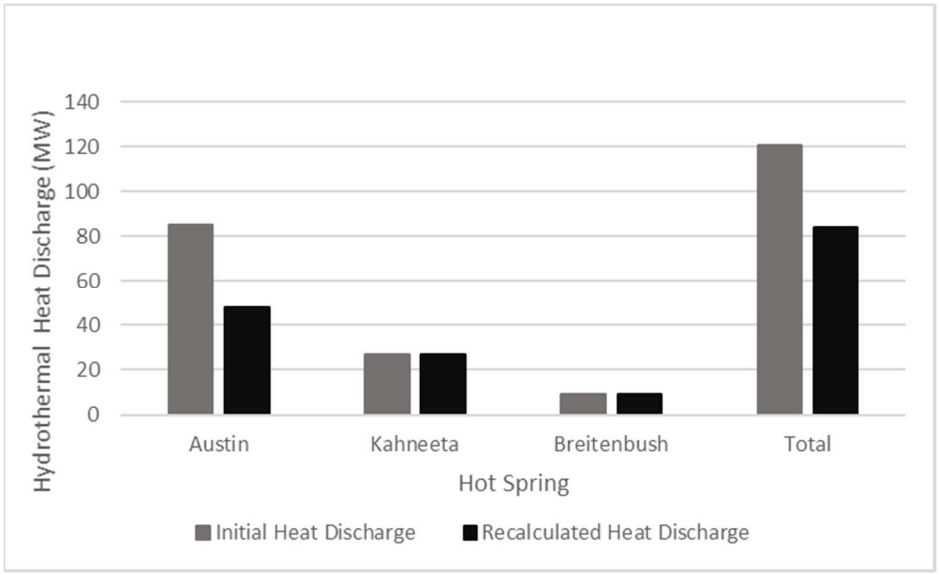

Figure 34. Change in Austin Hot Springs' contribution to total heat discharge from thermal springs in the north-central Cascades.

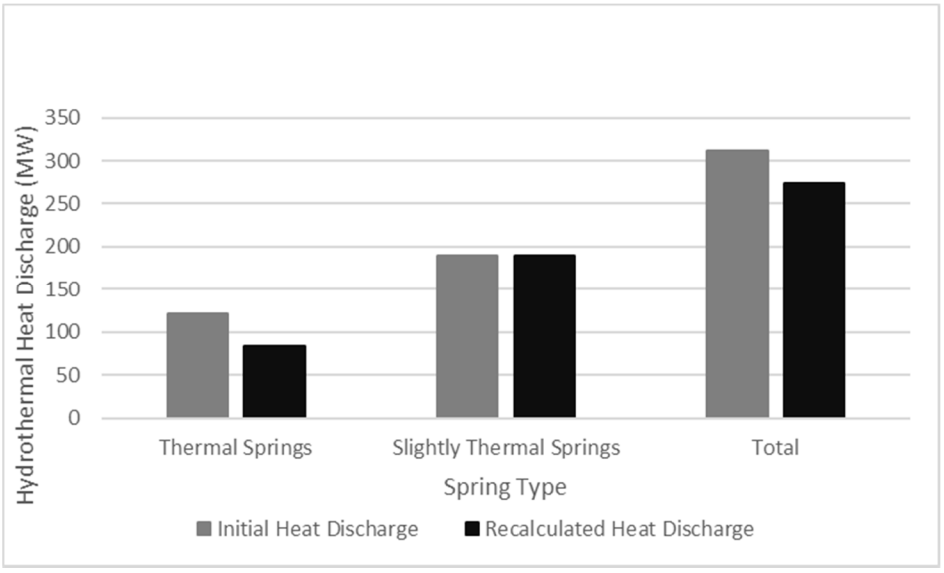

Figure 35. Change in total heat discharge in the north-central Cascades when accounting for input from slightly thermal springs.

5.2 Wind River

Reservoir temperature estimations for Tenzen wells using a cristobalite-based suite yield temperatures of 63.6 for WR AAT715 (Tenzen 1) and 66.2°C for WR AAT724 (Tenzen 2). These temperatures are close to the measured discharge temperatures of 64.5 and 56.3°C. Estimations calculated using a chalcedony suite yield a temperature of 87.6 and 89.4°C. While the cristobalite suite provides a tighter fit for more equilibrium minerals, the chalcedony suite provides a temperature more consistent with previously reported reservoir temperatures of St. Martins and Shipherds Hot Springs (Berri and Korosec, 1983; Czajkowski et al., 2013; Malkemus, 2016; Forson et al., 2017). The calculated reservoir temperature of 87.6-89.4°C for the Tenzen thermal waters is consistent with the temperature of 83-100°C for both St. Martins and Shipherds Hot Springs (Malkemus, 2016).

The lower calculated reservoir temperatures for Tenzen wells are consistent with previously reported reservoir temperatures of 65 and 73°C for St. Martins Hot Springs using Na-K-Ca and chalcedony geothermometers, respectively (Czajkowski et al., 2013). However, as with Bagby Hot Springs, the reservoir temperature of these waters cannot be less than their discharge temperatures. Because of this, the chalcedony-based suite is more suitable for all thermal waters in the Wind River Valley.

Water chemistries between Tenzen Wells and St. Martins Hot Springs are similar enough to suggest that the two systems share the same groundwater reservoir. Shipherds Hot Springs is more dilute than St. Martins and Tenzen waters and plots towards Na-mixed anion waters, similar to Bagby Hot Springs. Shipherds Fault Zone may act as a

zone of groundwater mixing between water from the east side of the Wind River Fault and groundwater from Wind River itself (Czajkowski et al., 2013). Based on current reservoir temperature estimations between 87.6 and 100°C, Shipherds, Tenzen, and St. Martins Hot Springs likely share the same hydrothermal reservoir. However, this does not account for the significantly different water chemistry of Shipherds Hot Springs. Shipherds Hot Springs discharges closer to Wind River and lies within Shipherds Fault Zone, so it is possible that mixing with dilute surface waters occurs during ascent or near the discharge point (Czajkowski et al., 2013). Optimizing gain or loss of water in RTEst yields an apparent loss of water ($-dH_2O$), suggesting mixing with surface or near-surface waters at Shipherds Hot Springs (Malkemus, 2016). This is consistent with the uniformly low ion concentrations measured in Shipherds Hot Springs. Mixing with surface water is not observed at St. Martin and Tenzen Hot Springs and results yield no significant gain or loss of water when optimized using RTEst. This may be attributable to their respective distances south of Shipherds fault zone and distances from Wind River: though St. Martins has slightly lower TDS than Tenzen wells (~1200 vs. ~1500 mg/kg), $\delta^{18}O$ and δD values are higher at St. Martins Hot Springs (Table 7; Figure 14). While these isotope values are comparable between Tenzen wells (mean $\delta^{18}O$ = -12.32; δD = -91.42) and St. Martins Hot Springs (mean $\delta^{18}O$ = -11.64; δD = -91.92), the more ^{18}O-enriched St. Martins Hot Springs has a higher calculated "andesitic water" component than Tenzen wells (8% vs. 4%). This range is comparable to the 4-8% calculated for samples collected from Breitenbush and Austin Hot Springs (Malkemus et al., 2017*)*.

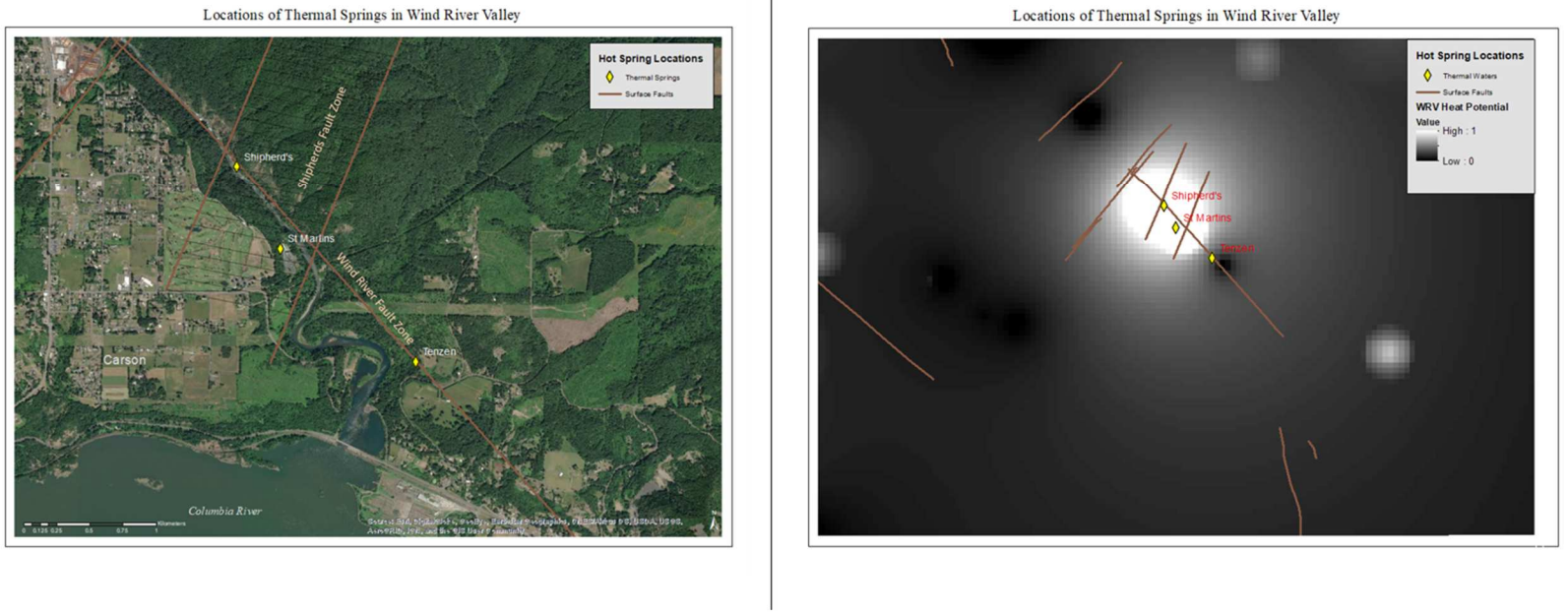

Figure 36. Wind River Valley fault locations superimposed on a Heat Potential raster created using data from Czajkowski et al., 2013.

5.3 Larger Tectonic Setting of Breitenbush-Bagby-Austin and Wind River

The higher conductive heat flow and increased thermal-spring discharge south of 45°15'N is heavily influenced by Basin and Range-style faulting (Ingebritsen and Mariner, 2010). The revised hydrothermal heat output for the north-central Cascades still supports structural control of Basin and Range impingement as a major control on heat production in this area (Ingebritsen and Mariner, 2010). Basin and Range impingement below 45°15'N both enhances crustal heat flow and provides deep permeability for fluid circulation via deep extensional-style faults. However, volcanic vent alignments near Wind River and north-south trending folds of the Yakima Fold Belt indicate extensional stress as far north as Mt. Adams (Jones and Malone, 2005; Hildreth, 2007). Heat-flow contour maps also show areas with >100 mW m^{-2} heat flow extending from central Oregon to the Wind River Valley. This heat flow pattern corresponds with a series of NW-trending faults following a clockwise-rotating trend (Figure 37). This rotating fault trend matches the steady rotation of the Siletz Terrane and the Cascade arc model by Wells and McCaffrey (2013). These faults are not mapped past the surface past Austin Hot Springs, though they do point to Wind River Valley.

Further evidence for this deeply faulted system extending further north is the andesitic water mixing line of both Breitenbush-Austin thermal waters and Wind River thermal waters (Figure 17) The discharge of deeply circulating thermal waters in the north-central Cascades is explained by presence of subvertical normal faults evident of Basin and Range impingement. Although extensional structures become less prominent past the assumed impingement latitude of 45°15, mixing with andesitic waters at depth

may continue north into the lower Wind River Valley near the Hood River Fault Zone where extensional-style tectonics is prominent (Figure 38). This is also reflected in the heat flow gradient map of the Pacific Northwest (Figure 37) and the normal faults of the lower Wind River Valley.

High chloride concentrations observed in these hydrothermal systems are explained by mixing with andesitic water, though total chloride concentrations could be a combination of magmatic volatiles partitioning to aqueous phase and leeching from marine rocks (Ingebritsen et al., 1992; Mariner et al., 1993, 2003). A conservative chloride concentration of 0.1 weight percent in the source magma coupled with an intrusion rate of 10 km^3/km arc length/m.y. would be sufficient to supply the flux of chloride observed in the north-central Oregon Cascades. The necessary intrusion rate of 10 km^3/km arc length/m.y. fits within the range of 9-33 km^3/km arc length/m.y. calculated by Ingebritsen et al. (1989). High chloride values similar to Austin and Breitenbush Hot Springs were observed in St. Martins and Tenzen thermal waters. Measured chloride concentrations of between 658 and 800 mg/L in the Wind River Valley lie within the range of concentrations measured at Austin (390 mg/L) and Breitenbush Hot Springs (1200 mg/L). No evidence of marine sedimentary rocks is observed in or proximal to Wind River Valley suggesting the high chloride concentrations further north are solely derived from magmatic sources (Czajkowski et al., 2013).

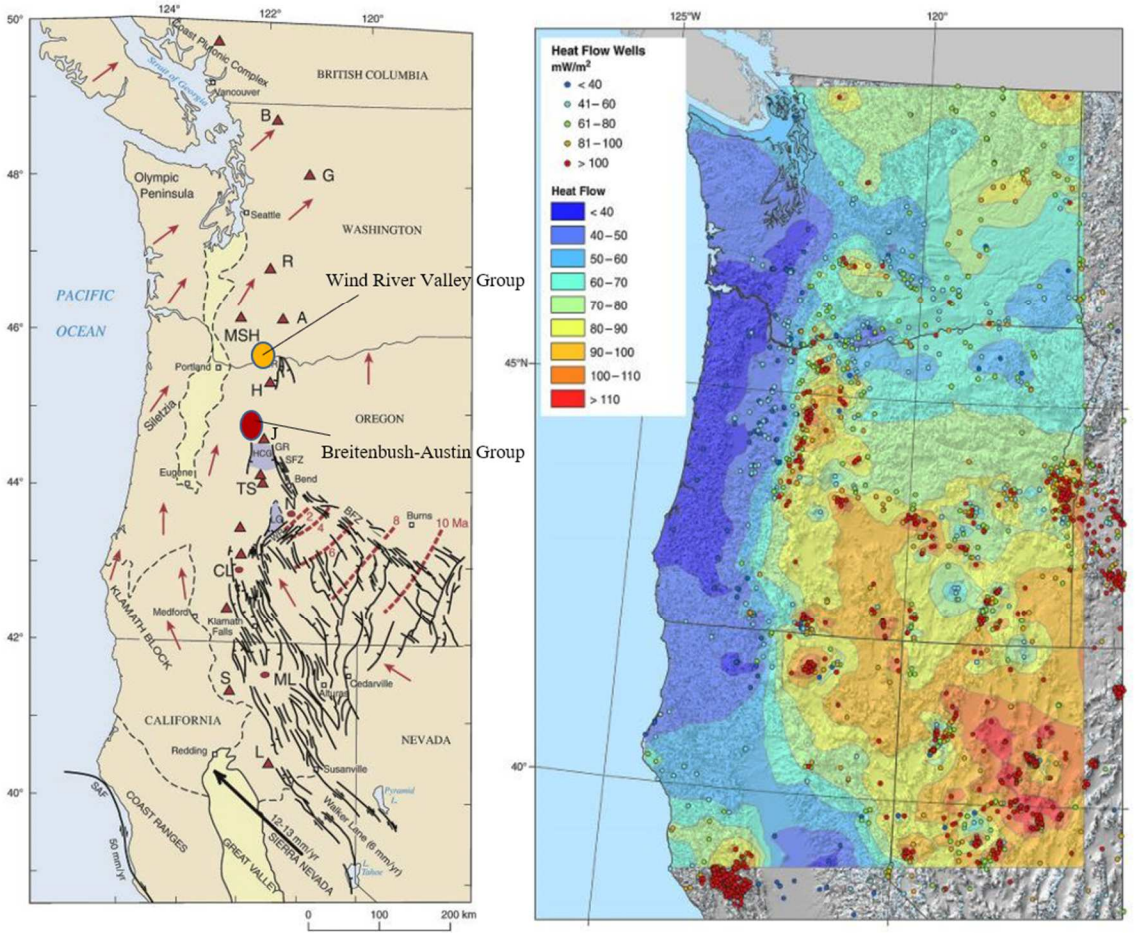

Figure 37. Tectonic setting and heat-flow gradient map of the Cascade Range (from Hildreth, 2007, and Williams and DeAngelo, 2008).

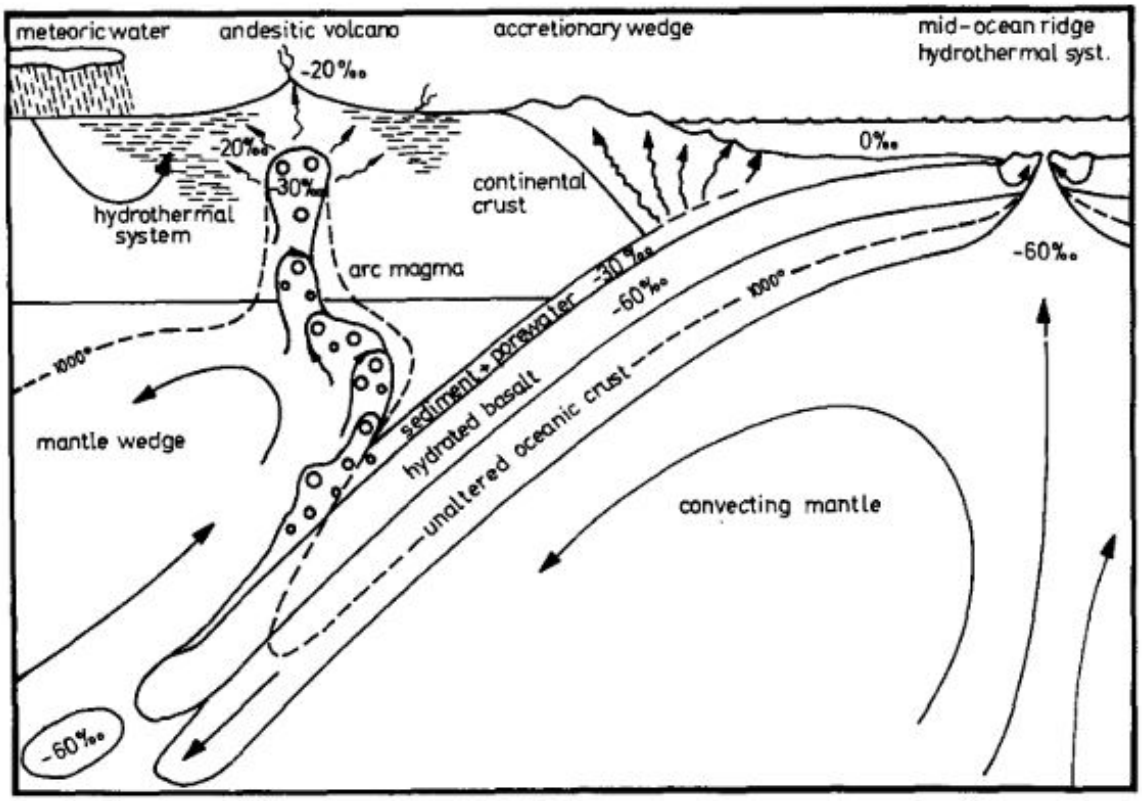

Figure 38. Schematic presentation of the production of andesitic waters from Giggenbach (1992). Minor fractionation due to degassing of subducting marine sediments shifts δD composition from -30 ± 10‰ to -20 ± 10‰.

A limited variable principal component analysis (PCA) of water samples along the north-central Western Cascades highlights similarities and differences between thermal waters in the region (Figure 39). This PCA was performed using a Pearson (correlation) matrix with six log normalized variables: boron, calcium, potassium, chloride, silica, and sodium. The complete list of chemical variables were narrowed down until 90% of the variance was explained by two factors (F1 and F2).

The upper right quadrant contains all Shipherds Hot Springs samples along with the samples "Austin Well" (Forcella, 1982) and W12 from Breitenbush (Malkemus, 2016). Samples in this quadrant have uniformly dilute ion concentrations. Because Shipherds Hot Springs has likely mixed with near-surface waters before discharging at the surface, the same mixing scenario is assumed with the "Austin Well" and W12 samples.

Springs of the central Cascades (Terwilliger, Bigelow, Belknap, Foley, Kitson, McCredie) all plot in the upper left quadrant. These springs do not form distinct clusters, though the springs in this area have only been sampled twice at most (Forcella, 1982; Mariner et al., 1993). Thermal waters from the Wind River Valley also plot in the same quadrant as springs in the central Cascades.

Most samples from Breitenbush plot with Austin Hot Springs in the lower left quadrant (Mariner et al., 1993), though Austin is not in the same distinct grouping as the Breitenbush waters. Tenzen well samples plot closer to Austin Hot Springs than Breitenbush, though both sites are considered Na-Cl waters (Ingebritsen et al., 1992; Mariner et al., 1993).

Bagby Hot Springs form a prominent grouping in the lower right quadrant. Though this group is closer to samples believed to have mixed with near surface waters than Breitenbush or springs of the central Cascades, Bagby Hot Springs is clearly isolated from all other springs based on this PCA.

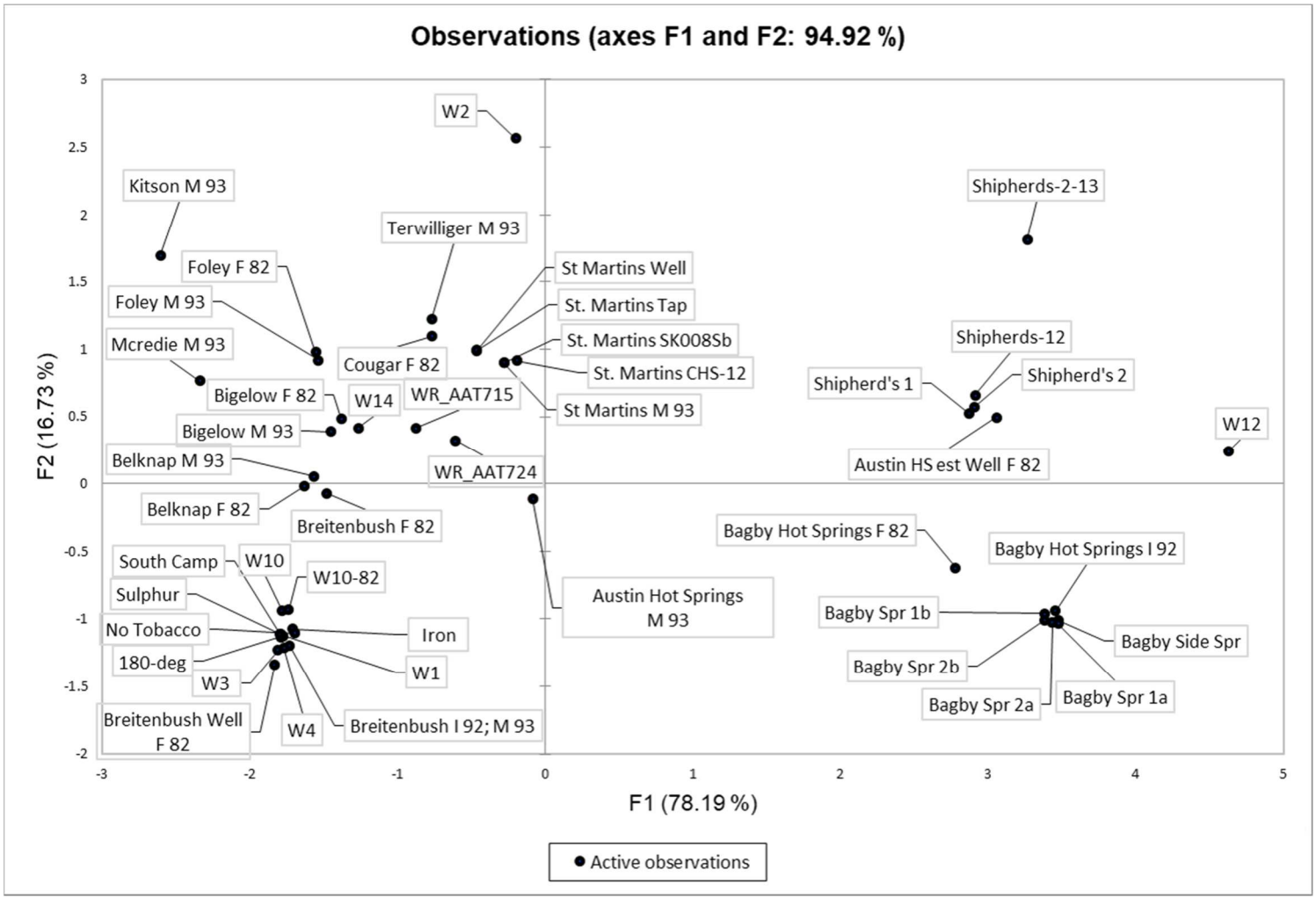

Figure 39. Principal component analysis for hot springs and wells in the north-central Cascades.

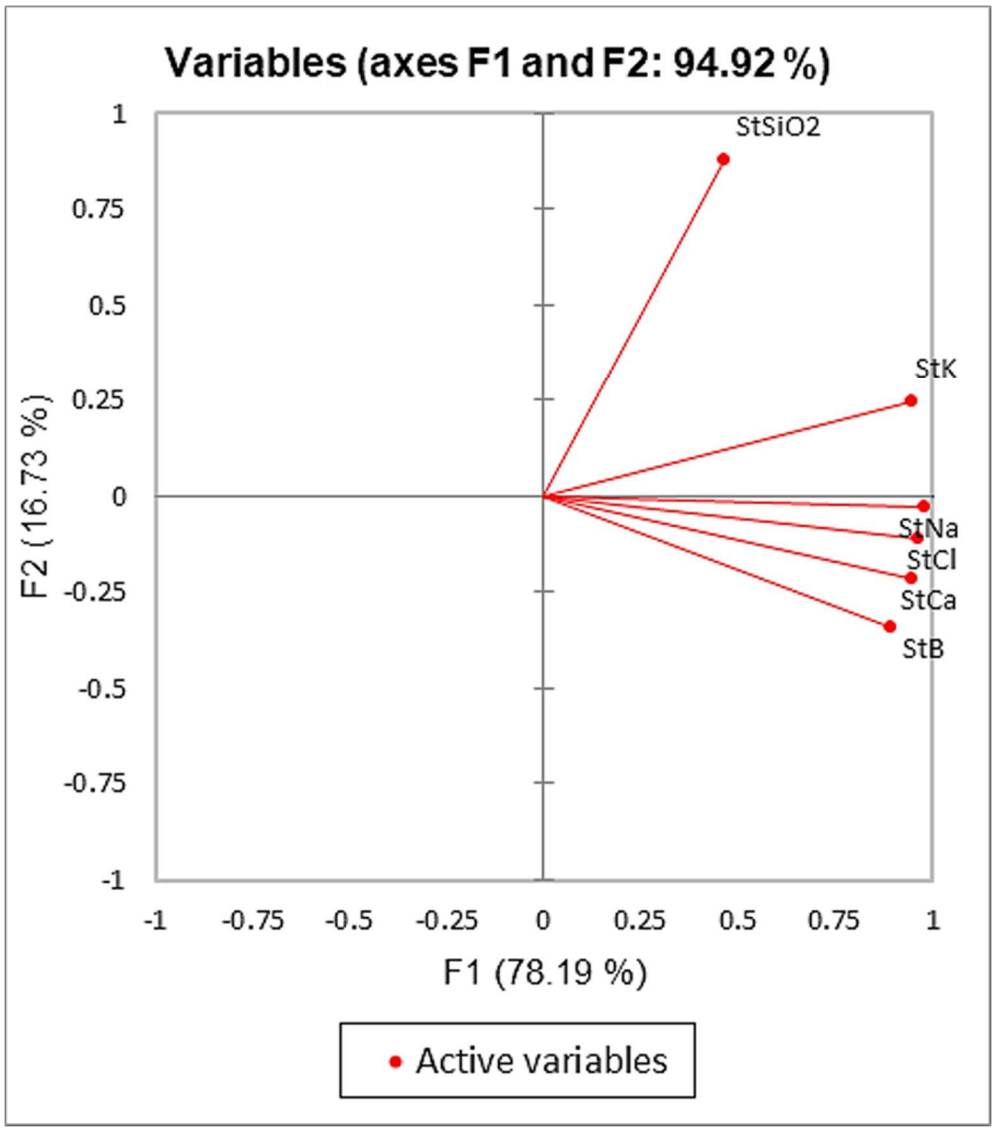

Figure 40. F1 and F2 variables for the Principal Component Analysis above. Variables for axes F1 and F2 are the logarithmic standardizations of boron, calcium, potassium, chloride, silica, and sodium.

6. Conclusions

In this study I provided revised estimated of reservoir temperatures for Austin and Bagby Hot Springs, and new reservoir temperatures based on geothermal well samples for the Wind River Valley. A revised temperature of 100.1 – 106.5°C was estimated for Austin Hot Springs using chalcedony-based mineral suites. This new reservoir temperature yields a corresponding hydrothermal heat discharge of 48 MW, which is lower than the previously reported 85 MW for Austin Hot Springs (Ingebritsen and Mariner, 2010) and lowers the overall hydrothermal heat discharge in the north-central Cascades from 121 to 88 MW and the total hydrothermal heat charge of hot and slightly-warm springs from 311 to 278 MW.

Values of $\delta D/\delta^{18}O$, He^3/He^4, and $\delta^{18}O\text{-}SO_4$ for Austin Hot Spring are similar to those measured at Breitenbush Hot Springs, and the stable water isotopes fall on the $\delta D/\delta^{18}O$ trendline established for Breitenbush thermal waters which project to the "andesitic water "of Giggenbach (2012). This indicates 4-8% water mixing with andesitic waters from the subducting slab for both Austin and Breitenbush Hot Springs. The new reservoir temperature estimate of 100.1 – 106.5°C is lower than one recently calculated for Breitenbush Hot Springs (Malkemus et al., 2017). This—together with the coincidence of the isotope data—support a scenario where Austin and Breitenbush Hot Springs are part of a common hydrothermal system with waters heated either by narrow intrusive sources beneath Mt. Jefferson and/or Mt. Hood. This setting is consistent with Austin Hot Springs' increased distance from both Mt. Jefferson and the crest of the Cascades.

A revised reservoir temperature of 66.3°C was calculated for Bagby Hot Springs using a cristobalite-based mineral suite (cristobalite, calcite, albite, laumontite). This estimated temperature is only 8°C higher than its discharge temperature of 58°C, though higher than the previously reported 52°C reservoir temperature that was approximately 6°C lower than measured discharge temperatures. Isotope values that lie close to the local meteoric water line (Brooks et al., 2012), lower He^3/He^4 ratios, dilute waters, and the separation of data points from all other north-central Western Cascade springs on PCA plots suggest that Bagby Hot Springs is an isolated thermal system.

A reservoir temperature of 87.6-89.4°C was calculated for samples collected from Tenzen wells at the Wind River Valley using a chalcedony-based mineral suite (chalcedony, clinoptilolite-Ca, calcite, daphnite-14A). This temperature range is consistent with reservoir temperatures between 83 and 100°C for St. Martins and Shipherds Hot Springs. Similar to St. Martins and contrasting Shipherds, Tenzen wells have not mixed with more dilute waters during ascent or discharge. St. Martins and Tenzen well waters show a similar andesitic water mixing line as Breitenbush and Austin Hot Springs with a calculated ratio of 4.2-8.5% andesitic water. Higher heat flow gradients extending into Wind River Valley follow the projection of the NW-trending clockwise-rotating faults ending at Austin Hot Springs.

Similar andesitic water mixing trendlines, heat flow gradients, and extensional features suggest the hydrothermal system encompassing Austin and Breitenbush Hot Springs is controlled by the same structural system as Wind River Valley. Mechanisms that govern the heating of groundwater in the north-central Oregon Cascades likely

extend into the lower Wind River Valley, with extensional structures facilitating the movement of deep thermal waters along the Western Cascades.

7. Future Work

Though water samples from most hot springs along the Oregon Cascades have been analyzed in previous studies, duplicate or triplicate ion chemistry data that includes aluminum concentrations would solidify the statistical groupings of thermal waters. The lack of aluminum data for Austin Hot Springs and Foley, Belknap, Terwilliger, and Bigelow Hot Springs require that aluminum concentrations are assumed in equilibrium with aluminum-bearing minerals such as potassium feldspar or illite. While these methods allow for the use of aluminum in geothermometric calculations and ultimately support measured aluminum values, addressing high aluminum error is only possible when aluminum concentrations are known.

$^{3}He/^{4}He$ and $\delta^{18}O/\delta D$ isotope chemistry from all sites will further support or refute the idea of a larger geothermal system along the north-central Oregon Western Cascades. This is especially true for $\delta^{18}O$ and δD, which can further address the proposed andesitic water mixing line of Malkemus et al. (2017) for all thermal waters in the region. Collecting these isotope data in duplicate or triplicate at different times of the year could address the possibility of mixing with surface waters or plausible evaporative trends. This can also be supported by $^{3}He/^{4}He$ ratios which highlight magmatic signatures of thermal waters. Sulfate and boron data for these springs may also provide insight to the relationship of thermal waters along the north-central Western Cascades, if not only to solidify the isolation of Bagby Hot Springs from Austin and Breitenbush.

References

Allen, D.M., Grasby, S.E., and Voormeij, D.A., 2006, Determining the circulation depth of thermal springs in the southern Rocky Mountain Trench, south-eastern British Columbia, Canada using geothermometry and borehole temperature logs: Hydrogeology Journal, v. 14, p. 159–172

Arnórsson, S., 1975, Application of the Silica Geothermometer in Low Temperature Hydrothermal Areas in Iceland: American Journal of Science, v. 275, p. 763-784

Bargar, K.E., 1988, Secondary mineralogy of core from geothermal drill hole CTGH-1, High Cascade Range, Oregon: GRC Transactions, v. 12, p. 283–289.

Bargar, K.E., and Oscarson, R.L., 1997, Zeolites and selected other hydrothermal minerals in the Cascade Mountains of northern Oregon: U.S. Department of the Interior U.S. Geological Survey

Bargar, K.E., 1994, Hydrothermal alteration in the SUNEDCO 58-28 geothermal drill hole near Breitenbush hot springs, Oregon: Oregon Geology, v. 56, p. 75–87.

Barth, S., 1993, Boron isotope variations in nature: a synthesis: Geologische Rundschau, v. 82. p. 640-651.

Berri, D.A., and Korosec, M.A., 1983, Geological and geothermal investigation of the lower Wind River valley, Southwestern Washington Cascade Range: Washington Division of Geology and Earth Resources Open File Report 83-5, 48 p.

Bethke, C.M., Farrell, B., and Yeakel, K., 2019, The Geochemist's Workbench Reference Manual, Aqueous Solutions LLC.

Bindeman, I., 2008, Oxygen isotopes in mantle and crustal magmas as revealed by single crystal analysis: Reviews in Mineralogy and Geochemistry, v. 69, p. 445–478

Blackwell, D.D., 1978, Heat Flow of Oregon: Oregon Department of Geology and Mineral Industries Special Paper, v. 4, p. 1-41.

Blackwell, D.D., Bowen, R.G., Hull, D.A., Riccio, J., and Steele, J.L., 1982, Heat flow, arc volcanism, and subduction in northern Oregon: Journal of Geophysical Research, v. 87, p. 8735-8754.

Blackwell, D.D., and Priest, G.R., 1993, Comment on “Heat Flow from Four New

Research Drill Holes in the Western Cascdes, Oregon, U.S.A." by S.E. Ingebritsen, M. A. Scholl, and D.R. Sherrod: Geothermics, v. 22, p. 151-163.

Blackwell, D.D., Steele, J.L., Kelley, S., and Korosec, M.A., 1990(a), Heat flow in the state of Washington and thermal conditions in the Cascade Range: Journal of Geophysical Research, v. 95, p. 19495-19516.

Blackwell, D.D., Steele, J.L., Frohme, M.K., Murphey, C.F., Priest, G.R., and Black, G.L., 1990(b), Heat flow in the Oregon Cascade Range and its correlation with regional gravity, Curie point depths, and geology: Journal of Geophysical Research, v. 95, p. 19475-19493.

Boden, J. R., 1985, Lithology, hydrothermal petrology and stable isotope geochemistry of three geothermal exploration drill holes, upper Clackamas River area, Cascade Range, Oregon: unpublished M.S. thesis, University of California Riverside, 137 p.

Brooks, J.R., Wigington, P.J., Phillips, D.L., Comeleo, R., and Coulombe, R., 2012, Willamette River Basin surface water isoscape (δ 18 O and δ 2 H): temporal changes of source water within the river: Ecosphere, v. 3, 21 p.

Clark, I. and Fritz, P., 1997. Environmental Isotopes in Hydrogeology. Lewis Publishers.

Clark, I. D., 2015, Groundwater geochemistry and isotopes: CRC Press.

Czajkowski, J.L., Bowman, J.D., Fusso, L.A., and Boschmann, D.E., 2013, Geologic mapping and geothermal assessment of the Wind River valley, Skamania County, Washington: 36 p.

Dilles, J.H., Solomon, G.C., Taylor, H.P., and Einaudi, M.T., 1992, Oxygen and hydrogen isotope characteristics of hydrothermal alteration at the Ann-Mason porphyry copper deposit, Yerington, Nevada: Economic Geology, v. 87, p. 44–63.

Dogramaci, S.S., Herczeg, A.L., Schiff, S.L., and Bone, Y., 2001, Controls on δ34S and δ18O of dissolved sulfate in aquifers of the Murray Basin, Australia and their use as indicators of flow processes: Applied Geochemistry, v. 16, p. 475–488.

Dyhrman, R. F., Geology of the Bagby Hot Springs Area, Clackamas and Marion Counties, Oregon [M.S. Thesis]: Oregon State University, 77 p.

Forcella, L., 1982, Geochemistry of Thermal and Mineral Waters in the Cascade Mountains of Western North America: Ground Water, v. 20, p. 39–47.

Forson, C., Steely, A., Cladouhos, T., Swyer, M., Davatzes, N., Anderson, M., Rtizinger, B., Glen, J., Peacock, J., Schermerhorn, W., Burns, E., and Telling, P., 2017, Geothermal Play-Fairway Analysis of Washington State Prospects: Phase 2 Technical Report, 232 p.

Fournier, R.O., 1989, Geochemistry and dynamics of the yellowstone national park hydrothermal system: Annual Review of Earth and Planetary Sciences, v. 17, p. 13-53.

Fournier, R.O., 1979, Geochemical and Hydrologic considerations and the use of enthalpy-chloride diagrams in the prediction of underground conditions in hot-spring systems: Journal of Volcanology and Geothermal Research, v. 5, p. 1-16.

Fournier, R.O., 1977, Chemical geothermometers and mixing models for geothermal systems: Geothermics, v. 5, p. 41–50.

Giggenbach, W.F., 1992, Isotopic shifts in waters from geothermal and volcanic systems along convergent plate boundaries and their origin: Earth and Planetary Science Letters, v. 113, p. 495–510.

Giggenbach, W.F., 1988, Geothermal solute equilibria. Derivation of Na-K-Mg-Ca geoindicators: Geochimica et Cosmochimica Acta, v. 52, p. 2749-2765.

Giggenbach, W.F., 1986, Graphical techniques for the evaluation of water/rock equilibration conditions by use of Na, K, Mg, and Ca-contents of discharge waters *in* Proceedings, 8th Geothermal Workshop, New Zealand: p. 37-43.

Gran, G., 1952, Determination of the Equivalence Point in Potentiometric Titrations. Part II: Analyst, v. 35, p. 236–242.

Hildreth, W., 2007. Quaternary magmatism in the Cascade Range — geologic perspectives. U.S. Geological Survey Professional Paper 1744, 125 p.

Ingebritsen, S.E., and Mariner, R.H., 2010, Hydrothermal heat discharge in the Cascade Range, northwestern United States: Journal of Volcanology and Geothermal Research, v. 196, p. 208–218.

Ingebritsen, S.E., Mariner, R.H., and Sherrod, D.R., 1994, Hydrothermal Systems of the

Cascade Range, North-Central Oregon, 91 p.

Ingebritsen, S.E., Sherrod, D.R., and Mariner, R.H., 1992, Rates and patterns of groundwater flow in the Cascade Range Volcanic Arc, and the effect on subsurface temperatures: Journal of Geophysical Research, v. 97, p. 4599–4627.

Ingebritsen, S.E., Sherrod, D.R., Mariner, R.H., 1989. Heat flow and hydrothermal circulation in the Cascade Range, north-central Oregon. Science, v. 243, p. 1,458–1,462.

Ingebritsen, S.E., Galloway, D.L., Colvard, E.M., Sorey, M.L., and Mariner, R.H., 2001, Time-variation of hydrothermal discharge at selected sites in the Western United States: Implications for monitoring: Journal of Volcanology and Geothermal Research, v. 111, p. 1–23.

Ishikawa T., Nakamura E., 1994, Origin of the slab component in arc lavas from across-arc variation of B and Pb isotopes: Nature, v. 370, p. 205-208.

James, E.R., Manga, M., Rose, T.P., and Hudson, G.B., 2000, The use of temperature and the isotopes of O, H, C, and noble gases to determine the pattern and spatial extent of groundwater flow: Journal of Hydrology, v. 237, p. 100–112.

Jones, J., Malone, S.D., 2005. Mount Hood earthquake activity: volcanic or tectonic origins? Bulletin. Seismological Society of America, v. 95, p. 818–832.

Keith, T.E.C., 1988, Hydrothermal alteration patterns in the Breitenbush Hot Springs area, Cascade Range, Oregon: Geothermal Resources Council Transactions, v. 12, p. 299-304.

Malkemus, D., 2016, Geothermometry of Two Cascade Geothermal Systems [M.S. Thesis]: Portland State University, 172 p.

Malkemus, D., Perkins, R. B., and Palmer, C. D., Geothermometry of the Breitenbush Hot Springs Area, Oregon, USA, *in* Proceedings 42nd Workshop on Geothermal Reservoir Engineering, Stanford University, Stanford, CA, 2017.

Mariner, R.H., Evans, W.C., Presser, T.S., and White, L.D., 2003, Excess nitrogen in selected thermal and mineral springs of the Cascade Range in northern California, Oregon, and Washington: sedimentary or volcanic in origin? Journal of Volcanology and Geothermal Research, v. 121, p. 99–114.

Mariner, R.H., Presser, T.S., and Evans, W.C., 1993, Geothermometry and water—rock interaction in selected thermal systems in the cascade range and modoc plateau, western United States: Geothermics, v. 22, p. 1–15.

Mariner, R.H., Presser, T.S., Evans, W.C., and Pringle, M.K.W., 1990, Discharge rates of fluid and heat by thermal springs of the Cascade Range, Washington, Oregon, and northern California: Journal of Geophysical Research, v. 95, p. 19517-19531.

Marschall, H.R., 2018. Boron Isotopes in the Ocean Floor Realm and the Mantle, *in* Marschall, H., Foster, G. (Eds.), Boron Isotopes: The Fifth Element. Springer International Publishing, Cham, p. 189-215.

McGowan, K. I., 1985, Geochemistry of alteration and mineralization of the Wind River gold prospect, Skamania County, Washington [M.S. Thesis]: Portland State University, 152 p.

Millot, R., and Négrel, P., 2007, Multi-isotopic tracing (δ7Li, δ11B, 87Sr/86Sr) and chemical geothermometry: evidence from hydro-geothermal systems in France: Chemical Geology, v. 244, p. 664–678.

Möller, P., Geyer, S., Salameh, E., and Dulski, P., 2006, Sources of mineralization and salinization of thermal groundwater of Jordan: Acta Hydrochimica et Hydrobiologica, v. 34, p. 86–100.

Palmer, C.D., 2015, Reservoir temperature estimator (RTEst) user's manual. *in* Mattson, E.D., Smith, R.W., Neupane, G., Palmer, D.D., Fujita, Y., McLing, T.L., Reed, D.W., Cooper, C., and Thompson, V.S., 2015, Improved geothermometry through multivariate reaction-path modeling and evaluation of geomicrobiological influences on geochemical temperature indicators: Idaho National Laboratory, INL/EXT-14-33959

Palmer, C.D., Ohly, S.R., Smith, R.W., Neupane, G., McLing, T., and Mattson, E., 2014, Mineral selection for multicomponent equilibrium geothermometry: Transactions - Geothermal Resources Council, v. 38, p. 453–459.

Palmer, M.R., 1991, Boron isotope systematics of hydrothermal fluids and tourmalines: A synthesis: Chemical Geology, v. 94, p. 111–121.

Palmer, M.R., and Sturchio, N.C., 1990, The boron isotope systematics of the

Yellowstone National Park (Wyoming) hydrothermal system: A reconnaissance: Geochimica et Cosmochimica Acta, v. 54, p. 2811–2815.

Pang, Z.H., and Reed, M., 1998, Theoretical chemical thermometry on geothermal waters: problems and methods: Geochimica et Cosmochimica Acta, v. 62, p. 1083–1091.

Penniston-Dorland, S., Liu, X.M., and Rudnick, R.L., 2017, Lithium isotope geochemistry: Non-Traditional Stable Isotopes, v. 82, p. 165–218

Powell, T. and Cumming, W., 2012, Spreadsheets for geothermal water and gas geochemistry 3rd edition: Proceedings, Thirty-fifth Workshop on Geothermal Reservoir Engineering, SGP-TR-188, 10 p.

Power, S.G., 1984, The "Tops" of Porphyry Copper Deposits - Mineralization and Plutonism in the Western Cascades, Oregon [Dissertation]: Oregon State University, 234 p.

Priest, G.R., and Vogt, B.F., 1982, Geology and Geothermal Resources of the Mount Hood Area Oregon, 104 p.

Reed, M., and Spycher, N., 1984, Calculation of pH and mineral equilibria in hydrothermal waters with application to geothermometry and studies of boiling and dilution: v. 48, p. 1479–1492.

Sherrod, D.R., Ingebritsen, S.E., Curless, J.M., Terry, K.E.C., Diaz, N.M., DeRoo, T.G., and Hurlocker, S.L., 1996, Water, rocks, and woods--A field excrusion to examine the geology, hydrology, and geothermal resources in the Clackamas, North Santiam, and McKenzie River drainages, Cascade Range, Oregon: Oregon Department of Geology and Mineral Industries, v. 58, p. 103–124.

Sherrod, D.R., and Conrey, R.M., 1988, Geologic setting of the Breitenbush-Austin Hot Springs area, Cascade Range, north-central Oregon, in Sherrod, D.R., ed., Geology and geothermal resources of the Breitenbush-Austin Hot Springs area, Clackamas and Marion Counties, Oregon: Oregon Department of Geology and Mineral Industries Open-File Report O-88-5, p. 1-14.

Spivack, A.J., and Edmond, J.M., 1986, Determination of Boron Isotope Ratios by

Thermal Ionization Mass Spectrometry of the Dicesium Metaborate Cation: Analytical Chemistry, v. 58, p. 31–35.

Spycher, N., Peiffer, L., Sonnenthal, E.L., Saldi, G., Reed, M.H., and Kennedy, B.M., 2014, Integrated multicomponent solute geothermometry: Geothermics, v. 51, p. 113–123.

Taylor, H. P., 1974, The application of oxygen and hydrogen isotope studies to problems of hydrothermal alteration and ore deposition: Economic Geology, v. 69, p. 843-883.

Utada, M., 2001, Zeolites in hydrothermally altered rocks: Reviews in Mineralogy and Geochemistry, v. 45, p. 305–322.

Walker, G.W., MacLeod, N.S., and Blakely, R.J., 1985, Mineral resource potential of the Bull of the Woods Wilderness, Clackamas and Marion Counties, Oregon: U.S. Geological Survey Open-File Report 85-247, 28 p.

Wells, R.E., and McCaffrey, R., 2013, Steady rotation of the Cascade arc: Geology, v. 41, p. 1027–1030.

Williams, C.F., DeAngelo, J., 2008. Mapping geothermal potential in the western United States. Transactions of the Geothermal Resources Council 32, p. 181–188.

Wise, W.S., 1961, The Geology and Mineralogy of the Wind River Area, Washington, and the Stability Relations of Celadonite [Ph.D. thesis]: The Johns Hopkins University, 158 p.

APPENDIX A: ION CHEMISTRY FOR GEOCHEMICAL MODELING

Appendix A contains two excel spreadsheets with ion data for hot springs in the north-central Oregon Cascades, central Oregon Cascades, and Wind River Valley. These data were used for geochemical modeling including piper diagrams in figures 11, 12, and 13. The first spreadsheet contains ion chemistry data divided by location and reported in moles. The second spreadsheet contains the same ion chemistry data reported in mg/L.

Filename: Appendix A_Ion Chemistry.xlsx

APPENDIX B: LABORATORY QUALITY CONTROL

Appendix B contains laboratory quality control for Bagby Hot Springs ICP-MS and IC, and $\delta^{18}O$ and δD isotopes.

Filename: Appendix B_Ion and Isotope QAQC.xlsx

APPENDIX C: RTEst and GWB Files

Appendix C contains .rea and .txt files for both the input and output of chemical models produced using the Reservoir Temperature Estimator (RTEst). These files require both Geochemist's Workbench and RTEst to run.

Filename: Appendix C_RTEst and GWB Files.rar